UNIVERSITA` DEGLI STUDI
DI PERUGIA

CORSO DI LAUREA MAGISTRALE IN INGEGNERIA MECCANICA

Advanced local approach for the fatigue assesment of aluminium weldments

Supervisors:

Prof. Ing. Filippo Cianetti

Prof. Ing Filippo Berto (NTNU)

Student:

Andrea Leonardi

Erasmus+

NTNU – Trondheim
Norwegian University of
Science and Technology

A.A. 2016/2017

Summary

Sommario

La prima fase di progettazione dei giunti saldati è alquanto complessa e difficile. Parametri come geometria del cordone della saldatura e il suo raggio di raccordo non sono quantificabili per la aleatorietà del processo tecnologico, neppure in un processo in cui la saldatura viene controllata in maniera ottimale. A tutto ciò si aggiunge un'ulteriore incertezza riguardo gli stress residui lasciati dal processo di saldatura stesso. Come prima conseguenza, in fase di progettazione di un giunto, l'intaglio che si genera tra componente e cordone di saldatura è modellato come un intaglio a spigolo vivo. Di seguito a ciò, il campo di stress assume un andamento asintotico (singolare) al variare della distanza, secondo il modello di Williams, la cui severità è quantificabile attraverso il fattore di intensificazione delle tensioni (NSIFs). In fase di progettazione l'impiego del NSIFs conduce ad una elevata dispersione di dati di riferimento (curve master), dato che le dimensioni caratterizzanti il NSIF dipendono da parametri geometrici con cui si modella l'angolo di apertura. Per superare tale aleatorietà può essere impiegata la densità di energia di deformazione (SED), valutata non su un volume infinitesimo ma su un volume di controllo dipendente dalla natura del materiale. Differenti lavori, precedentemente svolti, applicano il metodo di previsione a fatica attraverso SED a differenti tipologie di giunti.

In questo lavoro, per la prima volta, il metodo è applicato a giunti saldati di testa in lega di alluminio. La previsione della vita a fatica è stata condotta con tale metodologia, e confrontata con i dati sperimentali ricavati da prove svolte in laboratorio. Il lavoro è stato affrontato attraverso diversi step: un primo step è stato fare un'analisi dei vantaggi derivanti dell'impego del SED rispetto NSIFs (o stress). E' stata poi fatta un'analisi sperimentale dei giunti sollecitati a fatica, unendo i dati derivanti da prove sperimentali (numero di cicli di rottura) a dati derivanti dal FEM (valori della SED), ricostruendo le curve a fatica caratteristiche dei provini. Successivamente è stata fatta una previsione e un confronto della vita a fatica dei giunti attraverso metodologia SED ed una metodologia

più affermata quale quella denominata Nominal stress. Si è costruiti un modello in prims piano, poi si è creato un modello 3D al fine di comparare quali differenze sussistessero tra i due in termini del valore di SED. Da sudetta analisi è stato notato un comportamento singolare nel valore della SED, in prossimità del bordo libero. Tale effetto è caratteristico della geometria intagliata, prescindendo quindi dal componente saldato. Lo studio si è cosi incentrato, in un'ultima fase, nell'analisi di tali effetti rispetto le geometrie a disposizione nel caso di in questione, allontanandosi dal campo di studio delle saldature e spostandosi a quello della meccanica della frattura. Tali effetti tuttavia non portano a paricolari criticità per quanto riguarda la resistenza delle saldature, in quanto incrementano (nel caso di studio) il valore della SED del 10% nel caso peggiore.

Keywords: Alluminio, Giunti saldati, Approccio locale, Strain Energy Density, Mesh rada

Abstract

The first step in fatigue design of welded joint is particularly complex e difficult. Welded bead geometries can not be precisely definied. Parameters such as bead shape and toe radius change from joint to joint, even if in a well-controled manufacturing operations. Moreover, residual stress arising from welding process increase the overall uncertainty. Therefore, no exact weld radius will be modelled during the first design process step, and weldments are modelled as V-sharp notch in several cases for reason of simplicity. In the current case (zero radius of welded toe) the intensity of asymptotic stress distributions follows Williams' model, and they are quantified with the Notch Stress Intensity Factors (NSIFs). The main problem using NSIF in life fatigue assessment is related to its dimensions, changing for different opening angle. In this way, a grat number of reference data has to be available, each one for a respective geometry. Because of this, Lazzarin et all proposed another parameter, the Strain Energy Density (SED). This parameter is evaluated in a finite volume of control whose radius depends from material proprieties. By using SED method, several test lab evaluations of different welded joints were made in order to evaluate their fatigue life, mostly for cruciform and T-joint weldment geometries. In this work, for the first time, SED method is applied to butt joint of aluminium. In a first place, analysis of advantages arising from SED method are been analyzed and compared to NSIFs mehod. Following, experimental fatigue analysis has been made using butt welded. Moreover, numerical models have been made. Experimental data (number of cycles of failure) are been connected with numerical ones (SED values). Finally, a comparation between cycles assessed with SED method Nominal approach has been made. Firstly, a 2D FEM model for butt joints of 5 and 20 mm of thickness has been built. Following, a 3D model has been created in order to compare it with 2D. From 3D FEM model, particular effect arising from notch singularity have been noted and studied.

Keywords: Aluminium, Welded joints, Local approaches, Strain Energy Density, Coarse mesh

Introduction:

In mechanical components production, geometrical discontinuities are inevitable. Those imperfections produce a variation and an increase of local stress and strain state. Different criteria of static and fatigue life assessments have been formulated in order to approach fatigue design in presence of a notch. The current state of art shows that engineers can chose among four different methods: the first one using nominal stress, the second one using the peak values of stress, the third one using Notch Stress Intensity Factors while the last one based on a volumetric approach [1] and [2]. The Notch Stress Intensity Factor (NSIF) quantifies the severity of notch in stress state. The study of this parameter requires particular attention. Because of this, material strength decreases, especially in the fatigue field. In general, the fatigue life curve of notched components is lower than the fatigue life of the material. Therefore, the strength of a mechanical notched component is lower. Moreover, especially for brittle materials, if the imperfection has a very little radius close to zero, or is modelled as a zero-radius, NSIF is the only parameter used. From experimental analysis we can see that, when the radius of the notch decrease, the fatigue curve of the component doesn't decrease with the same velocity (for radius under a little value). So, from a phenomenologically point of view, we can say that is not the peak factor but an average value in a finite volume to rules the strength of the material [3].

Welded structural members have complex geometry and metallurgy in the proximity of the weld. They may contain porosity or other different defects, making it difficult to determinate real stress state. A great spread of geometries, material proprieties, average stress, weld shapes and quality can be noted. These defects make impossible to relate the behaviour of weldments to non-welded test material. As a result, the majority of the industrial design codes that perform welded structures employ S-N curves based on tests of actual welded members. The results are insensitive to the sub-class of structural metal involved, but highly sensitive to the geometric detail [4]. Different methods of welded

joints design are used as, nominal stress method, hot spot stress method, and NSIFs method [5]. Nominal stress is used only for very precise correspondence of geometry and load of structure with reference data. Hot spots stress analysis is suitable for not-conventional geometries. However those two methods don't provide detailed information on the stress field in the critical regions of the materials. If this is the aim, a more detailed approach related to Fracture Mechanics has to be applied, using parameter as NSIF, secceeding to characterize the local state of stress. In the field of weldments, the geometric parameters of the joints are not precisly known. Infact they can also change also in an optimal welding process control. For this reason, the geometry is generally modelled with a zero radius at the first design [1]. In the static or fatigue life assessment, the use of NSIFs requist a very fine mesh. However the main and greater problem related to use of NSIF is his dimensions. Infact NSIFs' dimensions depend from opening angle accordig to $\mathrm{MPa}\, mm^{\zeta}$ units of measurement, where ζ characterizes the opening angle. In this way, if fatigue life assessment wants to be made using NSIFs, different master curves has to be evaluated experimentally for each opening angle. Moreover, a very fine mesh has to be used to evaluate NSIFs. Lazzarin and Berto [6] propose the use of another parameter, the strain energy density (SED) instead of NSIF. The use of SED, mediated in a finite volume of control depending from the material, leads to some different benefits. The method based on this parameter succeeds to evaluate a local value characterizing stress field around the interested region. The main benefit is the indipendance of SED from opening angle, since its unit of measurement is $\mathrm{N}\, mm\, /mm^3$ for each opening angle. A very coarse mesh can be used in order to evaluate it. Moreover, for plane model, it's possible to recreate the stress field around the notch using relation among SED and NSIFs, using Williams' model. On the other hand, a more complex pre-processing has to be faced in order to evaluate this parameter, but more precise results can be found.

The aim of this work is to study SED method, its advantages and its disadvantages, beside its application for first time in fatigue life assessment of butt joint, largelly used in big structures and heavy carpentery. A fatigue life assessment comparation of results has been made using Nominal stress method's results as reference. In the end a comparation

af 2D model and 3D model has been made in order to comment the difference of SED values.

The job has been articulated in four chapter: The first chapter is related to basic theoretical concept, treating with a brief overview on weldments, conventional fatigue life assessment for welded joint, and some concepts of linear elastic fractur mechanics. In the second chapter there is description of experimental methods. In the third one numerical models can be found, for 2D and 3D cases, with the results of the study. In the last chapter a comment of the work has been made.

Chapter 1

Basic concepts

1.1 An overview on welded joints and main design criteria

Welding is a process where two divided components are connected togheter using heat or pressure. The joint is made through two surface belonging to each element. At the end of the process, the joint is irreversible. The process is made using a filler generally, but in some cases no filler is used and the weldments is defined autogene. The main advantages arising from weldments are low cost, the little time needed from process, and the possibility of automatization. The strength of the weldments depends from:

- Geometry of weldment
- Type of load

American Welding Society defines 50 tipologies of weldings, that can be macroscoply divided in 2 groups:

- Fusion Welding: Heat and filler are used for the process. The main welding process are:
- Arc Welding: Heat comes from an electrical shock arising from an electrode. Sometimes a pressure is used in addition. The contact between electrode and piece is necessary only in a first moment, at the start.
- Resistance welding: Heat comes from an electrical resistance;
- Oxifuel Gas Welding: Flame is used in order to generate heat and melt the components.

- State Solid Welding: The joint arises from application of pressure. Sometimes a little flux of heat is applied. No filler is used:
  - Diffusion Welding: Surfaces come in touch with high pressure and lightly heated;
  - Friction Welding: Heat is generated from friction among surfaces;
  - Ultrasonic Welding: A light pressure is applied with a high frequency vibration of the component

Different kinds of welded joint can be built:

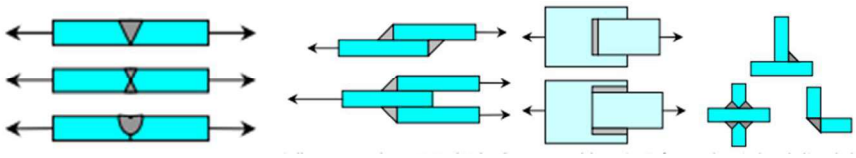

FIGURE 1: DIFFERENT TYPES OF WELDMENTS

Heating process produces some residual stress that lasts after the process. They can be reduced in different ways:

- Pre-heating of pieces to weld;
- Post treatament of weldments to stretch the material
- Using the same thickness of the joints.

The basic idea is to create a high local temperature in order to melt locally the component, following join. The high value of temperatur and heat flux generate different conformations of crystalline shapes, so that material proprieties change respect the original material ones.

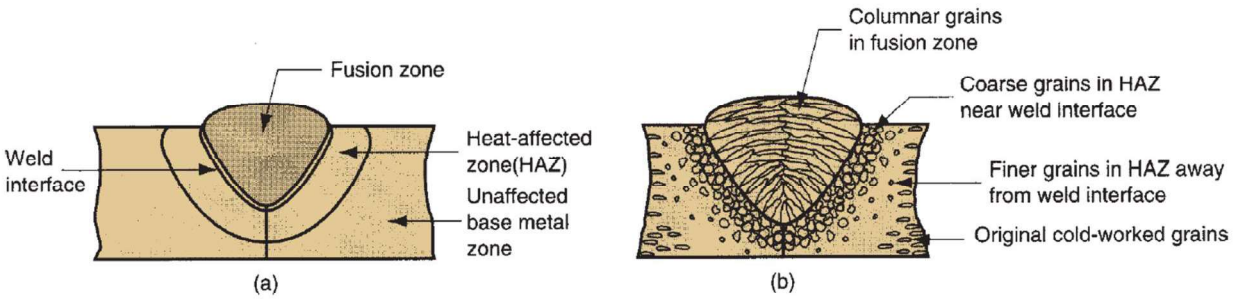

FIGURE 2:CHANGING OF MATERIAL PROPRIETIES

Four different zones can be defined:

- Fusion zone: Is the area where complete melt of the materiali is achieved. The nucleation of the material depends from boudary conditions and magnitude of heat flux;
- Weld interface: is the littlest area, dividing Heat Affected Zone from fusion zone;
- Heat Affected Zone (HAZ): The temperature here are not so high to melt the material, but much to change crystallographic conformation. Here the material is brittle.
- Unaffected base metal.

The high local temperature generates residual stress and deformation. Typically residual deformations can be seen ad in figure 3:

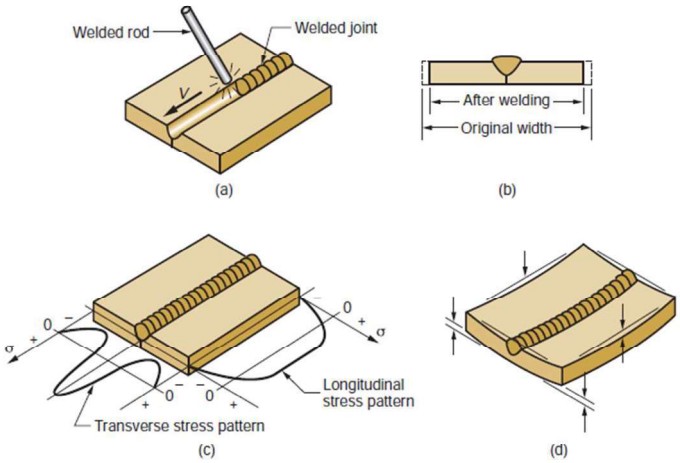

FIGURE 3: RESIDUAL STRESS

In a first design step, fatigue life assessment of mechanical components is very difficult and complex. Life fatigue assessment follows some exential basic step generally, that can be syntetised in figure 4:

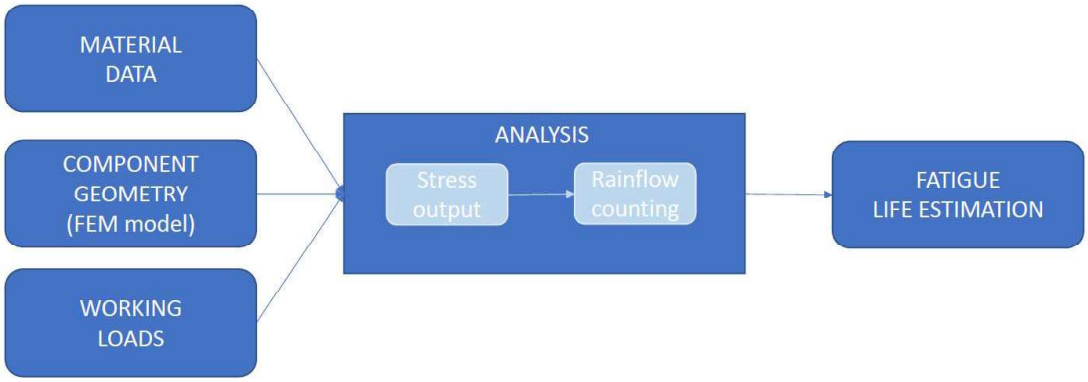

FIGURE 4: MAIN STEPS IN A FATIGUE LIFE ANALYSIS

Design of welding is generally more complex, because of different reasons:

- Uncertainness on material proprieties and data, mainly with fusion welding. The heat changes the material microstructure and so the mechanical proprieties. Different types of the same structural materials have indicatively the same behavior;
- High uncertainty on geometry, due to misalignment;
- High uncertain in weld shape.

For those reasons experimental data are essential in order to design a right weldment. Different criteria are used, and in general all of the arises from experimental data:

- NOMINAL STRESS

It is used only where a nominal stress can be planly defined. From the class of the weldment and type of load, a precise fatigue curve is defined, that is the 95% of probability of survival. Welded joints are classified by type, loading conditions and shape/geometry. The fatigue curves are based on rappresentative experimental investigations and thus they include the effects of:

- Local stress concentrations due to the weld geometry
- Direction of load
- Residual stress
- Welding process

Moreover, because of the heat trasfered during the welding process, the different types of the same material are not important.

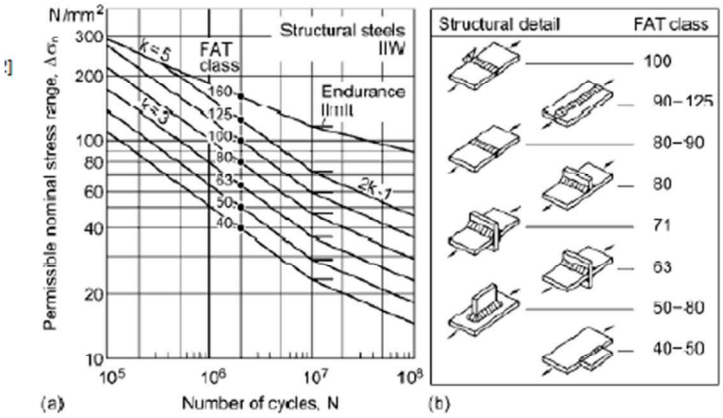

FIGURE 5: EXAMPLE OF NOMINAL STRESS DESIGN

The class of the weldments is related to nominal stress for number of cycles of failure $N_f = 2\,E + 06$. The effects of NSIF and residual stress are included because of the experimental method. The conditions of application of this method need to be the following:

- Nominal stress can be well and plain defined;
- Structural discontinuity is comparable to one of the classified details included in the codes/regulation

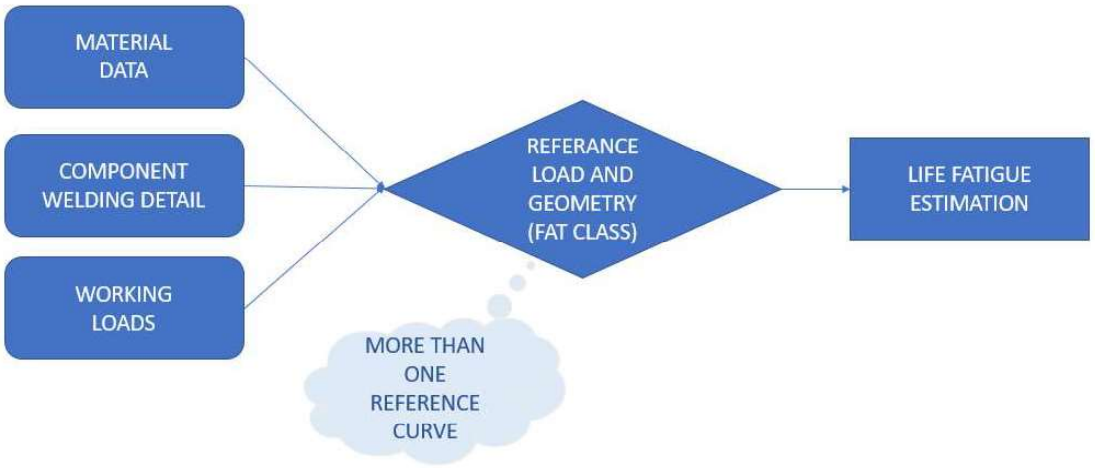

FIGURE 6: FLOW CHART FOR NOMINAL APPROACH DESIGN

- HOT SPOT STRESS

It is applied in general when nominal stress is not plain defined, for more complex structures. The idea of hot spot method is to study the geometric stress near the weldment, influenced only by geometry of the joints. In this way the interest is focused on the local geometry and not on the overall geometry. The fatigue design curves are referred according to their FAT number, that identify the local geometry closest to the weldment.

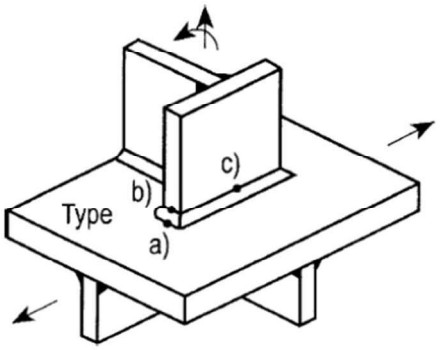

FIGURE 7: EXAMPLE OF STRUCTURE WHERE HOT SPOT STRESS IS APPLIED

The stress near the weld bead is composed by three effects: membrane one, flexional one a plastic one. Membrane and flexional effects are related to load a geometry, plastic one is not considered in this case

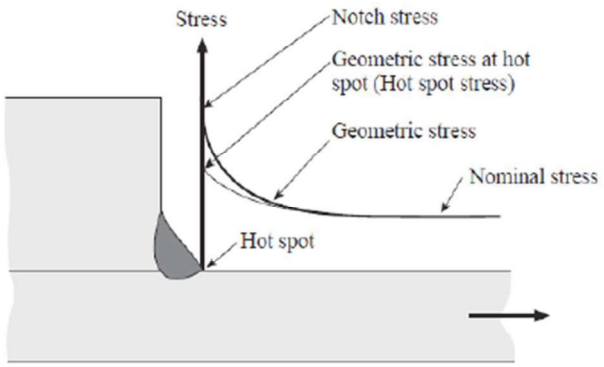

FIGURE 8: HOT SPOT STRESS EVALUATION

Hot spot stress come from interaction of geometries. They are evaluated using a linear (2 points) or parabolic (3 points) interpolation, taking in consideration 2 or 3 points being at a regulated distance from the notch [5]. A FEM model can be built and used for analysis.

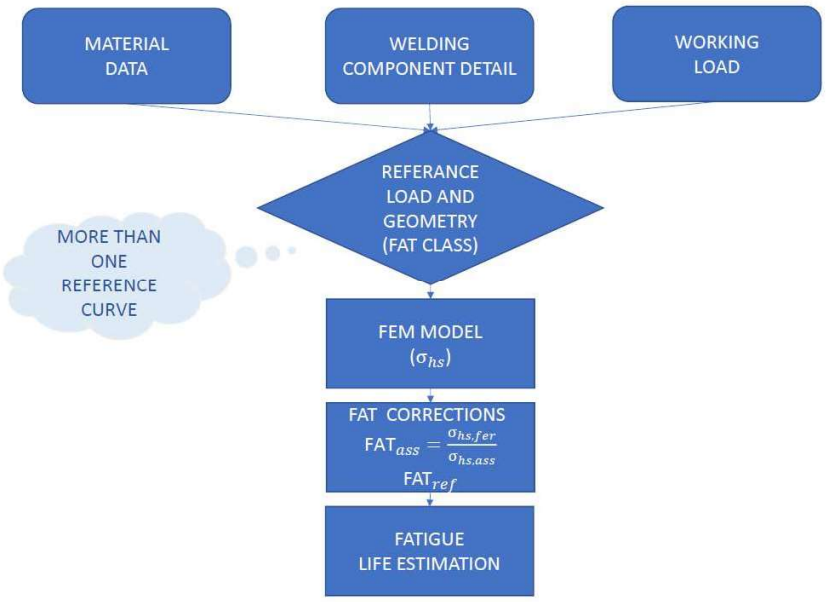

FIGURE 9: FLOW CHART FOR HOT SPOT STRUCTURAL DESIGN

1.2 Basic concepts of fracture mechanics

In some different cases, structural components go under loads that fail the component even if the load is below the yelding value and no macroscopic deformation can be seen.

Fracture mechanics is the matter treating with continuum mechanics with local defects, like cracks or voids or imperfection. It studies how local lacks change locally the stress and strain field in a limited zone. The importance of the fracture mechanical arises if the way of the failure of components wants to be studied and understood. Mainly in the fatigue field, the failure arises from local imperfections that, in some case, grow very fast. At the same time they increase their size too. Fracture mechanics is divided in three main branches:

- Linear Elastic Fracture Mechanics (LEFM), that studies the mechanical behaviour in linear elastic field;
- Elasto-plastic fracture mechanics, studing the material in plastic field;
- Visco-elastic fracture mechanics, studing the material with visco-elastic behaviour

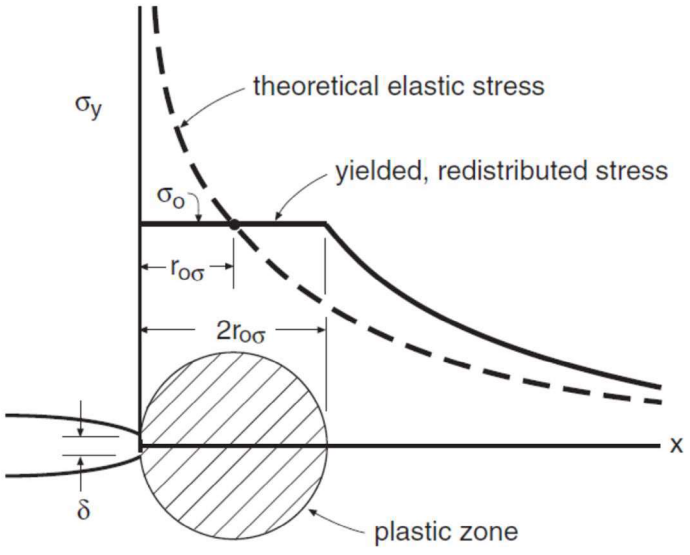

FIGURE 10: ELASTIC AND PLASTIC STRESS ZONES AROUND A NOTCH

Of course, the stress around the crack doesn't grow towords infinite value in the real behaviour of the material, but there will be an upper limit arising from the plastic behaviour or from the failure of material. Linear elastic fracture mechanics is the simplest, and the bases for more complex theory. In order to use linear model, the plastic zone around the notch has to be small enough, and the equation describing this situation is:

$$r_p/l_{min} < \frac{1}{5\,\pi} \qquad (1)$$

Where r_p radius of plastic area and l_{min} is the littlest dimension of the geometry.

The modelling of imperfection can be made with two main reference geometries: zero radius or a blunt discontinuity.

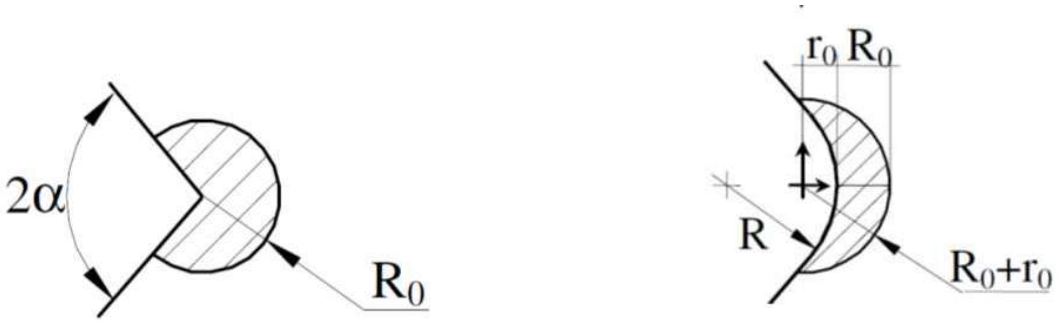

FIGURE 11: EXAPLE OF V AND U NOTCH

Stress state for zero-radius geometry has not an upper limit, at the contrary than blunt notch, considering only linear field. A crack can be moved in three different ways:

- Mode I: The crack is opened in Y direction;
- Mode II: The crack surfaces slide along x direction;
- Mode III: The crack is moved in Z direction)

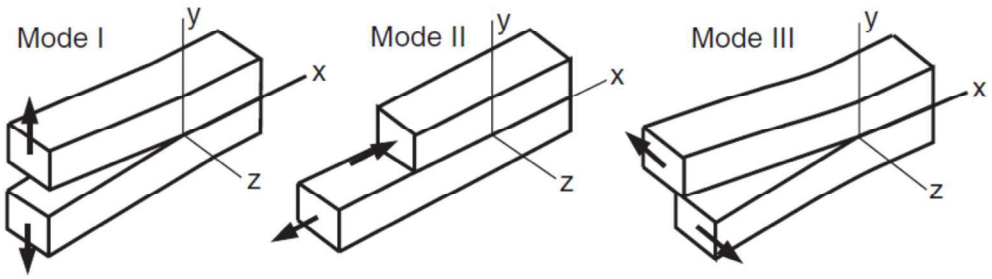

FIGURE 12: MODE I, II, III

The most dangerous mode is the Mode I.

1.2 Stress field around a crack

In the plane case, there are different models describing the stress around the notch. The first people concerning with this matter were Irwin, Westegaard and Williams. The mostly coordinate system used in order to describe the stress state is the cilyndrical one shown in figure 13.

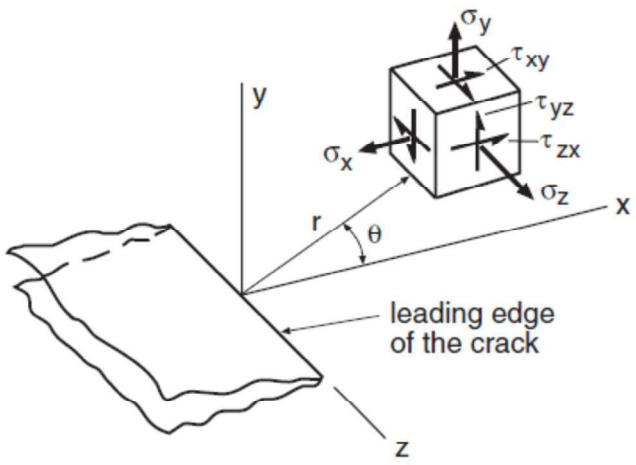

FIGURE 13:SYSTEM OF RIFERIMENT FOR NOTCH

If only the plane case x-y is considered, the strain field is rappresented by this following equation:

$$\varepsilon_{rr} = \frac{\partial u_r}{\partial r};\ \varepsilon_{\theta\theta} = \frac{\partial u_r}{r} + \frac{1}{r}\frac{\partial u_\theta}{\partial \theta};\ \varepsilon_{r\theta} = \frac{1}{2}\left(\frac{1}{r}\ \frac{\partial u_r}{\partial \theta} + \frac{\partial u_\theta}{\partial r} - \frac{u_\theta}{r}\right) \quad (2)$$

r and θ declair the radial and tangential direction. In all the bodies with a material discontinuity can be shown that the stress state around the notch is:

$$\sigma_{ij} = \left(\frac{k}{\sqrt{r}}\right) f_{ij}(\theta) + \sum_{m=0}^{\infty} A_m r^{\frac{m}{2}} g_{ij}^{(m)}(\theta) \quad (3)$$

The different letters mean:

- σ_{ij} Stress component;
- k is a costant increasing the stress state;
- f_{ij} is an adimensional function depending from the angle;
- g_{ij} is an adimensional function depending from the angle but for higher order terms;
- A_m is the amplitude of the higher order terms.

The equation (3) has two different terms:

- The first one describes the stress around the notch and its values increases when the distance decreases;
- The second one is a sum of different terms, which increase togheter with the distance.

In order to describe the stress around the notch, only the first one has to be considered. The stress is so defined singular, and the costant k depends from the different modes, so that we have 3 different costants K_I, K_{II}, K_{III}.

The stress is so described:

$$\lim_{r\to 0} \sigma_{ij}^{I} = \frac{K_I}{\sqrt{2\,\pi\, r}}\, f_{ij}^{I}(\theta) \tag{4.1}$$

$$\lim_{r\to 0} \sigma_{ij}^{I} = \frac{K_{II}}{\sqrt{2\,\pi\, r}}\, f_{ij}^{II}(\theta) \tag{4.2}$$

$$\lim_{r\to 0} \sigma_{ij}^{I} = \frac{K_{III}}{\sqrt{2\,\pi\, r}}\, f_{ij}^{III}(\theta) \tag{4.3}$$

And the total stress will be

$$\sigma_{ij}^{total} = \sigma_{ij}^{I} + \sigma_{ij}^{II} + \sigma_{ij}^{III} \tag{5}$$

1.2.1 Airy'S Function

Airy's funtion is a scalar function which satisfies the equilibrium and the conguence conditions in plane cases of stress and strain. From this function the stress can be described using equations in table 1:

TABLE 1: RELATIONS BETWEEN AIRY'S FUNCTION AND STRESS COMPONENTS

Coordinate cartesiane	Coordinate polari
$\Psi = \Psi(x,y)$	$\Psi = \Psi(r,\theta)$
$\sigma_{xx} = \frac{\partial^2 \Psi}{\partial x^2}$	$\sigma_{rr} = -\frac{1}{r}\frac{\partial \Psi}{\partial r} + \frac{1}{r^2}\frac{\partial^2 \Psi}{\partial \theta^2}$
$\sigma_{yy} = \frac{\partial^2 \Psi}{\partial y^2}$	$\sigma_{\theta\theta} = \frac{\partial^2 \Psi}{\partial \theta^2}$
$\sigma_{xy} = -\frac{\partial^2 \Psi}{\partial x\, \partial y}$	$\sigma_{r\theta} = -\frac{1}{\partial r}\left(\frac{1}{r}\ \frac{\partial \Psi}{\partial r}\right)$

Describing equilibrium in plane case, equations (6) are obtained:

$$\frac{\partial \sigma_{xx}}{\partial x} + \frac{\partial \sigma_{xy}}{\partial y} = 0 \ ; \ \frac{\partial \sigma_{yy}}{\partial y} + \frac{\partial \sigma_{xy}}{\partial x} = 0 \tag{6}$$

And using Airy's funtion equation (7) is achieved:

$$\nabla^2 \nabla^2 \Psi = \frac{\partial^4 \Psi}{\partial y^4} + \frac{\partial^4 \Psi}{\partial x^4} + \frac{\partial^4 \Psi}{\partial y^2 \partial x^2} = 0 \tag{7}$$

that satisfies both equilibriun and congruence.

1.2.2 Westergaard's model: stress around a crack

Westergaard's model describes the stress state around a crack, that is a geometric discontinuity in the material having only one dimension. Along this, the joint of the crack surface forms the crack front. When a load is applied to the body, the crack front is moved and the two surfaces have a relative displacement. In order to describe the stress state, complex analysis is used. The solution came from a plate loaded by nominal biaxial stress. The a-parameter is the half-crack length. Different solutions are computed by Westeergard for different mode. In mode I case, the boundary condition around the crack are:

$$\sigma_{xy} = \sigma_{yy} = 0 \rightarrow |x| < a \;\&\; y = 0 \tag{8}$$

$$\sigma_{xx} = \sigma_{yy} = \sigma_0 \,, \sigma_{xy} = 0 \rightarrow x^2 + y^2 \rightarrow \infty \tag{9}$$

The reference geometry in figure 14 is used for describing the problem:

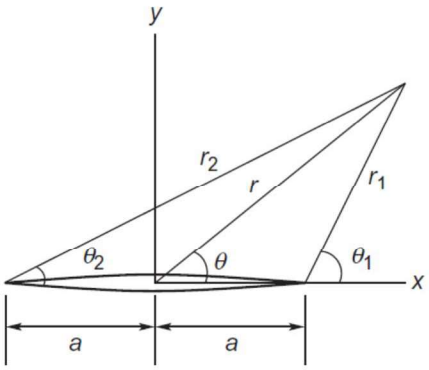

FIGURE 14: GEOMETRY FOR WEESTERGARD MODEL

The parameters used in the description of stress state are:

- r_1, r_2 e r are the distance from the end of the crack and from the centre;

- $\theta, \theta_1\ e\ \theta_2$ are the corners made from r directions and crack length.

$$\sigma_{xx} = \sigma_0 \frac{r}{\sqrt{r_1 r_2}} \left[\cos\left(\theta - \frac{\theta_1 + \theta_2}{2}\right) - \frac{a^2}{r_1 r_2} \sin(\theta) \sin(\frac{3}{2}(\theta_1 + \theta_2)) \right] \quad (10)$$

$$\sigma_{yy} = \sigma_0 \frac{r}{\sqrt{r_1 r_2}} \left[\cos\left(\theta - \frac{\theta_1 + \theta_2}{2}\right) + \frac{a^2}{r_1 r_2} \sin(\theta) \sin(\frac{3}{2}(\theta_1 + \theta_2)) \right] \quad (11)$$

$$\sigma_{xy} = \sigma_0 \frac{r}{\sqrt{r_1 r_2}} \left[\frac{a^2}{r_1 r_2} \sin(\theta) \sin(\frac{3}{2}(\theta_1 + \theta_2)) \right] \quad (12)$$

Close to the crack some simplification can be made:

$$\frac{r_1}{a} \ll 1\ ;\ \theta \approx 0\ ;\ \theta_2 \approx 0\ ;\ r \approx a\ ;\ r_2 \approx 2a \quad (13)$$

And writing the equations using hypothesis (13):

$$\sigma_{xx} = \sigma_0 \frac{\sqrt{a}}{\sqrt{2r_1}} \cos\left(\frac{\theta_1}{2}\right) \left[1 + \sin\left(\frac{\theta_1}{2}\right) \sin\left(\frac{3}{2}\theta_1\right) \right] \quad (14)$$

$$\sigma_{yy} = \sigma_0 \frac{\sqrt{a}}{\sqrt{2r_1}} \cos\left(\frac{\theta_1}{2}\right) \left[1 + \sin\left(\frac{\theta_1}{2}\right) \sin\left(\frac{3}{2}\theta_1\right) \right] \quad (15)$$

$$\sigma_{xy} = \sigma_0 \frac{\sqrt{a}}{\sqrt{2r_1}} \sin\left(\frac{\theta_1}{2}\right) \cos(\frac{\theta_1}{2}) \cos(\frac{3}{2}\theta_1) \quad (16)$$

Analyzing stresses around the crack length:

$$\sigma_{xy} = 0 \tag{17}$$

$$\sigma_{yy} = \sigma_0 \frac{\sqrt{\pi a}}{\sqrt{2\pi r_1}} \tag{18}$$

So, for the mode, I the NSIF is defined following equation (19):

$$K_I = \sigma_0 \sqrt{\pi a} \tag{19}$$

1.2.3 Williams' model: stress around V-sharp notch

This model created by Williams in 1952 decribes the stress around a V-notch and it can be considered an extension of Westergaard's model.

The geometry used is the one reppresented in figure 15:

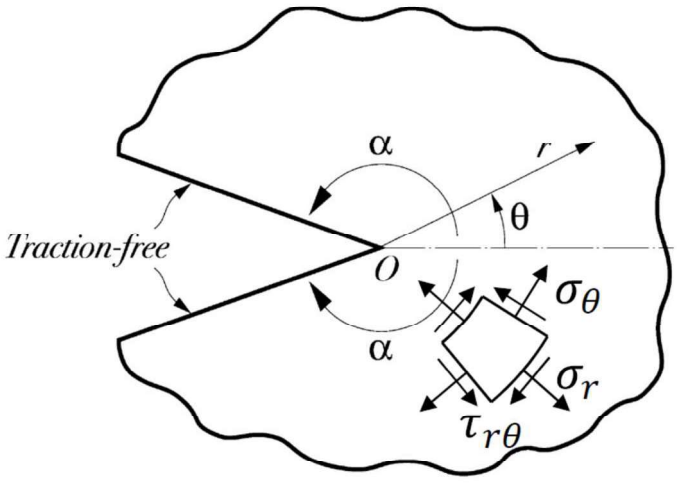

FIGURE 15: GEOMETRY OF WILLIAMS' MODEL

In order to find a solution for the problem, Airy's function described in equation 20 is assumed:

$$\Psi = r\hat{}(1+\lambda)\ (C1\sin[(1+\lambda)\theta] + C2\cos[(1+\lambda)\theta + C3\sin[(\lambda-1)\theta] + \cos[(\lambda-1)\theta]) \quad (19)$$

Deriving Airy's function, stress component (21) e (22) are obteined:

- Modo I:

$$\begin{Bmatrix}\sigma_{\theta\theta}\\ \sigma_{rr}\\ \sigma_{r\theta}\end{Bmatrix} = \frac{1}{\sqrt{2\pi}}\frac{r^{\lambda_1-1}K_1^N}{(1+\lambda_1)+\chi_1\ (1-\lambda_1)}[\begin{Bmatrix}(1+\lambda_1)\cos(1-\lambda_1)\theta\\ (3-\lambda_1)\cos(1-\lambda_1)\theta\\ (1-\lambda_1)\sin(1-\lambda_1)\theta\end{Bmatrix} + \chi_1\ (1-\lambda_1)\begin{Bmatrix}\cos(1+\lambda_1)\theta\\ -\cos(1+\lambda_1)\theta\\ \sin(1+\lambda_1)\theta\end{Bmatrix} \quad (20)$$

- Modo II:

$$\begin{Bmatrix}\sigma_{\theta\theta}\\ \sigma_{rr}\\ \sigma_{r\theta}\end{Bmatrix} = \frac{1}{\sqrt{2\pi}}\frac{r^{\lambda_2-1}K_2^N}{(1+\lambda_2)+\chi_2\ (1-\lambda_2)}[\begin{Bmatrix}-(1+\lambda_2)\sin(1-\lambda_2)\theta\\ -(3-\lambda_2)\sin(1-\lambda_2)\theta\\ (1-\lambda_2)\cos(1-\lambda_2)\theta\end{Bmatrix} + +\chi_2\ (1+\lambda_2)\begin{Bmatrix}-\sin(1+\lambda_2)\theta\\ \sin(1+\lambda_2)\theta\\ \cos(1+\lambda_2)\theta\end{Bmatrix} \quad (21)$$

Where K_1^N and K_2^N are the NSIFs for mode I and mode II, λ_1 e λ_2 are the eigenvalues of Williams' problem,,that depend from the boundary conditions and opening angle, as χ_1 χ_2.

So, the parameters λ1, λ2, and χ1, χ2 describe the problem from a geometic point of view.

The values of eigenvalues define the singolarity of the different modes of problem. In order to be singular, the Williams' eigenvalues have to be littler than zero.

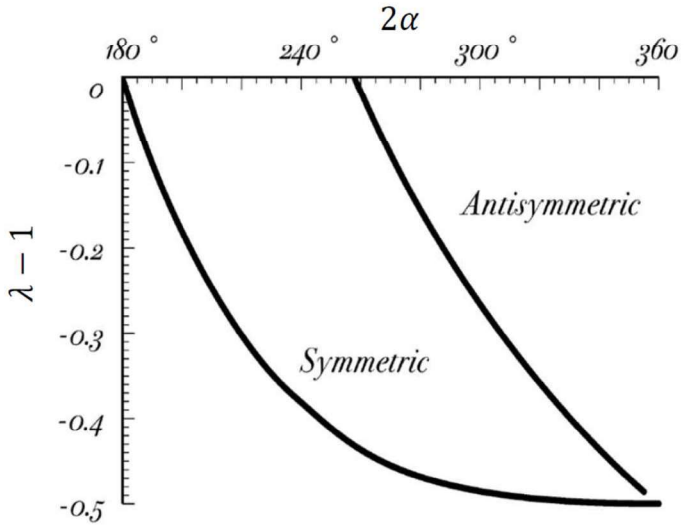

FIGURE 16: MAGNITUDE OF SINGULARITY

In the event that both modes are singular, the superposizion of effects is applied. The boundary conditions, as plane stress or strain, define the geometrical parametres.

$$B \leq 2.5 \left(\frac{K_{Ic}}{S_y}\right)^2 \rightarrow \text{plane stress} \tag{23}$$

$$B \geq 2.5 \left(\frac{K_{Ic}}{S_y}\right)^2 \rightarrow \text{plane strain} \tag{24}$$

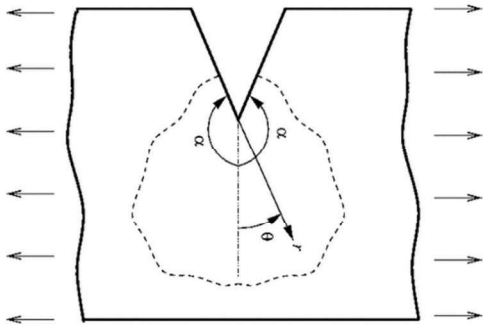

FIGURE 17: WILLIAMS' MODEL

From the equations (20) and (21) can be seen as the mode I is symmetric and the mode II is anti-symmetric respect the bisector direction. Studing the stress changing only the angle parameter, for costant distance from the V-notch, can be seen that, for $\theta = 0$:

- Mode I

$$\begin{Bmatrix}\sigma_{\theta\theta}\\ \sigma_{rr}\\ \sigma_{r\theta}\end{Bmatrix} = \frac{1}{\sqrt{2\pi}} \frac{r^{\lambda_1 - 1} K_1^N}{(1+\lambda_1) + \chi_1 (1-\lambda_1)} \left[\begin{Bmatrix}(1+\lambda_1)\\ (3-\lambda_1)\\ 0\end{Bmatrix} + \chi_1 (1-\lambda_1) \begin{Bmatrix}1\\ -1\\ 0\end{Bmatrix} \right] \tag{25}$$

- Mode II

$$\begin{Bmatrix}\sigma_{\theta\theta}\\ \sigma_{rr}\\ \sigma_{r\theta}\end{Bmatrix} = \frac{1}{\sqrt{2\pi}} \frac{r^{\lambda_2 - 1} K_2^N}{(1+\lambda_2) + \chi_2 (1-\lambda_2)} \left[\begin{Bmatrix}0\\ 0\\ 1-\lambda_2\end{Bmatrix} + \chi_2 (1+\lambda_2) \begin{Bmatrix}0\\ 0\\ 1\end{Bmatrix} \right] \tag{26}$$

tangential component has a maximum value and shear stress in zero in the same point.

The opposite happens for the mode II. The stress components are so uncopuled, and from them NSIFs can be calculated:

$$K1 = \sqrt{2 * pi} \lim_{r \to 0} \left(\sigma_{\theta\theta}\right)_{\theta=0} r^{1-\lambda_1} \tag{27}$$

$$K2 = \sqrt{2 * pi} \lim_{r \to 0} \left(\sigma_{r\theta}\right)_{\theta=0} r^{1-\lambda_2} \tag{28}$$

Using so the FEM model, along the bisector direction strees can be taken and using the equations (27) and (28) NSIFs can be computed

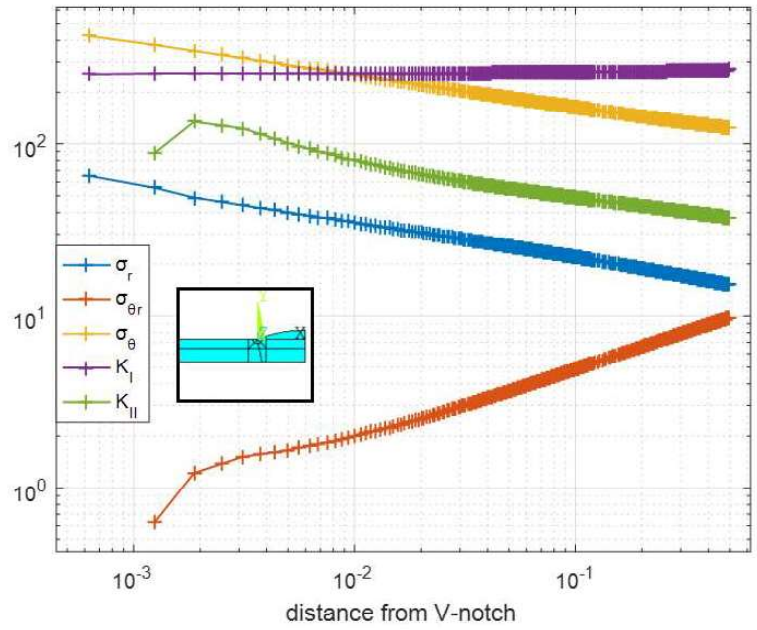

FIGURE 18: EXAMPLE OF STRESS AND NSIFS FOR V-NOTCH

1.2.4 Kirsch's model: stress around blunt notch

The simplest case for a blunt notch is when the notch is circular, whose radius is a.

The plate in the figure 19 in stretched by a nominal uniform stress, applied on the edge:

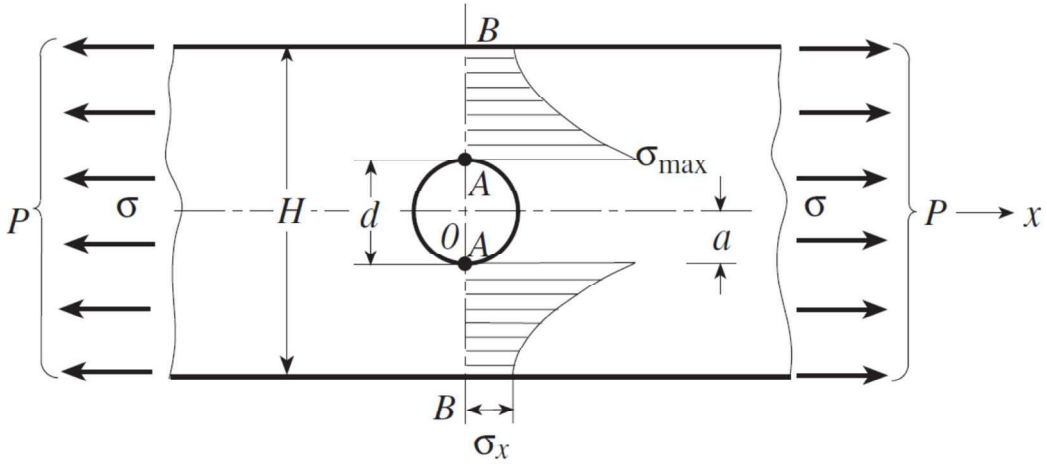

FIGURE 19: KIRSCH'S MODEL

The solution of the elastic problem generates the stress components (29) (30) (31):

$$\sigma_{\theta\theta} = \frac{p_0}{2}\left[1-\left(\frac{a}{r}\right)^2\right]+\frac{p_0}{2}\left[1+3\left(\frac{a}{r}\right)^4-4\left(\frac{a}{r}\right)^2\right]\cos(2\theta) \quad (29)0)$$

$$\sigma_{rr} = \frac{p_0}{2}\left[1+\left(\frac{a}{r}\right)^2\right]-\frac{p_0}{2}\left[1+3\left(\frac{a}{r}\right)^4\right]\cos(2\theta) \quad (30)0)$$

$$\sigma_{r\theta} = -\frac{p_0}{2}\left[1-3\left(\frac{a}{r}\right)^4+2\left(\frac{a}{r}\right)^2\right]\sin(2\theta) \quad (31)1)$$

For values of the r going to radius value, the components $\sigma_{r\theta}$ e σ_{rr} are zeros and the component $\sigma_{\theta\theta} = p_0[1-2\cos(2\theta)]$, so that the maximun of the stress is 3σ .

1.3 Strength criteria for notched component using NSIFs

For the assessment of notched components NSIF is used and it is compared with fracture toughness, in the case of static verification, or with ΔKc in case of fatigue assessment. The NSIf is index of a combination stress-defect generating instable propagation of the fracture. Its unit of mesurement is $[\mathrm{Kc}] = [\mathrm{MPa}][\mathrm{mm}]^{0.5}$, it is referred to the different modes and for a crack geometry.

The stress around the crack can be plane stress or plane strain. Between them, plane strain is the most severe one, so that it is considered like referement and it makes easier the propagation of yelded zone.

Clearly, the verification of the component is valid when the equation (32) is verified:

$$K_i \leq K_c \quad (32)$$

Kc value is defined experimentally, failing a sample of B thickness with a defect.

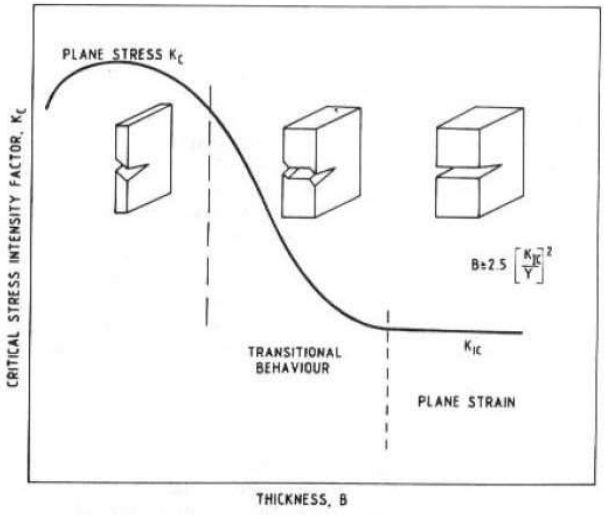

FIGURE 20: FRACTURE TOUGHNESS VS THICKNESS

From the figure 20 can be seen like, when the thickness grows, Kc decrease because of the more severe stress state.

1.4 Strain Energy Density (SED)

Strain Energy Density (SED) is the reversible elastic deformation accumulated by an infinitesimal volume of the elastic body when the body is going under loads/deformations. In the event of an elasitc body is loaded, a state of stress and strain are generated, and so an elastic energy of deformation is stored. It is measured in Joule. If we consider the absolute value, it depends from the dimensions of the body, from material e from loads. The parameter so defined doesn't permit comparation with other elastic body, neither to study how locally each point is stressed. It so introduced the density of strain energy, an energy of deformation divided by an infinitesimal volume around the point. The unit of mesurament is $N\ mm/mm^3$ The locally parameter so

definid let us to compare different points of different parts of the body. Its evaluation can be made in different modes, the simplest one is application of superposition of effects considering uniaxial model.

Two cases are considered:

- Normal deformations
- Shear deformations.

For first esemplification, let consider a body with concentred elastic parametres made by a mass and a linear spring, under a force. The energy accumulated by the sistem is the integral of the Force vs displacement curve.

$$U = \int_{l0}^{lf} P\, ds = \frac{1}{2}\, P\, \Delta \tag{33}$$

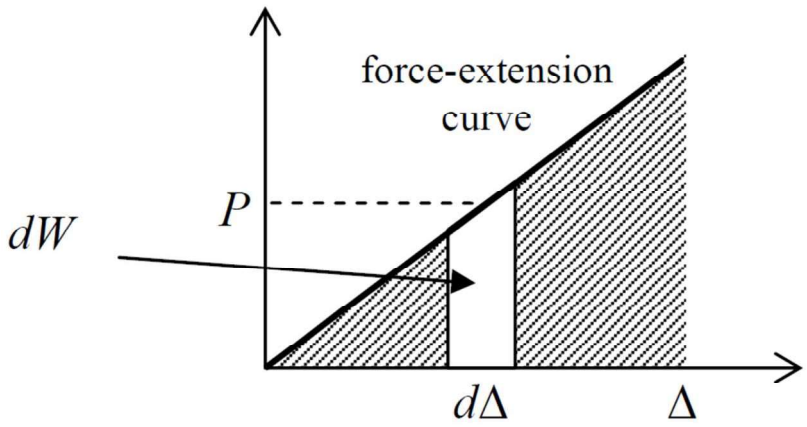

FIGURE 21: FORCE VS DISPLACMENT FOR A CONCETRED PARAMETRES SYSTEM

Now let cosider the continuum body:

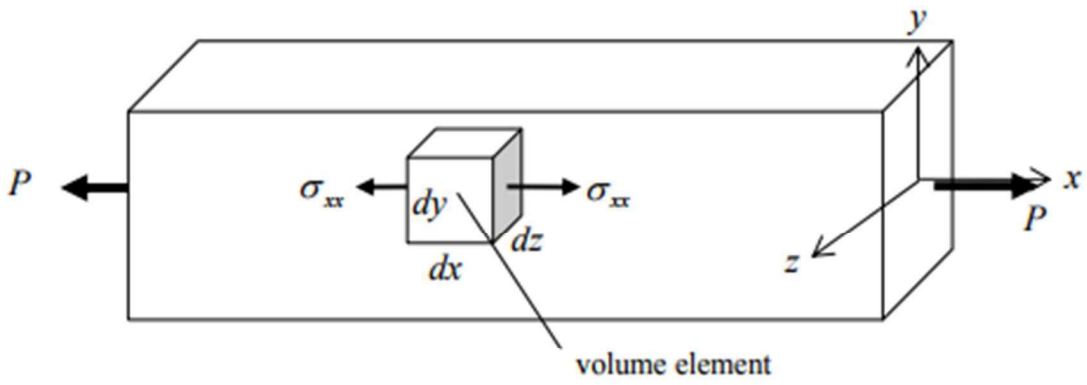

FIGURE 22: CONTINUUM ELASTIC UNIAXIAL BODY

The infinitesimal volume is $dV = dx\ dy\ dz$. If the force and the displacement is rebuilt by continuum mechanics can be obtained: $P = \sigma_{xx} dz\ dy$ and $ds = \varepsilon_{xx} dx$. The costitutive equation is applied, so that: $\varepsilon_{xx} dx = \frac{\sigma_{xx}}{E}$, and the energy in the infinitesimal volume can be evalueted $U = \frac{\sigma_{xx}^2}{2E}\ dxdy\ dz$. If the density of the energy is computed, the result (34) is obtained:

$$u = \frac{(\sigma_{xx}^2)}{2E} \tag{34}$$

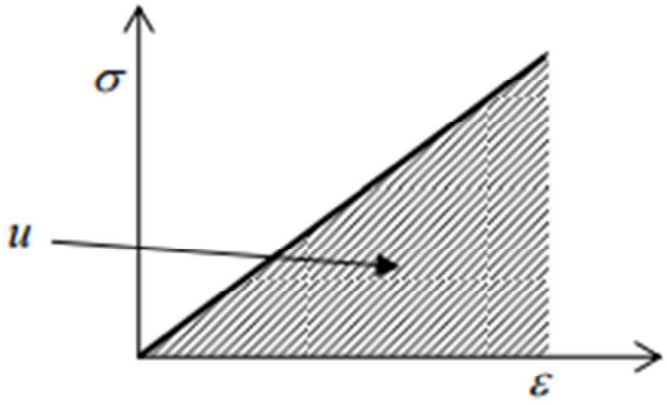

FIGURE 23: ELASTIC ENERGY IN CONTINUUM SYSTEM

Now the shear deformations can be considered:

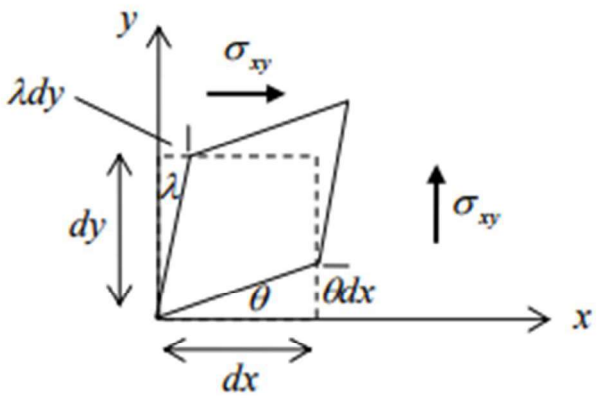

FIGURE 24: SHEAR DEFORMATION

The shear elastic deformations skew the geometry and it defines angles of deformation λ and θ ($\lambda = \frac{du}{dy}$ and $\theta = \frac{dv}{dx}$).

Force and the displacement can be newly built:

- $P_1 = \sigma_{yx} dz\, dx$ and displacement is $ds_1 = \lambda\, dy$;
- $P_2 = \sigma_{yx} dz\, dy$ and displacement is $ds_2 = \theta\, dx$

So that the total work avaraged on the volume is:

$$u = \sigma_{xy}\, \varepsilon_{xy} \tag{35}$$

Rotating all the possible direction and applying the superposition of effects, the final equations (36.1) and (36.2) can be achieved:

$$u = \frac{1}{2E}\left(\sigma_{xx}^2 + \sigma_{yy}^2 + \sigma_{zz}^2\right) - \frac{\nu}{E}\left(\sigma_{xx}\sigma_{yy} + \sigma_{xx}\sigma_{zz} + \sigma_{zz}\sigma_{yy}\right) + \frac{1}{2\mu}\left(\sigma_{xy}^2 + \sigma_{zy}^2 + \sigma_{xz}^2\right) \tag{36.1}$$

$$u = \frac{\mu\nu}{1-2\nu}\left(\varepsilon_{xx} + \varepsilon_{yy} + \varepsilon_{zz}\right)^2 + \mu\left(\varepsilon_{xx}^2 + \varepsilon_{yy}^2 + \varepsilon_{zz}^2\right) + 2\mu(\varepsilon_{xz}^2 + \varepsilon_{zy}^2 + \varepsilon_{xy}^2) \tag{36.2}$$

The equations (36.1) and (36.2) can be characterized for plane state of stress and strain.

1.4.1 Strain energy density for V-notched element

If SED wants to be evaluated for a V-notched component, Williams' stress-strain model and SED definition have to be used.

The geometry in figure 25 is used in order to model:

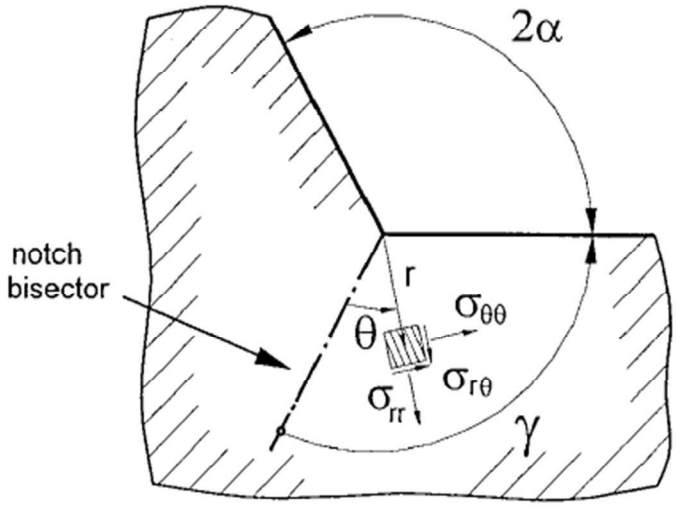

FIGURE 25: MODEL FOR SED OF V-NOTCHED COMPONENT

The stress components are reported in eq. 37, using cilyndrical system of referiment:

$$\begin{Bmatrix} \sigma_{\theta\theta} \\ \sigma_{rr} \\ \sigma_{r\theta} \end{Bmatrix} = r^{\lambda_1 - 1} K_1^N \begin{bmatrix} \sigma_{\theta\theta}^{(1)} & \sigma_{r\theta}^{(1)} & 0 \\ \sigma_{r\theta}^{(1)} & \sigma_{rr}^{(1)} & 0 \\ 0 & 0 & \sigma_{zz}^{(1)} \end{bmatrix} + r^{\lambda_2 - 1} K_2^N \begin{bmatrix} \sigma_{\theta\theta}^{(2)} & \sigma_{r\theta}^{(2)} & 0 \\ \sigma_{r\theta}^{(2)} & \sigma_{rr}^{(2)} & 0 \\ 0 & 0 & \sigma_{zz}^{(2)} \end{bmatrix} \qquad (37)$$

The equation (37) is for both I mode and II mode. Treating with a plane case, zθ and rz stress components are zero and SED equation is:

$$u(r,\theta) = \frac{1}{2E}\{(\sigma_{xx}^2 + \sigma_{yy}^2 + \sigma_{zz}^2) - 2\nu\,(\sigma_{xx}\sigma_{yy} + \sigma_{xx}\sigma_{zz} + \sigma_{yy}\sigma_{zz}) + 2(1+\nu)\sigma_{xy}^2\} \tag{38}$$

Using stress equations in SED definition:

$$u(r,\theta) = u_1(r,\theta) + u_2(r,\theta) + u_{12}(r,\theta) \tag{39}$$

The SED can be seen like combination of three factors, one describing mode I, one describing mode II and the third combining mode I and II. Now a finite volume is considered, that is an Area of R radius in plane case defined by +-ϒ corners. In this region Energy density can be computed for integration. Total elastic energy is:

$$E(R) = \int_A u\,dA = \int_0^R \int_{-\Upsilon}^{+\Upsilon} [u_1(r,\theta) + u_2(r,\theta) + u_{12}(r,\theta)]\,r\,dr\,d\theta \tag{40}$$

The $u_{12}(r,\theta)$ contribution is neglected because of the symmetri of the problem:

$$E(R) = E1(R) + E2(R) = \frac{1}{E}\frac{I_1\,(\Upsilon)}{4\lambda_1}\,(K_1^N)^2\,R^{2\lambda_1} + \frac{1}{E}\frac{I_2\,(\Upsilon)}{4\lambda_2}\,(K_2^N)^2\,R^{2\lambda_2} \tag{41}$$

I_1 and I_2 are the values of the integral in $\pm\Upsilon$ range, keeping inside information about the geometry of the problem [3]. Computing value of area as:

$$A(R) = \int_0^R \int_{-\Upsilon}^{+\Upsilon} r\, dr\, d\theta = R^2\, \Upsilon \tag{42}$$

Avarage SED can be calculated:

$$\bar{E} = \frac{E(R)}{A(R)} = \frac{1}{E} e_1\ (K_1^N)^2 R^{2(\lambda_1 - 1)} + \frac{1}{E} e_2\ (K_2^N)^2 R^{2(\lambda_2 - 1)} \tag{43}$$

1.6 Strenght criteria using SED

The failure of the components is achieved when the value of average strain energy in the control area achieves the critical value characterizing the material. The critical value for which the component breaks is, for brittle material:

$$Wc = \frac{\sigma_R^2}{2E} \tag{44}$$

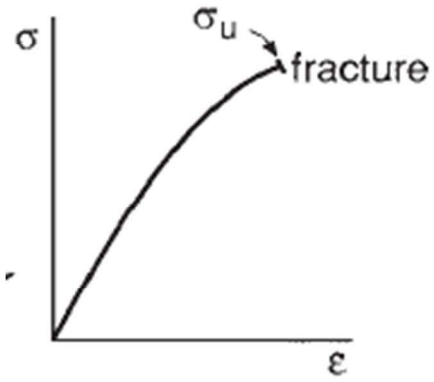

FIGURE 26: STRESS-STRAIN CURVE FOR BRITTLE MATERIAL

Wc can be related to NSIFs. For semplicity, Mode II can be assumed not singular and SED is related only to mode I.

$$K_1^N = \sqrt{\frac{4E\lambda_1 \Upsilon}{I_1(\Upsilon)} W}\ R^{(1-\lambda_1)} \tag{45}$$

The critical condizion for K is:

$$K_c^N = \sqrt{\frac{2\lambda_1 \Upsilon}{I_1(\Upsilon)}}\ \sigma_R\ R^{(1-\lambda_1)} \tag{46}$$

The value under square root is defined as a function $f(2\alpha) = \sqrt{\frac{2\lambda_1 \Upsilon}{I_1(\Upsilon)}}$, taking into account the geometry of the notch. When the component is broken, can be assumed that NSIF is related to fracture thougness:

$$K_c^N = K_{Ic} = f(0°)\ \sigma_R\ R^{0.5} \rightarrow\ \ R = \left(\frac{K_{Ic}}{f(0°)\ \sigma_R}\right)^2 \tag{47}$$

A semplification is made (considering a 0° angle) because of the experimental consideration for evaluation of fracture toughness is made with a crack. So, a quantification of critical radius can be achieved:

$$K_{Ic} = f(2\alpha)\ \sigma_R \left(\frac{K_{Ic}}{f(0°)\ \sigma_R}\right)^{0.5} \tag{48}$$

The main advantage in using SED and not NSIFs is related to his unit of mesurement. In fact the unit of mesurement of NSIF is related to open angle of the notch:

[MPa mm^$(1-\lambda)$]. At the contrary, SED as a unit of measurement insesible to opening angles, and it is [N mm/mm^3].

1.7 SED method in fatigue design for weldments

The fatigue life assessment using SED method goes to evaluate the values of Strain Energy Density in a control volume whose radius depends from material:

- Rc=0.12 mm for aluminium;
- Rc=0.28 mm for steel.

Fatigue method based on SED deals with calculation of SED in different interesting points. Then a comparation of those values with the fatigue curve of the material has made, INDIPENDENTLY from the geometric shapes of the welded joints. Only the paramenter is used, and nothing else.

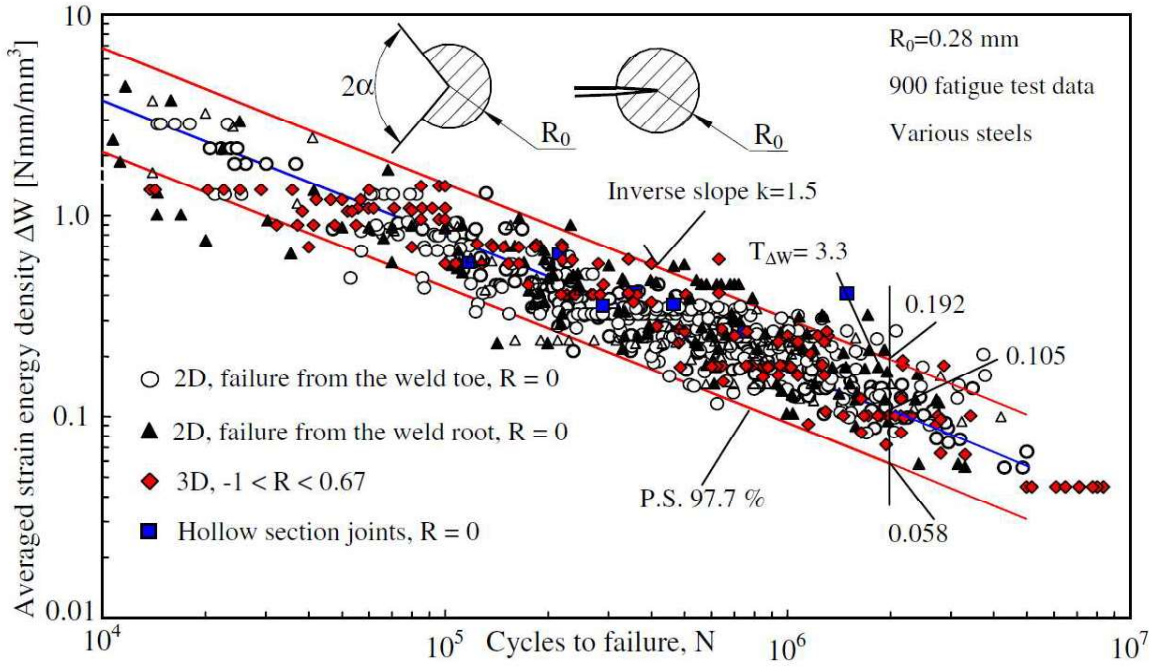

FIGURE 27: EXAMPLE OF MASTER CURVE FOR FATIGUE DESIGN OF WELDMENTS IN STEEL

This method, respect the Nominal stress or Hot Spot methods, offers advantage that only one curve has to be taken as reference, and a global parameter surrounding the notch is studied. Geometry lose importance. On the other hand, a more complex FEM model has to be built in order to evaluate the SED values.

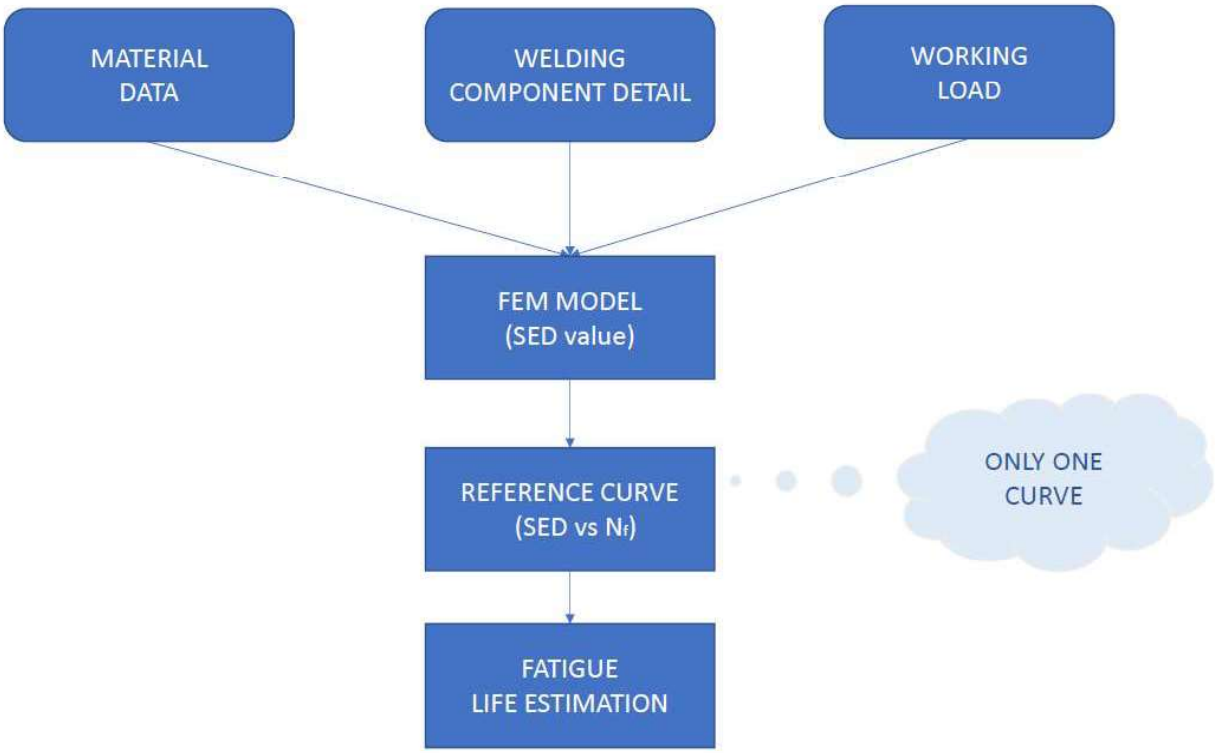

FIGURE 28: FLOW CHART FOR SED APPROACH DESIGN

1.8 Strain energy in FEM model

Finite elements method has been developed with the using of automatic calculation. The method is in general applied to problem described by differental equations, and hence applied to elastic problem. A finite element is a little and finite object defined by a precise number n of nodes. Every node has a number of degree of freedom m. So, generally, the

total degree of freedom of single node is nxm. Loads and displacement are definted using a local coordinate sistem of element. The vector describing the displacements of the system has nxm length. The displacements vector is related to force vector with stiffness matrix.

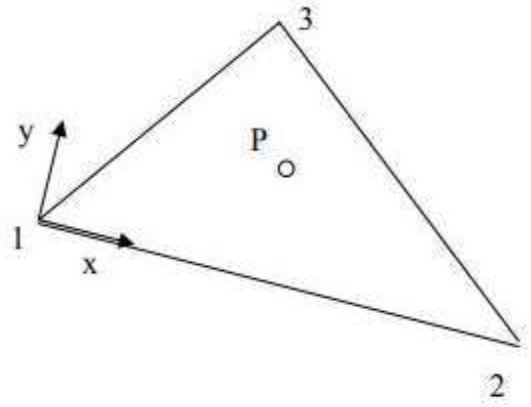

FIGURE 29: EXAMPLE OF FINITE ELEMENT

Nodal and load vectors are defined as follows:

$$\{x\} = \begin{Bmatrix} \{x\}_1 \\ \vdots \\ \{x\}_n \end{Bmatrix} = \begin{Bmatrix} x_1 \\ \vdots \\ x_{nxm} \end{Bmatrix} \rightarrow \{f\} = \begin{Bmatrix} \{f\}_1 \\ \vdots \\ \{f\}_n \end{Bmatrix} = \begin{Bmatrix} f_{11} \\ \vdots \\ f_{nxm} \end{Bmatrix} \tag{49}$$

$\{x\}_i$ is the displacement vector of node i, keeping inside all the dofs of node i.

Element's displacements are described using their node's displacement $\{x\}_i$, describing all the dof of the node i, and depending generally from local coordinates of the element:

$$\{x(P)\} = [N(P)]\{x\} \tag{50}$$

[N(P)] is Matrix of shape function. The functions are polynomial, whose degree depends from boundary conditions, so that thay can be respected. [N(P)] matrix is a nxm dimension matrix, containing nxm equations approximating the real nodal displacement. From displacements, deformation field can be evaluated for derivation:

$$\{\varepsilon(P)\} = \frac{\partial}{\partial P}[N(P)]\{x\} = [B(P)]\{x\} \tag{51}$$

From equation (51), using costitutive equation of material, stress components can be computed:

$$\{\sigma(P)\} = [D]\{\varepsilon(P)\} = [D][B(P)]\{x\} \tag{52}$$

Using finally virtual work principle, elastic problem can be closed:

$$L_e = \partial\{x\}^T\{f\} = L_i = \int_V \{\varepsilon\}^T\{\sigma\}\, dV = \partial\{x\}^T\left[\int_V [B]^T[D][B]\{x\}dV\right]\{x\} \tag{53}$$

From equation (53), stifness matrix can be obtained:

$$[K] = \int_V [B]^T[D][B]\{x\}dV \tag{54}$$

The problem described is related to singular element. A finite elements model is composed by a great number of elements, linked one each other.

A matrix of structur is so defined, keeping in count the constraints coming from the joint of the different elements.

For the elastic-static problem, the parameters early introduced are enough for the solution of the problem. In order to know displacement field is sufficient to calculate the inverse matrix of stiffness matrix and moltiply the forces vector for the invers one. Let's defining with B letter the set of constrained nodes, and with L the set of free nodes. In order to sort the matrix in a usefull way, free nodes (L) from constrained nodes (B) can be divided:

$$\begin{Bmatrix}\{f\}_L\\ \{f\}_B\end{Bmatrix} = \begin{bmatrix}[K]_{LL} & [K]_{LB}\\ [K]_{LB} & [K]_{bB}\end{bmatrix}\begin{Bmatrix}\{x\}_L\\ \{x\}_B\end{Bmatrix} \tag{55}$$

From equation of free nodes displacement can be computed, and substituing them in constrained nodes equation, raction froces can be solved. SED value can be evaluated as indicated in equation (56):

$$u = \frac{1}{2}\{\varepsilon\}^T\{\sigma\} = \frac{1}{2}\{x\}^T[B]^T[D][B]\{x\} \tag{56}$$

The energy stored in the finite volume of control is:

$$E = \int_V u\, dV = \frac{1}{2}\{x\}^T \int_V [B]^T[D][B]\, dV\ \{x\} = \frac{1}{2}\{x\}^T[K]\{x\} \tag{57}$$

From equation (57) can be seen that the elastic energy stored depends only from nodal displacements, and not from its derivation like stress. The complexity of displacement function is the one to defining the exact value of SED, and it is less sensible to the refinement of mesh.

Chapter 2

Experimental methods

Experimental analysis has been made in NTNU's fatigue laboratory "Paolo Lazzarin". Different samples of aluminium butt welded joints are been built and tested. All the samples arise from two big welded plate. The plate, after weldeing process, has been cut in order to produce singular welded butt samples.

2.1 Materials

Pure aluminium is not used in any case. In general, pure aluminium proprieties are not so good and some alloyng materials are used, like Magnesium, Silicium, Copper, Zinc and Manganese. The alloyng materials can been used singularly. Sometimes more then two materials can be used togheter, and they improve strength characteristics as:

- Silicium: improve the castablility and reduce the thermal expansion coefficients;
- Magnesium: increase corrosion strength;
- Manganese: increase mechanical and corrosion strength;
- Copper; increase mechanical strength in warm enviroments;
- Zinc: Manly used with magnesium, further increse mechanical proprieties.

Different nomeclatures to define the different alloyes are used. One of the most diffused is ASTM, American Society for Materials. Every alloy is defined using a code of 4 numebrs plus one letter (H or T) and a further number, for examples 7020-T6. The first number

rapresent the main alloyng material, the second one defines if a second alloyng is used with a reduced percentage respect the first one.

TABLE 2: ALLOYNG MATERIAL NOMENCLATURE

Number	Alloyng Element
1	none
2	Copper
3	Manganese
4	Silicium
5	Magnesium
6	Magnesium+Silicium
7	Zinc
8	Others

The third and fourth number characterize the sub-class of the same alloyes using the same alloyngs. The letters declair the type of heat treating used:

TABLE 3: MECHANICAL AND HEAT TREATING

Letter	Treating
F	Manufacturing raw
O	Annealed
H	Strain Hardened
W	Solubilized
T	Heat Treating

In our case of study an 6082-T6 aluminium is been used.

The material's proprieties used are: Young's module and Poisson's ratio.

TABLE 4: MATERIAL PROPRIETIES

Material proprieties	Value
Young's module [MPa]	70000
Poisson's ratio [--]	0.3

2.2 Welding Process, geometry and experimental method

The welding process used in order to create the samples is Metal Inert Gas (MIG) welding.

Gas metal arc welding (GMAW), sometimes referred to by its subtypes metal inert gas (MIG) welding or metal active gas (MAG) welding, is a welding process in which an electric arc forms between a consumable wire electrode and the workpiece metal(s), which heats the workpiece metal(s), causing them to melt and join. The samples arise from two plates with the same thickness (5 an 20 mm) welded togheter and following cut generating samples 30 mm wide.

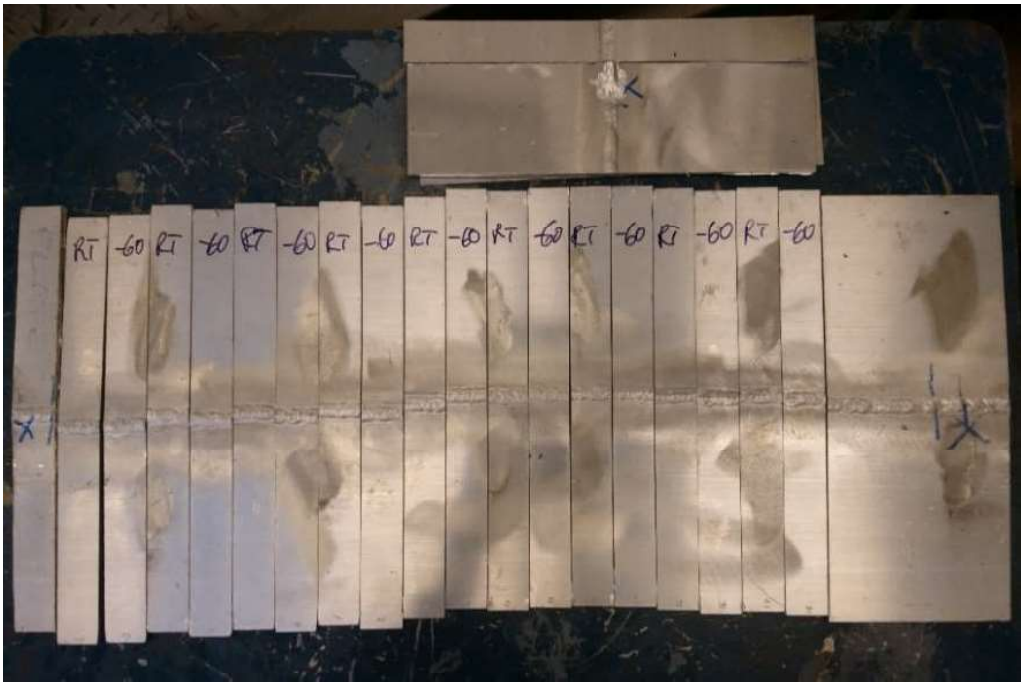

FIGURE 30: SAMPLES CAME FROM BUTT WELDED PLATES

Each sample contains geometric imperfection coming from welding process, as misalignent and eccentricy, measure in order to derive the correction factors for the FEM analysis.

FIGURE 31: WELDED JOINT 20 MM THICK

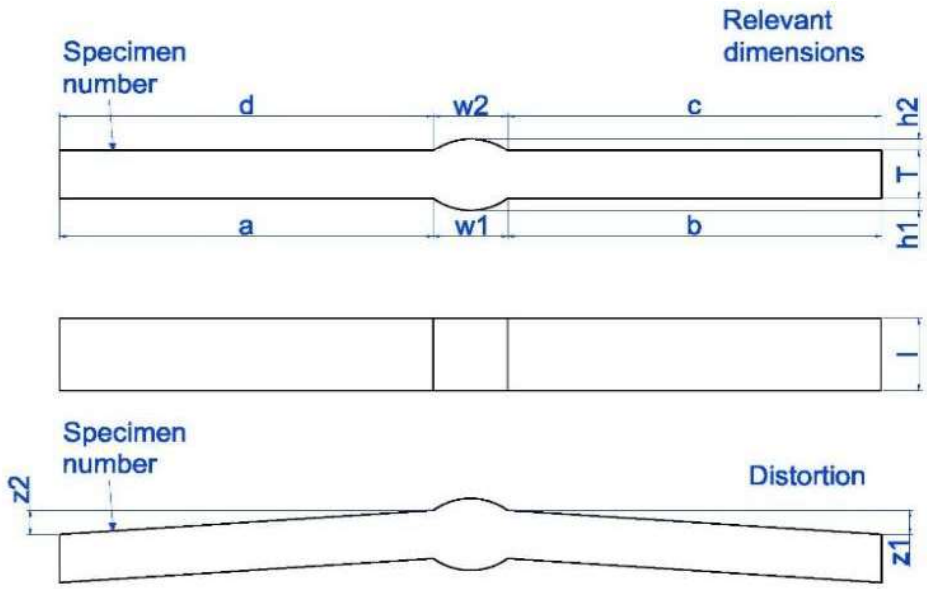

FIGURE 32: GEOMETRIC RAPPRESENTAZION OF WELDED JOINTS' SAMPLE AND MISALIGNMENET

The synthesis of the main dimensions of the welded joints are rapresented in the table number 4 and 5:

TABLE 5: DIMENSION OF 5 MM THICKNESS SAMPLES

Sample N°	A	B	C	D	Z1	Z2	W1	W2	H1	H2
1	144,33	143,81	143,43	144,88	4,12	3,8	11,01	11,54	1,25	0,96
2	144,17	144,03	143,57	145	2,93	2,81	9,92	9,93	1,15	1
3	144,58	142,67	143,04	145,47	2,67	2,29	11,17	10,42	1,28	0,85
4	30,1	144,04	144,41	144,4	143,56	4,98	4,61	9,74	1,1	0,58
5	143,75	144,43	144,11	143,84	5,02	4,61	10,26	10,34	0,93	0,94
6	144,18	144,19	143,52	144,36	2,43	2,56	9,78	10,48	1,21	0,87
7	144,05	144,04	143,27	143,93	3,98	4,07	10,1	11,79	1,33	0,44
8	143,44	144,15	144,15	143,37	5,76	5,81	9,98	11,04	1,52	0,85
9	144,07	144,32	143,39	143,95	4,45	4,39	10,13	11,66	0,96	0,85

*** T=5 mm thickness**

TABLE 6: DIMENSIONS OF 20 MM THICKNESS SAMPLES

Sample N°	A	B	C	D	Z1	Z2	W1	W2	H1	H2
1	164.86	164.16	167.17	164.16	1.18	0.78	28.69	25.92	2,83	2
2	164.82	163,5	163,11	167,11	0,88	1,05	29,42	26,55	3,61	2,31
3	164,83	163,79	168,39	162,02	1,39	0,79	28,39	27,07	3,02	2,48
4	164.08	164,79	169,18	162,21	1,59	1,17	28,22	26,11	3,37	1,87
5	164,88	165,26	169,35	162,17	1,62	1,32	26,53	26,59	2,79	2,78
6	164,26	165,29	162,4	170,11	2,07	1,73	27,31	25,76	2,38	3,25
7	163,82	165,48	169,21	163,14	1,9	1,5	25,23	28,4	2,03	3,01
8	164,06	165,09	169,34	163,09	1,71	1,26	27,77	24,4	2,83	2,51
9	164,81	163,53	168,26	163,24	1,72	1,23	28,43	26,11	2,36	3,8

***T=20 mm thickness**

Each specimen is been loaded in idraulic machine for fatigue tests setting load amplitude, mean load value and the frequency of the load, taking as output data the number of failure cycles. The frequency has been set at 10 Hz with a sinusoidal form.

Chapter 3

Numerical models

The FEM models have been created using Ansys APDL. Because of the simmetry of the problem, a quarter of welded joint has been modelled as 2D model, applying symmetric conditions. Through numerical model, the values of the SED have been extracted from control volume, and the corrected with correction factor.

A first analysis has seen the following considerations:

- Analysis of sensitivity changing the refinement of the mesh;
- Stress state has been rebuilt around the V-notch using SED coming from coarse and

  refine mesh, and a comparation with stress coming from Ansys for a very refine mesh.

The last step has been to make a fatigue life assessment using SED master curves for aluminium and using nominal approach. Moreover, joining SED values arising from FEM models and number of cycles of failure coming from experimental data, characteristic curves of samples have been built end compared with master curve of nominal stress and SED. In each case, a singular model has been solved, for a unit pressure in traction, and the superposition of the effects has been applied. Furthermore, a 3D model has been built in order to compare the difference of SED values between 2D model and 3D model.

3.1 Plane model

A first plane model has been built in order to evaluate Strain Energy Density in the control volume

3.1.1 Geometry of the model

FEM model has been created in Ansys APDL. Because of all the main parametres of samples have a dispersion in misalignement (mainly for 5 mm of thickness), a reference aligned geometry has been used, arising from the average dimensions of all joints. For both the geometries, FEM analysis have been made, but for syntesis, only the analysis for 5 mm joints is described. The first model is a quarter of joint, representing the trasversal section (middle plane) of the butt joint.

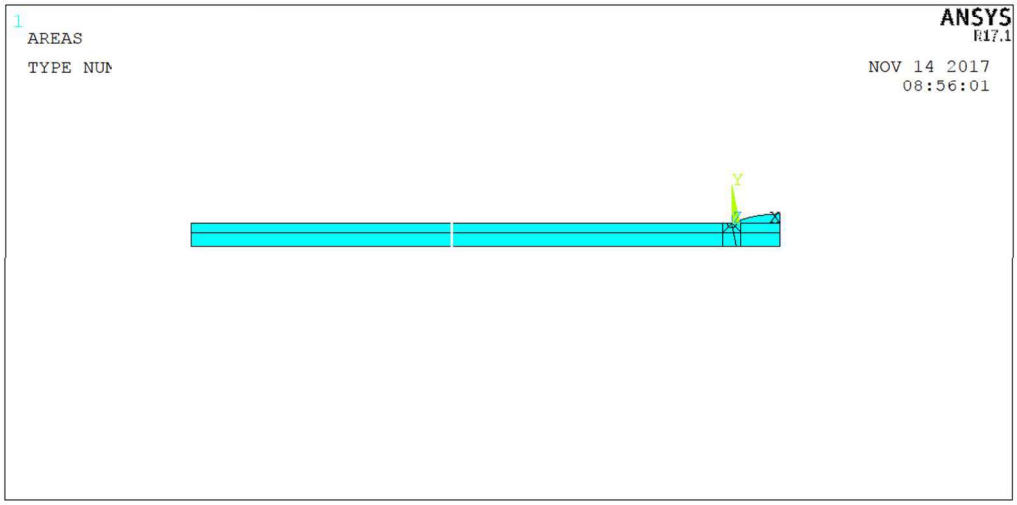

FIGURE 33: FEM MODEL OF QUARTER BUTT JOINT

The model has been made with plane elements and areas are been used in order to build the geometry. Another semplification is been made drawing the arc of the weldments

like a perfect arc of circonference. The criteria used to build the FEM model is the bottom-up, creating keypoints, lines and area. Another esemplification for the component has been the application of symmetrical conditions.

At the start of modelling process, V-notch has been generated, considering so a zero radius. Following, the critical volume has been generated, whose radius is 0.12 mm. A bigger circunferential arc has been drawn in order to adapt the mesh. The bisector of the welding arc has been made in order to extract the stress components following Williams' model and evaluate NSIFs.

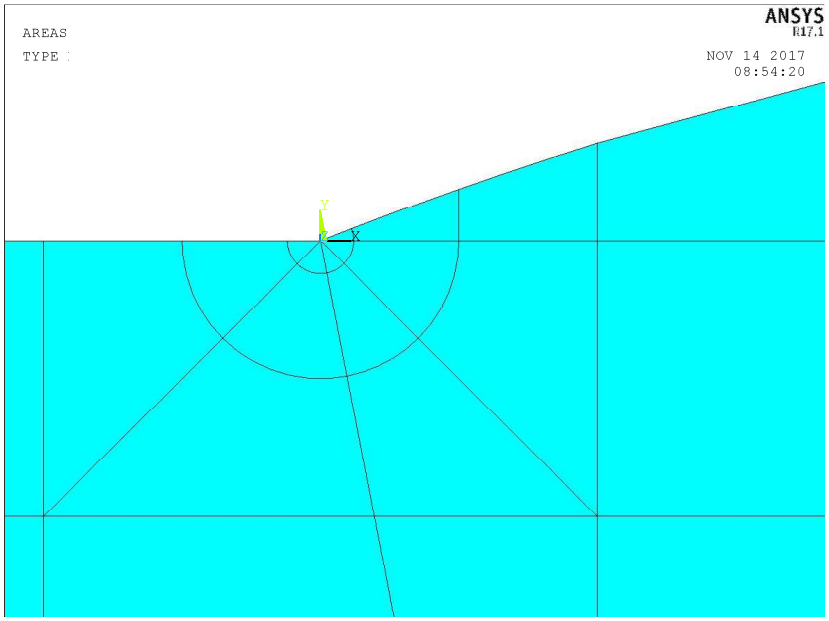

FIGURE 34: CRITICAL VOLUME MODEL

As last step, the completed geometry of the samples has been made. The real length of the welded joint has been calculated considering the penetration of the clamp, that is 50 mm.

3.1.2 Elements, material and proprieties

In order to mesh the model, PLANE 183 of Ansys has been choosen. This kind of element has a quadratic shape function, so that it can be adopted in not so regular meshing as well, taking in consideration that shape function is the only important parameter in FEM model for SED value evaluation.

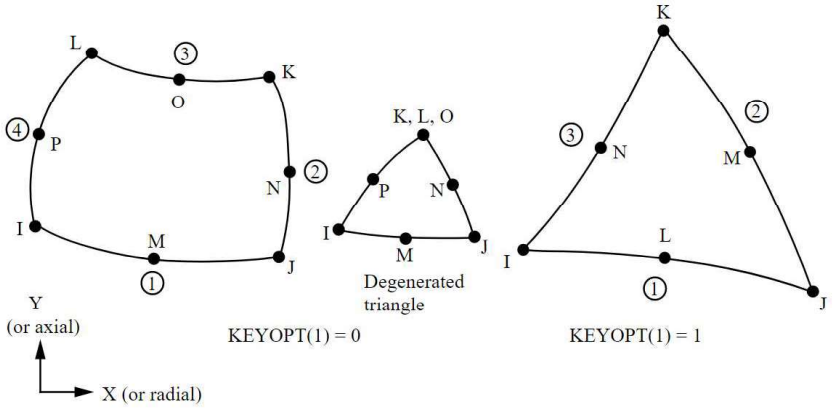

FIGURE 35: ELEMENT PLANE 183

Each element is characterized by 2 degrees of freedom for each node. They are the two traslation in x and y directions. Because of the thickness of the joints, plain strain condition is adopted in Ansys. The material proprieties set are the ones defined in table 4. Like output from our element, Stress components x,y,z and xy, in cylindrical coordinates, strain energy and volume are been extracted.

3.1.3 Constraint and load conditions:

The constrain conditions are been applied so that, along line of symmetry, conditions arising from bi-pendulum are applied. In order to apply loads, a pressure along a line has been used. The value of the pressure has been choosen as unit value, so that superposition of effects has been applied in order to built the real values of the stress and SED. The scale values used to creat the real condition of load is Rs so defined:

$$RS = \left(\frac{P_{input}}{P_{unitary}}\, f_{misalignment}\right) \rightarrow \begin{cases} Stress = Stress_{unitary} \cdot RS \\ SED = SED_{unitary} \cdot RS^2 \end{cases} \quad (58)$$

3.1.4 Validation of FEM model

In order to verify the FEM model, some considerations are been made:

1- For a first qualitative evaluation of notch effects, X stress has been evaluated along the model. This component has to be near the nominal value because of the first component in traction is the bisgst one. Some bounder effect coming from notch has to there be so that the stress is bigger close to notched edge, as can be seen in figure 36.

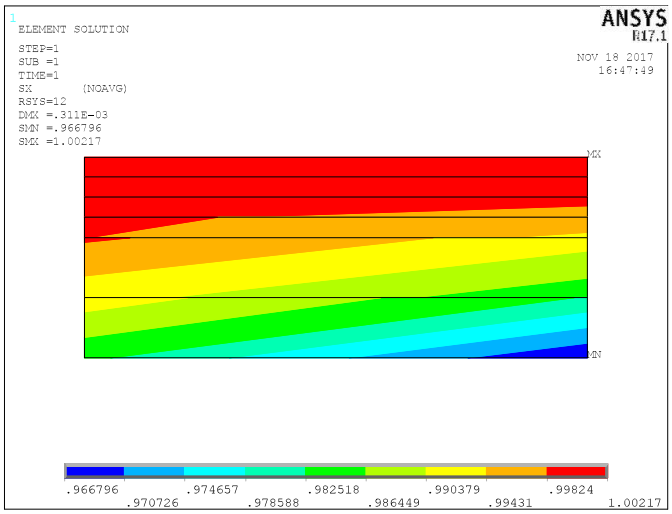

FIGURE 36: X COMPONENT OF STRESS

2- Stress around the notch are been calculated, setting a cilyndrical coordinates system whose origin is at V-notch. In this case, x component of stress is the radial one and y component of stress is the tangential one. Keeping in consideration Williams' model, y component of strees has to be maximum along bisector of the notch, and it has to decrease for all the corners from the bisector direction (Figure 37).

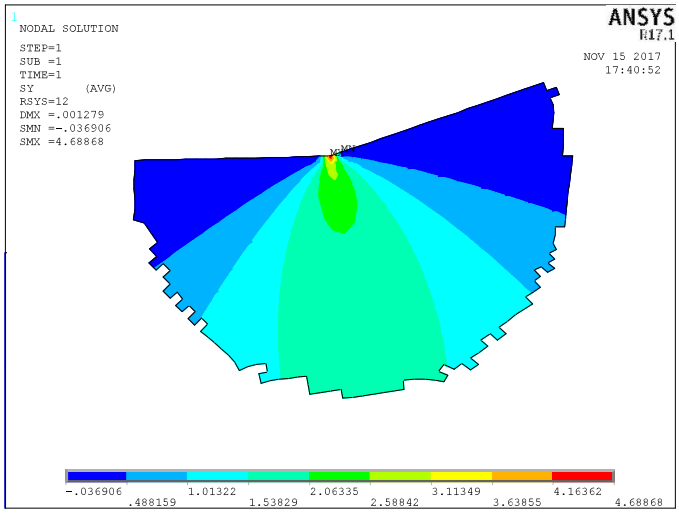

FIGURE 37: TANGENZIAL STRESS COMPONENT DISTRIBUTION

3.1.5 Sensitivity analysis for different elements in the critical volume

One of the main advantages in the study of fatigue behaviour for notched components through SED parameter (welded components in this case), is the insensitivity of the SED respect the number of elements in the critical volume. For the analysis made, the parameters used to generate the mapped mesh are listed below and can be seen in the figure 38:

- Divdiag: Number of divisions of the diagonal;
- Divragcrit: Number of divisions of critical radius;
- Divragest: Number of divisions of radius among the two circumferences, the external one and the critical one;
- Arcdiv: Number of divisions of arcus of circumference, both external and criticalo ne;
- Divsegvertc: Number of divisions of vertical line being out of the nominal thickness of the plate;

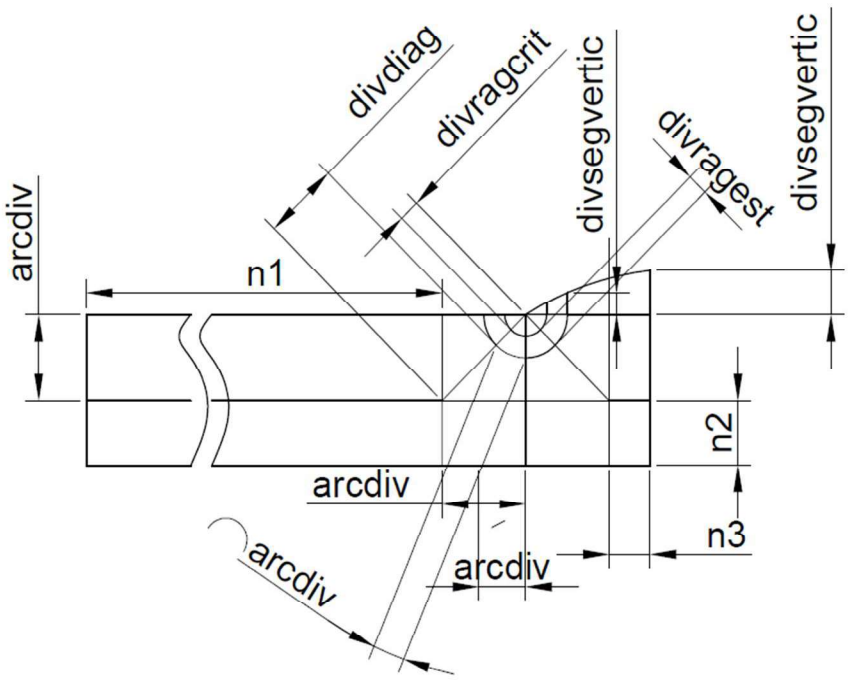

FIGURE 38: PARAMETERS USED FOR MAPPED MESH

The number of elements used in the different meshes go from 10 (mesh 1), until 64000 ca. in the mesh number 5. The mesh number 6 has a number of elements contained among mesh number 4 and mesh number 5 because of is been made in a later stage. For what concerns the values of the parametres used, in table 7 can be found a synthesis:

TABLE 7: VALUES OF PARAMETRES USED

	MESH1	MESH2	MESH3	MESH4	MESH6	MESH5
DivRagCrit	2	4	6	48	96	192
Arcdiv	1	2	4	32	64	128
Divragest	1	2	4	32	64	128
Divdiago	3	3	3	3	3	3
Divsegmvert	1	2	3	4	5	5
N1, N2, N3	1	1	1	1	1	1
Num. Elements	10	31	74	3814	15598	63956

In figure 39, the different pictures of the meshes made can be seen:

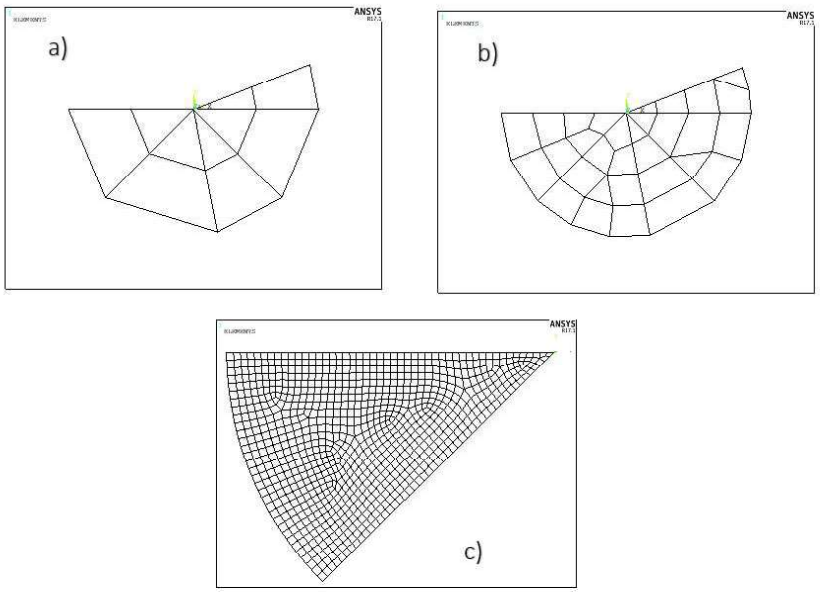

FIGURE 39: DIFFERENT GRADES OF MESH, A) MESH1, B) MESH2, C) MESH 6

For each kind of mesh, the same analysis has been made, setting a unit input in pressure, evaluating the Strain Energy Density in the control volume and evaluating the stress along the bisector direction. The stresses are evaluated in cilyndrical coordinates in order to compare with Williams' model. From Williams' model, the Notch stress intensity factors are so formulated:

$$K_I = \sqrt{2\pi} \lim_{r\to 0} \sigma_{\theta\theta}\ r^{1-\lambda 1} \tag{59}$$

$$K_{II} = \sqrt{2\pi} \lim_{r\to 0} \sigma_{r\theta}\ r^{1-\lambda 2} \tag{60}$$

One first consideration is about K_{II}, that is, for the opening of the angle, not singular, and so neglected. Infact its value is different order of magnitude littler than K_I. Morover, the definitions in equations 60 and 61 can be considered of interest for mesh number 4,5 and 6, because of the number of points in the other meshes are too coarse. Post-processing results in Matlab, can be underlined that:

1) The values of SED in the control volume is very insensible if the number of elements is changing in the volume; the maximum error is 1.2%, considering the mesh 1 and mesh 5 like reference (Figure 40).

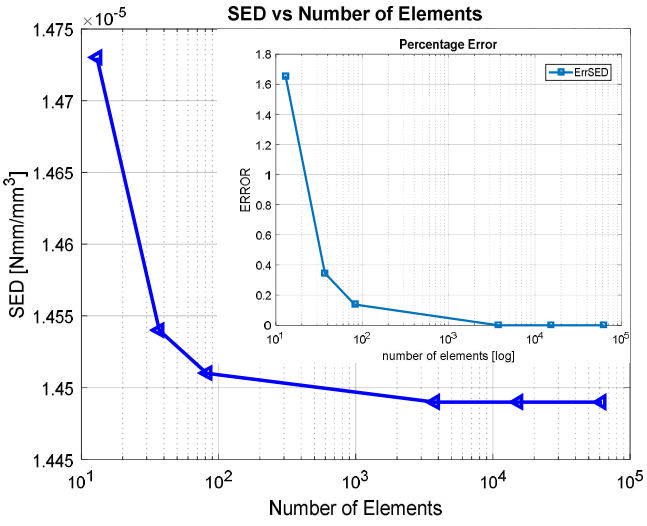

FIGURE 40: SED VALUES RESPECT DIFFERENT NUMBER OF ELEMENTS

TABLE 8: VALUES OF SED FOR DIFFERENT MESH

Num.Elem	10	31	74	3814	15598	63956
SED [MPa]	1.472E-5	1.452E-5	1.45E-5	1.449E-5	1.449E-5	1.449E-5

2) Can be seen that stress state depends from the refinement of the mesh. Infact, along the V-notch, tangential stress component grows up very fast increasing the number of elements, as can be seen in figure 42.

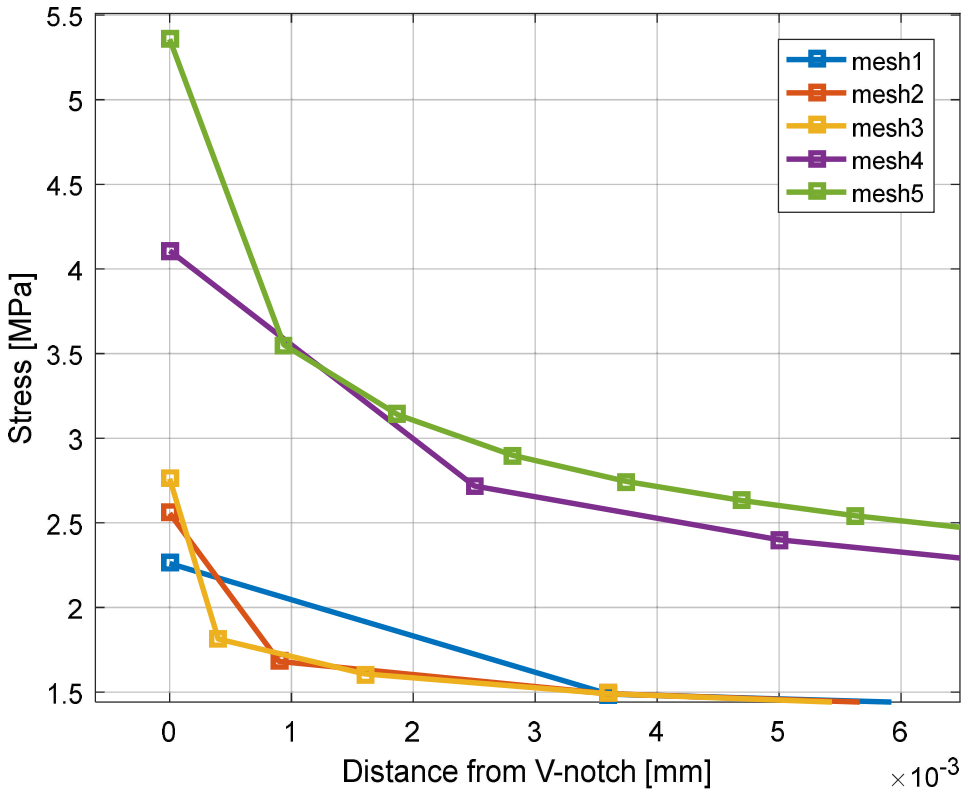

FIGURE 42: TANGENTIAL STRESS FOR DIFFERENT VALUES OF SED

Angular coefficient of normal tangential stress in bi-logaritmic system has been calculated for the different kind of mesh. These values have to be close to the eigenvalues of Williams' model, for the same opening angle. From Figure 43 and table 9 some values can

be red. For the opening angle of the samples, whose value is 158°, Williams' eigenvalues have been evalueted as linearization on the values available.

P. Lazzarin and R. Zambardi

Table 1. Values of the integrals I_1 and I_2.

2α (deg)	γ/π (rad)	λ_1	λ_2	Plane stress		Plane strain	
				$I_1(\gamma)$	$I_2(\gamma)$	$I_1(\gamma)$	$I_2(\gamma)$
0°	1	0.5000	0.5000	1.0250	2.3250	0.8450	2.1450
15°	23/24	0.5002	0.5453	1.0216	2.1608	0.8431	2.0087
30°	11/12	0.5014	0.5982	1.0108	2.0091	0.8366	1.8810
45°	7/8	0.5050	0.6597	0.9918	1.8688	0.8247	1.7610
60°	5/6	0.5122	0.7309	0.9642	1.7385	0.8066	1.6479
90°	3/4	0.5445	0.9085	0.8826	1.5018	0.7504	1.4379
120°	2/3	0.6157	1.1489	0.7701	1.2887	0.6687	1.2437
135°	5/8	0.6736	1.3021	0.7058	1.1883	0.6201	1.1505
150°	7/12	0.7520	1.4858	0.6386	1.0908	0.5678	1.0590
160°	5/9	0.8187	1.6305	0.5930	1.0269	0.5315	0.9986
170°	19/36	0.9000	1.7989	0.5481	0.9635	0.4957	0.9383

FIGURE 43: VALUES OF WILLIAMS' EIGVALES AND OTHER COSTANTS

TABLE 9: VALUES OF ANGULAR COEFFICIENT

mesh	1	2	3	4	5	6
1-lambda	-1.9405	-0.1853	-0.1802	-0.1829	-0.184	-0.1836
Err(%)	----	4.79	7.3954	6.02	5.45	5.7

For the most coarse mesh, the value is not calculated because of the few number of datas

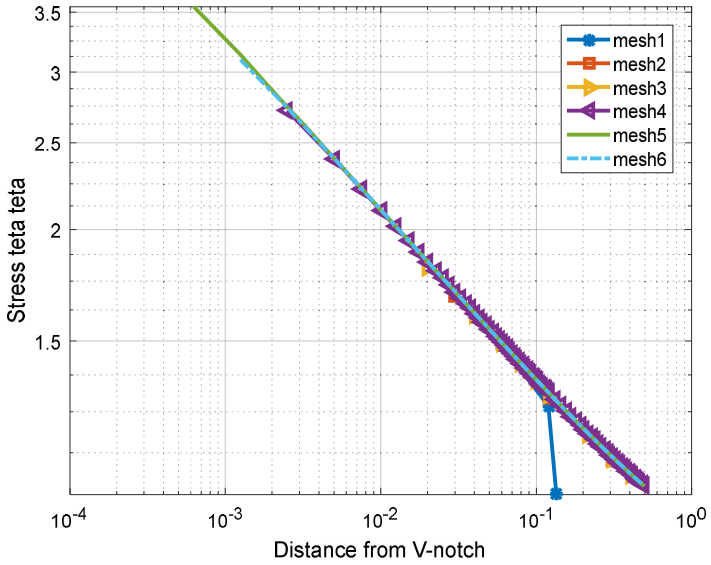

FIGURE 44: STRESS FOR DIFFERENT MESH IN BILOGARITMIC SYSTEM

3.1.6 Verification of relation between KI and SED

The verification has been made taking as reference the NSIF K_I evaluated through equation (60) of Williams' model, considering the finst mesh.

The equation used in order to evaluate NSIF relate to SED are written in table 10:

TABLE 10: RELATION AMONG NSIFS AND SED

NSIF (KI)	Relazione con SED
K1rif	$K1 = \sqrt{2\pi} \lim_{r\to 0} \sigma_{\theta\theta}\ r^{1-\lambda 1}$
KIA	$K1 = \sqrt{\frac{4E\lambda\Upsilon}{I1(\Upsilon)}} W R^{1-\lambda 1}$
KIB	$K1 = \sqrt{\frac{EW}{e1}} R^{1-\lambda 1}$

Where $e1$ is a function of opening angle:

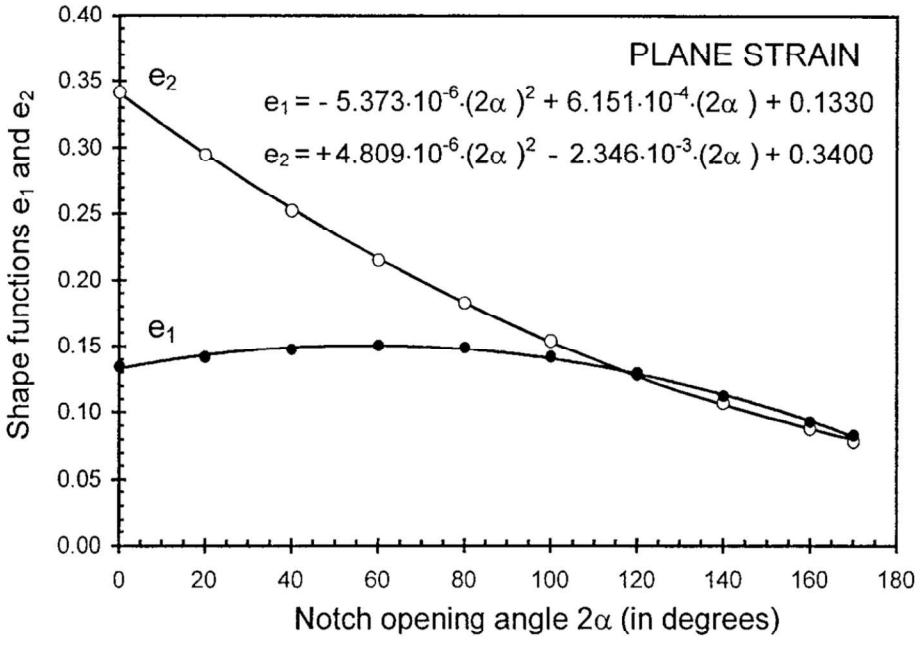

FIGURE 45: SHAPE FUNCTION FOR DIFFERENT OPENING ANGLES (°)

The value of K_I in Williams' model is 2.1796, evaluated through linearizazion of values in figure 43.

TABLE 11: VALUES OF KI RELATED TO SED

	Mesh1	Mesh2	Mesh3	Mesh4	Mesh5	Mesh6
SED [N mm/mm^3]	0.1472	0.1452	0.145	0.1449	0.1449	0.1449
KIA= $\sqrt{\frac{4E\lambda\Upsilon}{I1(\Upsilon)}}WR^{1-\lambda1}$	2.1809	2.1670	2.1650	2.1647	2.1647	2.1647
KIB= $\sqrt{\frac{EW}{e1}}R^{1-\lambda1}$	2.1672	2.1534	2.1513	2.1511	2.1511	2.1511

In each case, evaluating the K_I as linear function or with shape function of figure 45, the results are very close, with error under the 5%. So, with the different values of NSIF, stress field can be rebuilt using only the exact solution of Williams' model:

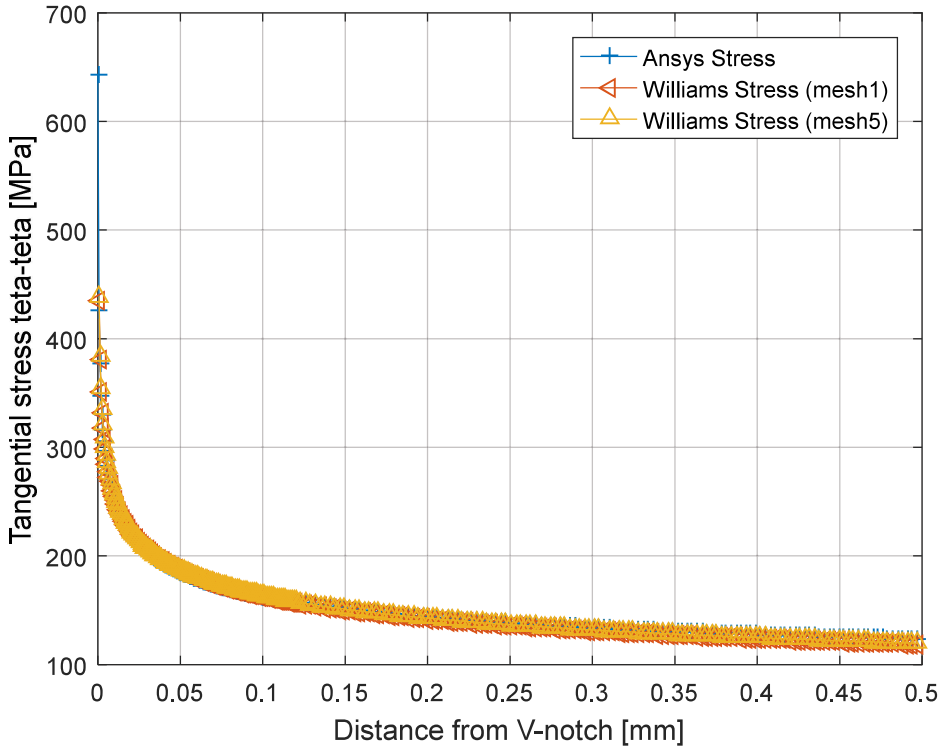

FIGURE 46: STRESS TETA TETA USING KI FROM SED

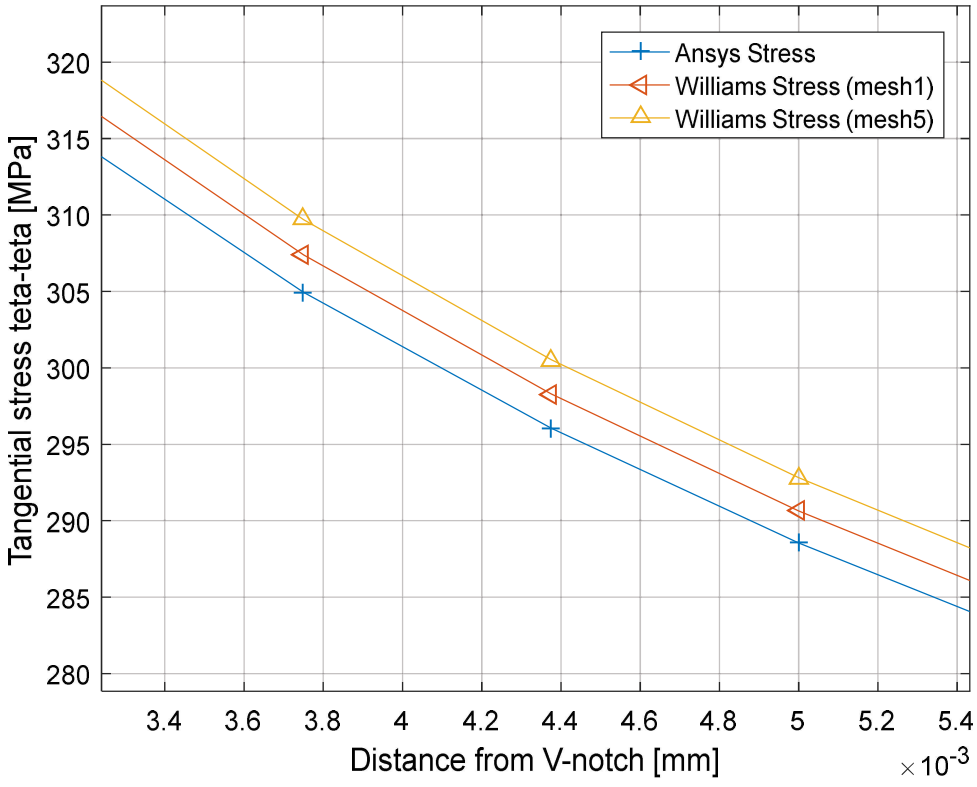

FIGURE 47: ZOOM OF STRESS TETA TETA

3.1.7 Analysis for real loads

In order to deal with fatigue life assessment for welded butt joints, two groups of samples have been made. The first one with 5 mm of thickness, composed from 17 samples. The second group has been composed from 18 samples of 20 mm of thickness. All the experiments have been made with a load ratio R=0. The load plane executed is reported in the table 12 and 13:

TABLE 12: 5 MM THICKNESS SAMPLES

SAMPLE	1	2	3	4	5	6	7	8	9
NOMINAL Stress	120	100	100	120	80	80	60	60	35
LOAD [KN]	18	15	15	18	12	12	9	9	5

TABLE 13: 20 MM THICKNESS SAMPLES

Sample	1	2	3	4	5	6	7	8	9
Nominal Stress	125	100	80	80	100	125	60	60	40
Load [kN]	75	62.5	50	50	62.5	75	37.5	37.5	25

Each analysis ariese from the FEM model with unitary input, and then modified by with scale factor coming from stress and misalignment factor, remembering that SED in a quadratic form respect stress. The synthesis of SED, without correction factor, is summarized in table 14:

TABLE 14: VALUES OF SED FOR DIFFERENT THICNKESS AND LOAD CONDITIONS

Loads	SED [N mm/mm^3]	Loads	SED [N mm/mm^3]
Unit	1.4493E-05	Unit	2.3779e-05
60	0.0522	60	0.0522
80	0.09276	80	0.09276
100	0.14497	100	0.14497
120	0.2087	125	0.2087
*Plate thickness 5 mm		*plate thickness 20 mm	

In order to synthesize, some comments only for sample of 5 mm of thickness and load of 120 MPa are made. Stress state for non-corrected component has been build from the datas came from FEM model. They are plotted in the figure 48:

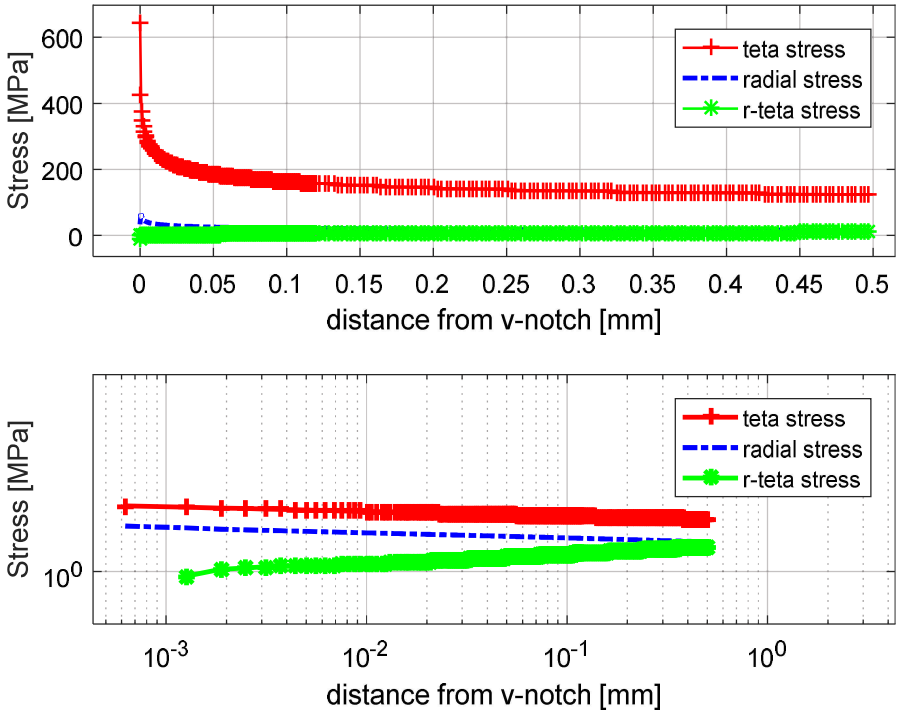

FIGURE 48: STRESS COMPONENT FOR SAMPLE OF 5 MM OF THICKNESS AND 120 MPA OF LOAD

The stress components are agree with Willliam's model. Moreover NSIFs, through Williams' definition are been calculated and plotted in figure 42:

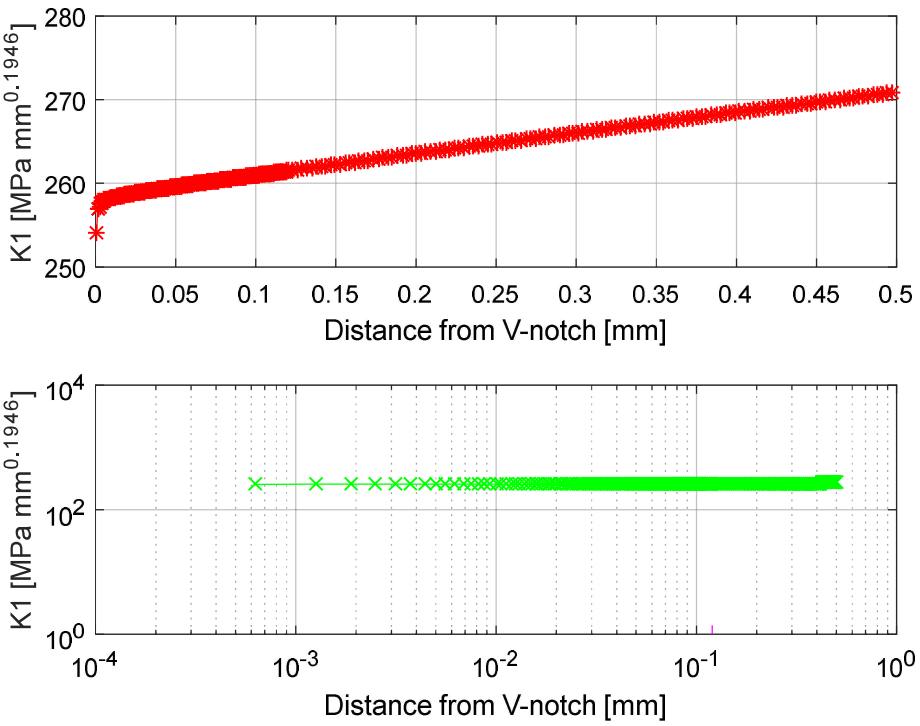

FIGURE 49: KI FOR BUTT WELDED JOINTS

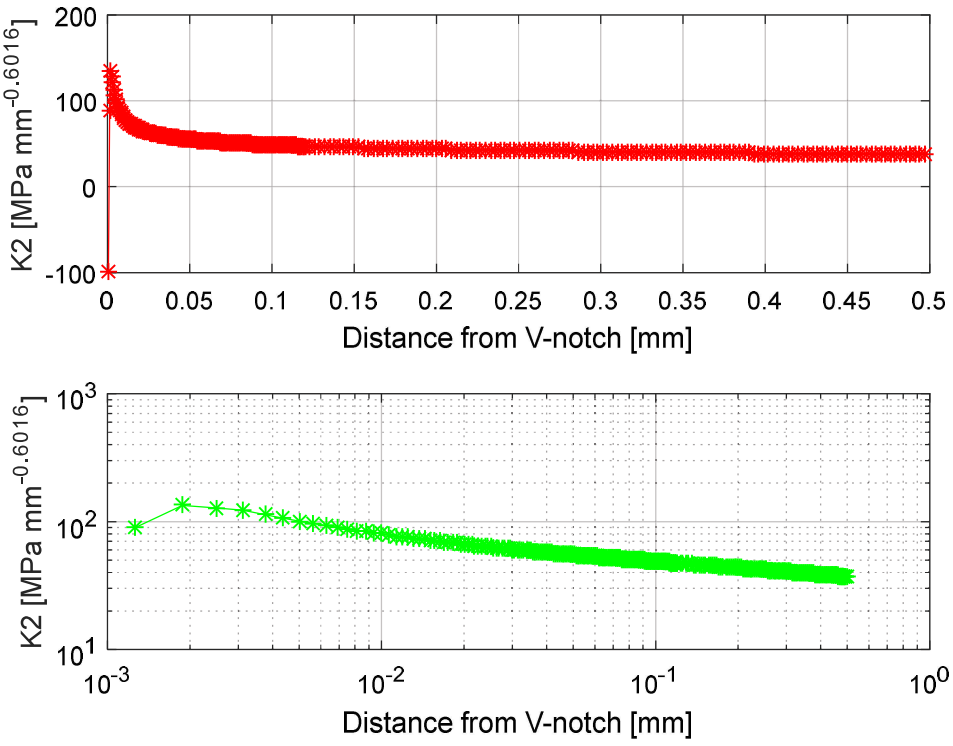

FIGURE 50: KII FOR BUTT WELDED JOINTS

3.1.8 life fatigue assessment

Life fatigue assessment has been made in order to assess fatigue life of samples. For each samples load plane followed is in the table 15 and 16:

TABLE 15: EXPERMENTAL PLANE FOR SAMPLES OF 5 MM OF THICKNESS

Sample N°	Nominal Δσ [MPa]	Nominal ΔF [kN]	N (Cycles of failure)	Correction factor	Corrected Δσ [MPa]
1	125	75	57157	1.1	137.5
5	125	75	65951	1.15	143.75
2	100	60	106330	1.1	110.0
6	100	60	160518	1.19	119.0
3	80	48	305548	1.11	88.8
4	80	48	375412	1.14	91.2
7	60	36	1112251	1.16	69.6
8	60	36	1137888	1.18	70.8
9	40	24	3800000 (R.O.)	1.15	46.0
***Load rate R=0, 20 mm of thickness**					

TABLE 16: EXPERMENTAL PLANE FOR SAMPLES OF 20 MM OF THICKNESS

Sample N°	Nominal Δσ [MPa]	Nominal ΔF [kN]	N (Cycles of failure)	Correction factor	Corrected Δσ [MPa]
1	125	75	57157	1.1	137.5
5	125	75	65951	1.15	143.75
2	100	60	106330	1.1	110.0
6	100	60	160518	1.19	119.0
3	80	48	305548	1.11	88.8
4	80	48	375412	1.14	91.2
7	60	36	1112251	1.16	69.6
8	60	36	1137888	1.18	70.8
9	40	24	3800000	1.15	46.0
***Load rate R=0, 20 mm of thickness**					

An inevitable problem, came from welding process, is the misalignment originating from residual stress. This problem creates a bending moment around the weldments and it increase the values of stress and so SED, how can be seen in figure 51:

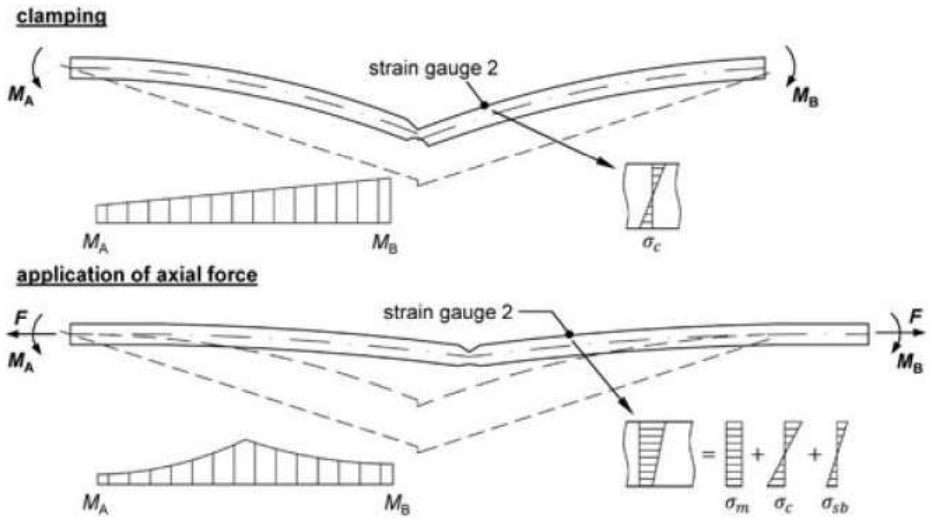

FIGURE 51: MISALIGNENT PROBLEM

The differen stress represented in figure 43 are:

1- σ_c, coming from boundary condition of the clamp that deform the samples;
2- σ_m, coming from axial component of the load around the samples, and generating a membranal stress;
3- σ_{sb}, coming from the bending moment generated from axial force having a not zero arm.

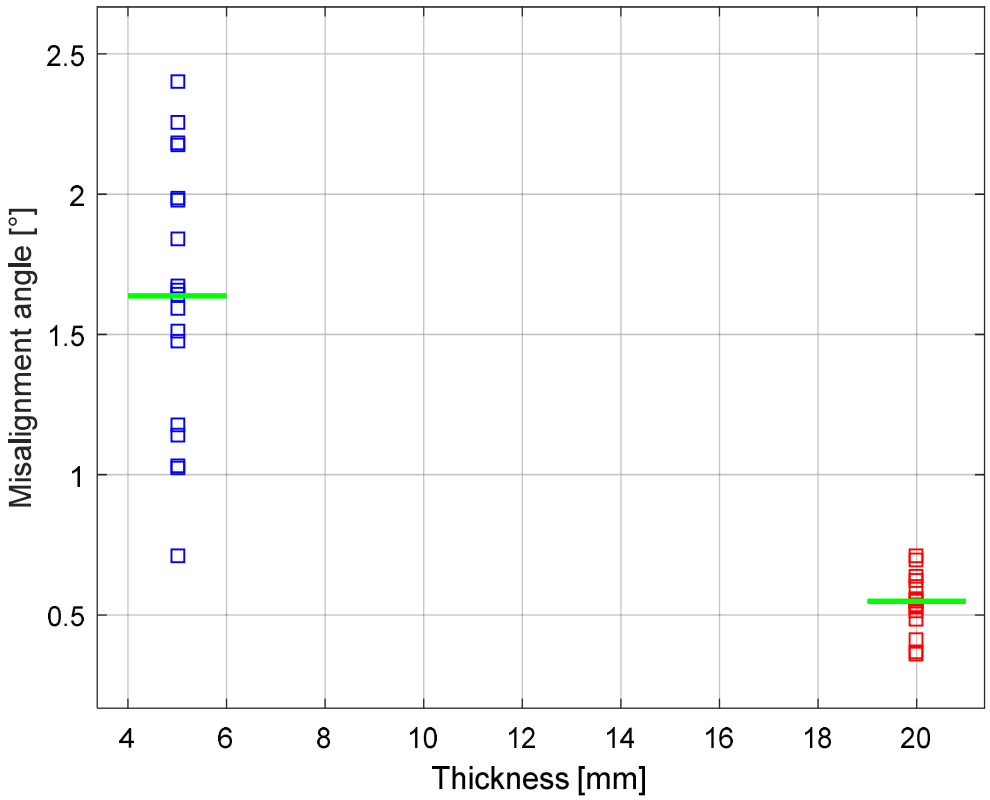

FIGURE 52: SPREAD OF ANGULAR MISALIGNEMENT

In order to correct the FEM result of not misalignent sample, two ways can be walked:

1- To create a FEM model of misalignmed sample, but in this case the original measuraments have to be very precise;
2- Correction factor can be taken fro different regulations

A first misalignemt model has been made, but the original measurament weren't so precise and so correction factors from regulations have to be taken in account:

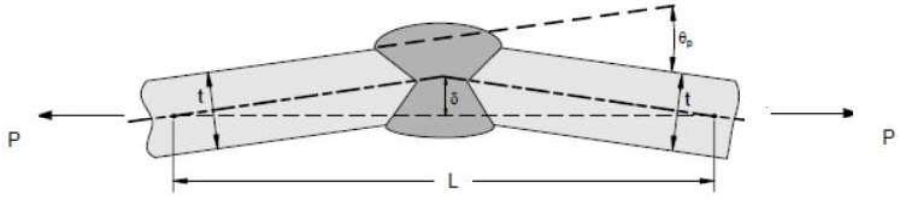

FIGURE 53: EXAMPLE OF MISALIGNEMENT

Type	Detail	Bending stress, σ_s
e) Angular misalignment between flat plates	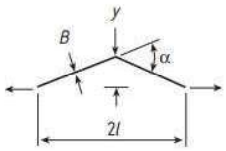 α in radians	Assuming boundary conditions equivalent to: — fixed ends: $\frac{\sigma_s}{P_m} = \frac{3y}{B}\left\{\frac{\tanh(\beta/2)}{\beta/2}\right\}$ $= \frac{3\alpha}{4}\frac{2l}{B}\left\{\frac{\tanh(\beta/2)}{\beta/2}\right\}$ — pinned ends: $\frac{\sigma_s}{P_m} = \frac{6y}{B}\left\{\frac{\tanh(\beta)}{\beta}\right\}$ $= \frac{3\alpha}{2}\frac{2l}{B}\left\{\frac{\tanh(\beta)}{\beta}\right\}$ where, in each case $\beta = \frac{2l}{B}\left(\frac{3\sigma_m}{E}\right)^{0.5}$

FIGURE 54:MISALIGNED CORRECTION FACTORS

FIGURE 55:EXAMPLE OF MISALIGNED SAMPLE

The misalignment correction factor came from [9]. The reference curves for fatigue life assessment are taken from [3] and reported in figure 55:

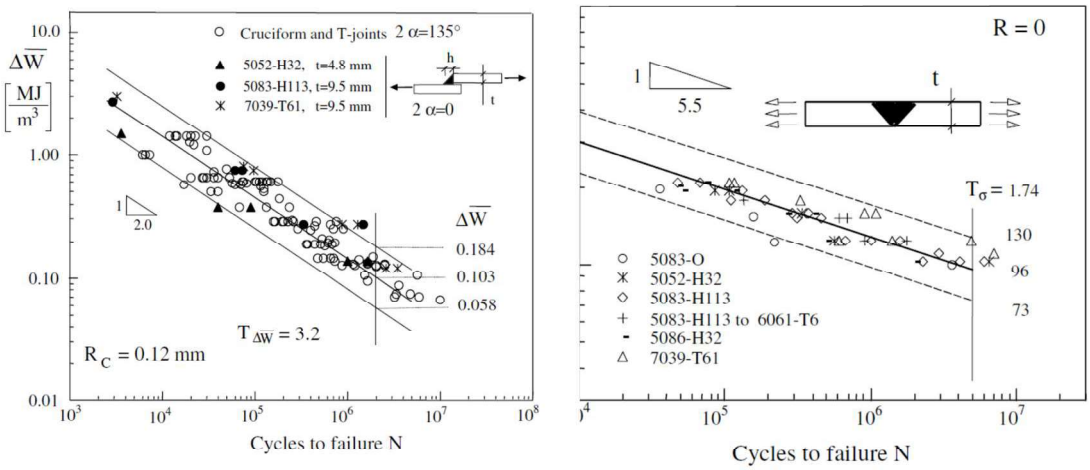

FIGURE 56: REFERENCE CURVES

The values of SED used for fatigue life assessments are reported in table 17 and 18:

TABLE 17: EXPERMENTAL DATA FOR SAMPLES OF 5 MM OF THICKNESS

Sample N°	SED [N mm/mm^3]	N (cycles of failure)
1	0.818	87980
2	0.9825	104228
3	0.4488	205920
4	0.3964	558585
5	0.4991	190297
6	0.268	573254
7	0.2479	613673
8	0.4119	429261
	*** 5 mm thick**	

TABLE 18: EXPERMENTAL DATA FOR SAMPLES OF 20 MM OF THICKNESS

Sample N°	SED [N mm/mm^3]	N (cycles of failure)
1	0.4496	57157
2	0.4914	65951
3	0.2877	106330
4	0.3367	160518
5	0.1875	305548
6	0.1978	375412
7	0.1152	1112251
8	0.1192	1137888
9	0.0503	3800000 (R.O.)
	***20 mm thick**	

Number of cycles are taken and joined to value of SED coming from FEM from experiments. From figure 56 can be seen how, without the use of correction factors, the fatigue assessment gives wrong results, mainly for samples of 5 mm of thickness characterized by a grat values of misalignment:

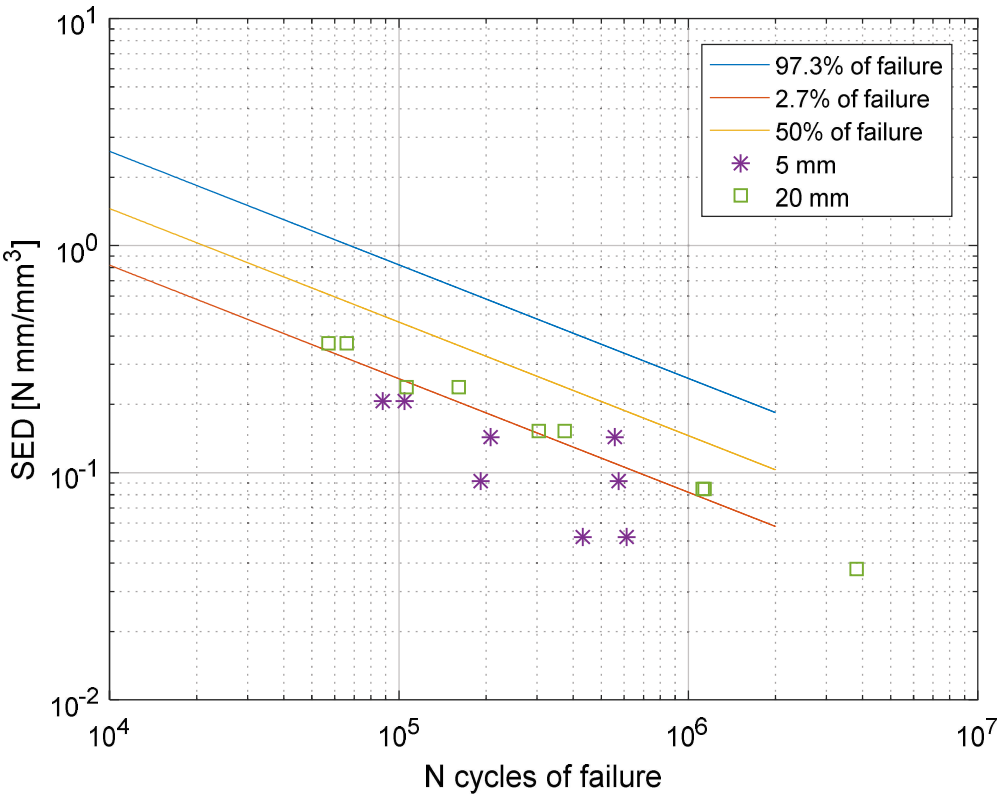

FIGURE 57: NOT CORRECTED VALUES OF SED

In this way the necessity of using correction factors are inevitable. Using correction factors, the corrected values of SED are reported in table 18, togheter to cycles of failure and forecasted number of failure:

TABLE 19: EXPERMENTAL RESULTS FOR SAMPLES OF 5 MM OF THICKNESS

N°	SED [N mm/mm^3]	N essessed (97.7 %)	N experimental
1	0.818	0.1005E05	0.87980E5
2	0.9825	0.0697E05	1.04228E5
3	0.4488	0.3340E05	2.05920E5
4	0.3964	0.4282E05	5.58585E5
5	0.4991	0.2701E05	1.90297E5
6	0.268	0.9363E05	5.73254E5
7	0.2479	1.0948E05	6.13673E5
8	0.4119	0.3966E05	4.29261E5
--	------	------	------

*5 mm of thickness

TABLE 20 : EXPERMENTAL RESULTS FOR SAMPLES OF 20 MM OF THICKNESS

N°	SED [N mm/mm^3]	N assessed (97.7 %)	N experimental
1	0.4496	0.0333E06	0.057157E6
2	0.4914	0.0279E06	0.065951E6
3	0.2877	0.0813E06	0.106330E6
4	0.3367	0.0593E06	0.160518E6
5	0.1875	0.1914E06	0.305548E6
6	0.1978	0.172E06	0.375412E6
7	0.1152	0.507E06	1.112251E6
8	0.1192	0.4735E06	1.137888E6
9	0.0503	2.6592E6	3.80E6

*20 mm of thickness

In figure 57 can be seen how experimental corrected data go inside the fatigue scatter band of SED, with some problem for 5 mm of thickness came from the big values of misalignment.

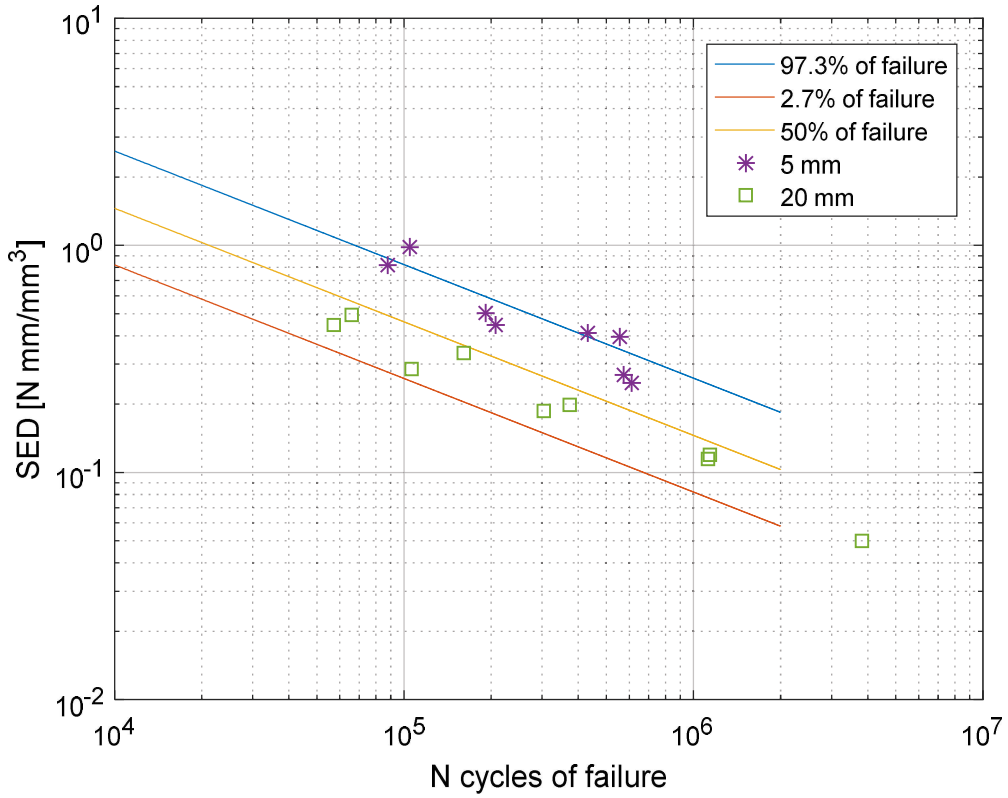

FIGURE 58: EXPERIMENTAL DATA FOR SAMPLES OF 5 MM AND 20 MM OF THICKNESS

3.1.9 Life fatigue assessment comparation between SED method and Structural/Nominal approach:

In order to verify SED method, a life fatigue assessment for butt welded joints have been made using Nominal stress approach, from reference curve from [9]:

- Nominal reference curve for nominal approach: FAT 32;

Infact, for this type of weldment, the average toe angle is less the 50° and misalignment is <10% of the plate thickness.

Life cycles of failure have been extracted from the different assessments and then they are compared between them and with the experimental data related to samples. Furthermore, a wrong life fatigue assessment has been made using the curve related to butt ground welded joint, to underline the necessity of linking geometries of samples to exact experimental data.

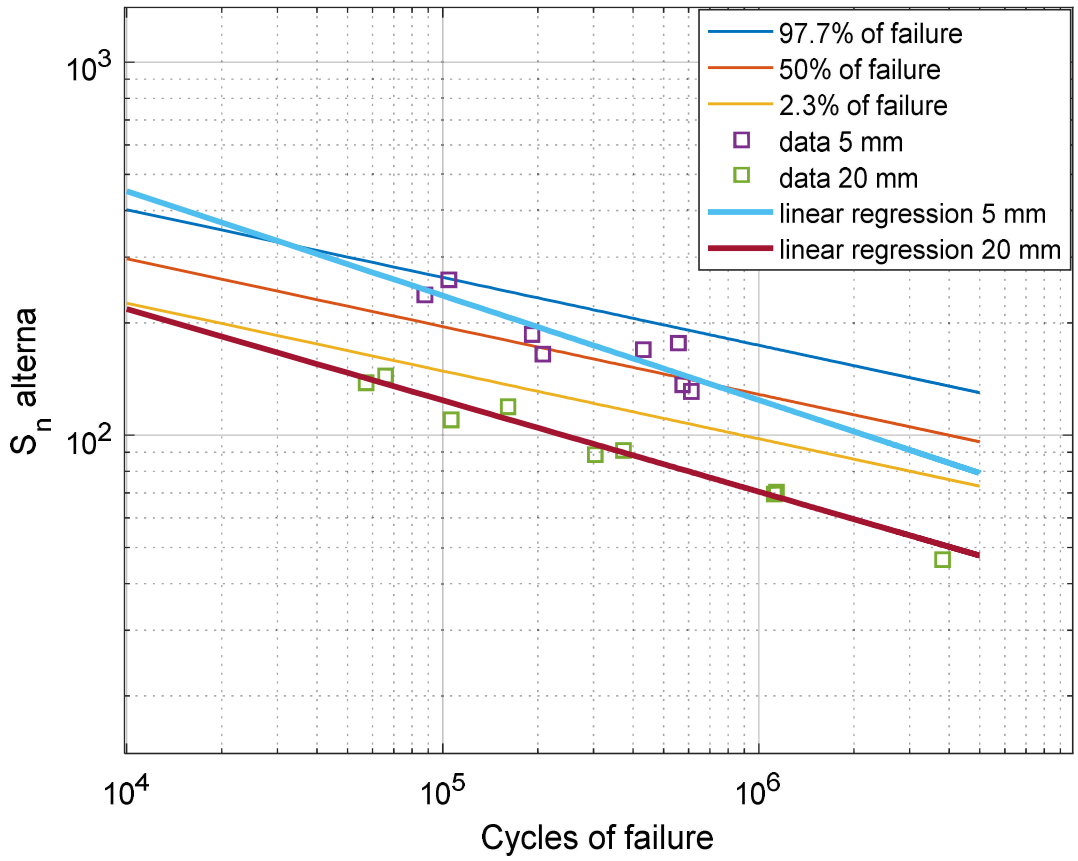

FIGURE 59: COMPARATION BETWEEN BUTT GROUND WELDED JOINTS AND BUTT JOINTS FROM EXPERIMENTAL DATA

In figure 58 can be seen how changing in geometry (transforming a toe in a ground joint) changes the behaviour of the weldments. Infact the angular coefficient of the trend of experimental data is very different from the reference curves. In Figure 59 experimental data and trend of linear regression are compared with FAT 32 reference curve that can be used for a fatigue life assessment in this case.

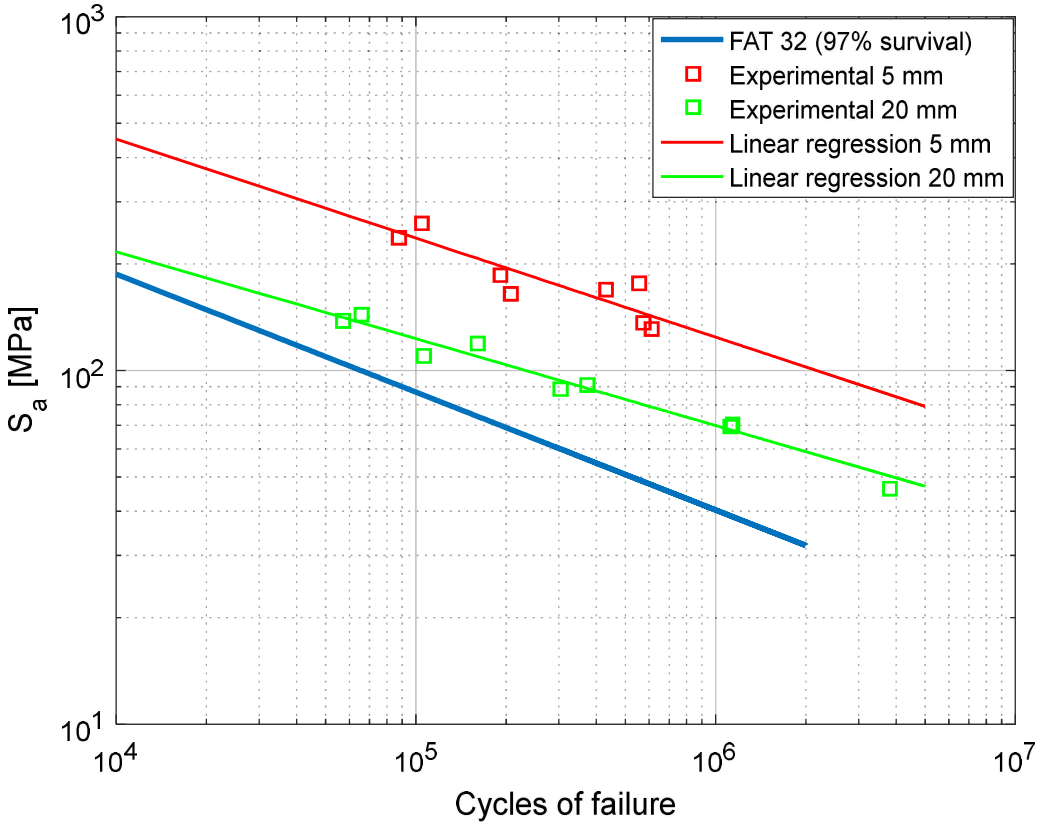

FIGURE 60: LIFE FATIGUE COMPARATION BETWEEN FAT32 REFERENCE CURVE AND EXPERIMENTAL DATA

Now a comparation among different methods can be made evaluating the number of cycles of failure expected from reference curves of each methods (97% probability of survival). In table 21 data are resumed:

TABLE 21: LIFE FATIGUE ASSESSMENT WITH DIFFERENT METHODS FOR 5 MM BUTT JOINTS

Cycles of failure Nf			
SAMPLE	FAT32	SED	Experimental
1	0.4843e+04	1.0050e+04	87980
2	0.3675e+04	0.6970e+04	104228
3	1.4510e+04	3.3400e+04	205920
4	1.2011e+04	4.2820e+04	558585
5	1.0234e+04	2.7010e+04	190297
6	2.5813e+04	9.3630e+04	573254
7	2.8992e+04	10.9480e+04	613673
8	1.3529e+04	3.9660e+04	429261
*5 mm thickness			

In figure 60 a comparation among the different method can be seen. In both the tests case can be seen that SED method is always conservative, and more precise than FAT method.

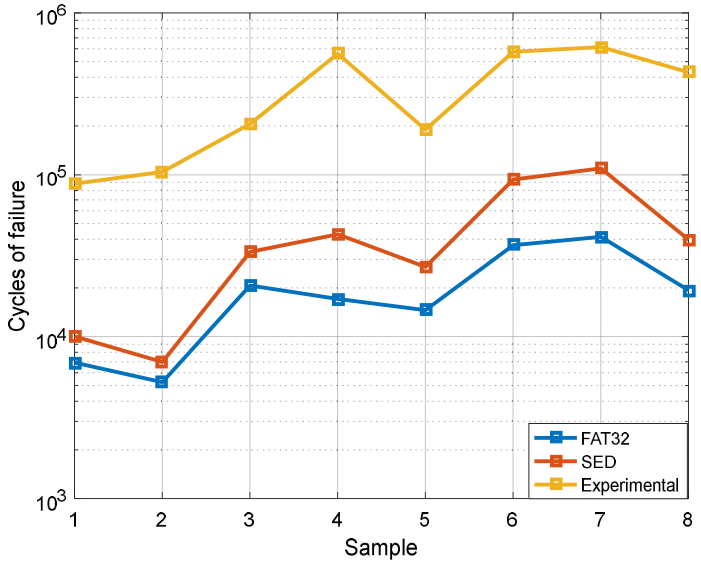

FIGURE 61: GRAPHICAL COMPARATION BETWEEN DIFFERENT METHOD FOR SAMPLE 5 MM THICK

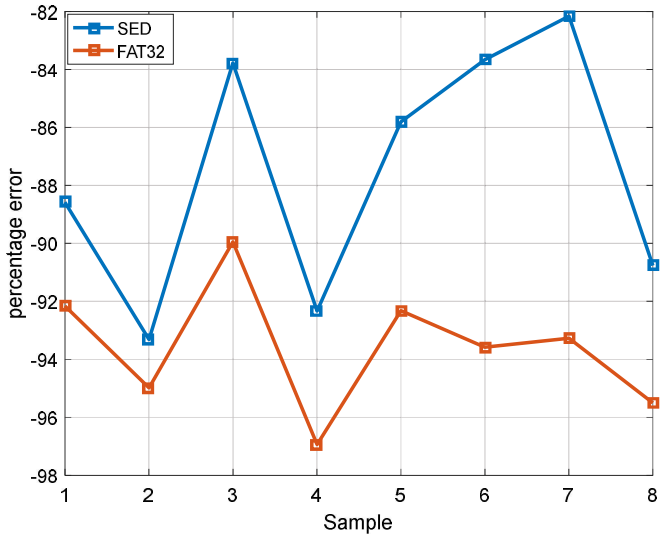

FIGURE 62: PERCENTAGE ERROR BETWEEN SED AND FAT32 RESPECT EXPERIMENTAL NUMBER OF CYCLES (5 MM)

TABLE 22: LIFE FATIGUE ASSESMENT WITH DIFFERENT METHODS FOR 20 MM BUTT JOINTS

Cycles of failure Nf			
SAMPLE	FAT32	SED	Experimental
1	0.2521e+05	0.333e+05	57157
2	0.2206e+05	0.279e+05	65951
3	0.4924e+05	0.813e+05	106330
4	0.3889+05	0.593e+05	160518
5	0.9359e+05	1.914e+05	305548
6	0.8640e+05	1.72e+05	375412
7	1.9438e+05	5.07e+05	1112251
8	1.8466e+05	4.735e+05	1137888
9	6.7330e+05	26.592e+05	3800000
*20 mm thickness			

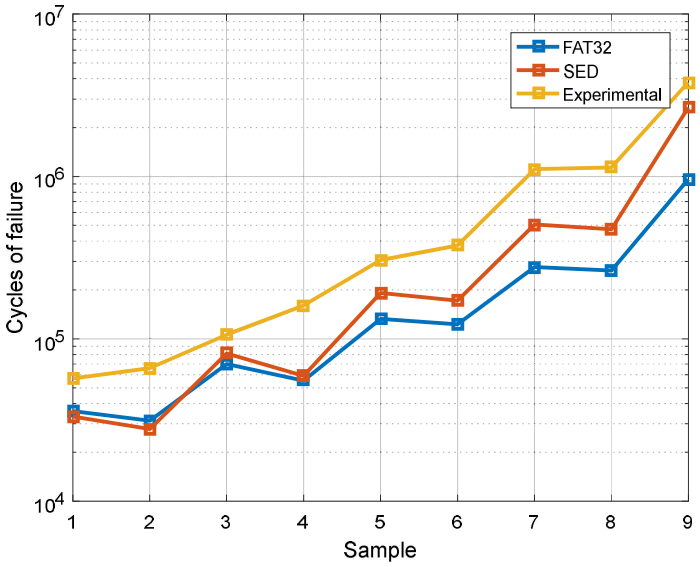

FIGURE 63: GRAPHICAL COMPARATION BETWEEN DIFFERENT METHOD FOR SAMPLE 20 MM THICK

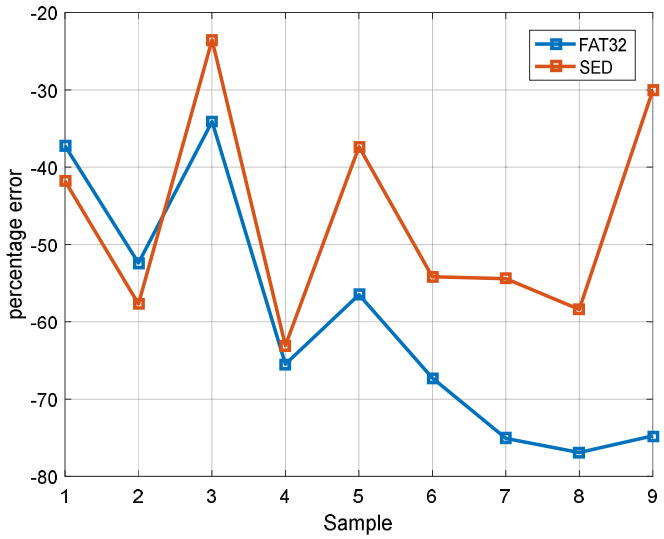

FIGURE 64: PERCENTAGE ERROR BETWEEN SED AND FAT32 RESPECT EXPERIMENTAL NUMBER OF CYCLES (20 MM)

3.1.10 Consideration on SED method:

Can be seen that the method base on SED gives very good results for samples of 20 mm of thickness. For the samples of 5 mm datas are in the upper failure curve line (2.5% of survival) because of the great uncertain of misalignement measurament. The iss been proved to be good for precision and reliability of results in a first design. Infact the results are all conservative respect the real cycles of failure. The master curves coming from a great number of experiments for different geometry can be used in butt welded joints design too, underlining the fact that SED methond is indipendent from the geometry. The interpolation fatigue line of data is very similar to master curve for what oncerns trend of fatigue curves, both samples of 20 mm of thickness and for the 5 mm ones.

For what concerns the 5 mm of thickness samples, the fatigue trend curve is a bit different because of the grat value of misalignment. Anyway, using the other method, as nominal approach, all the fatigue curve interpolating data deviate from reference curve FAT32, more than what happens in SED mothod.

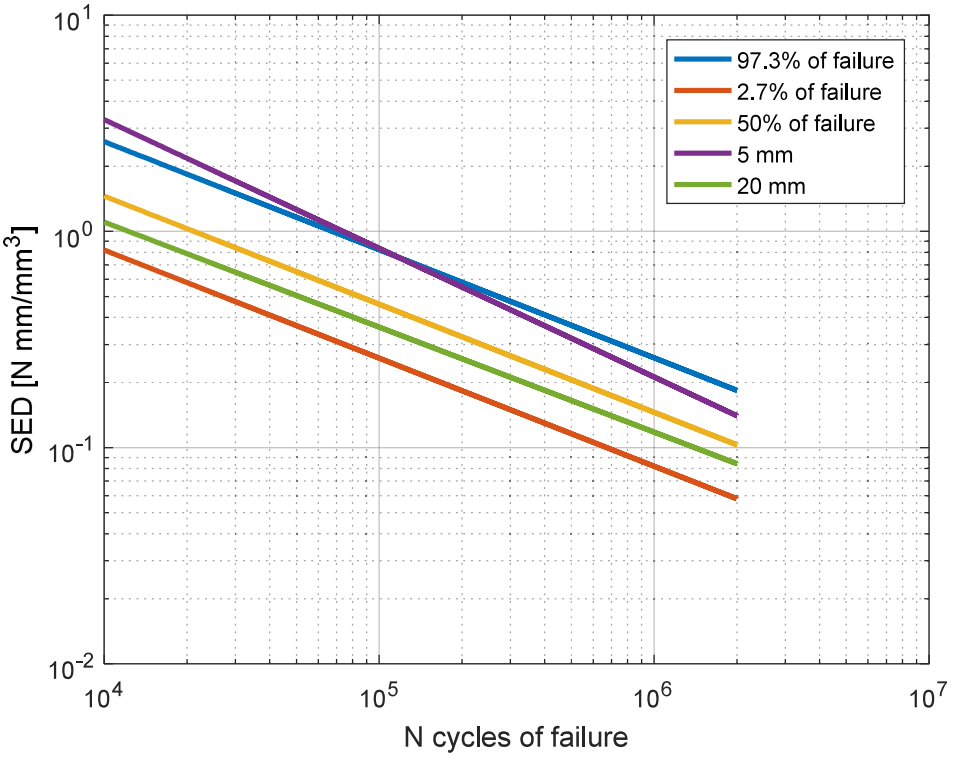

FIGURE 65: EXAMPLE FOR FATIGUE DESIGN WITH SED METHOD

Moreover, from the figure 62, can be noted how the method can be applied for all the different type of geometries used for welded joints.

Infact the linear regression of the experimental data (corrected with correction factors), have a trend very close to the reference fees.

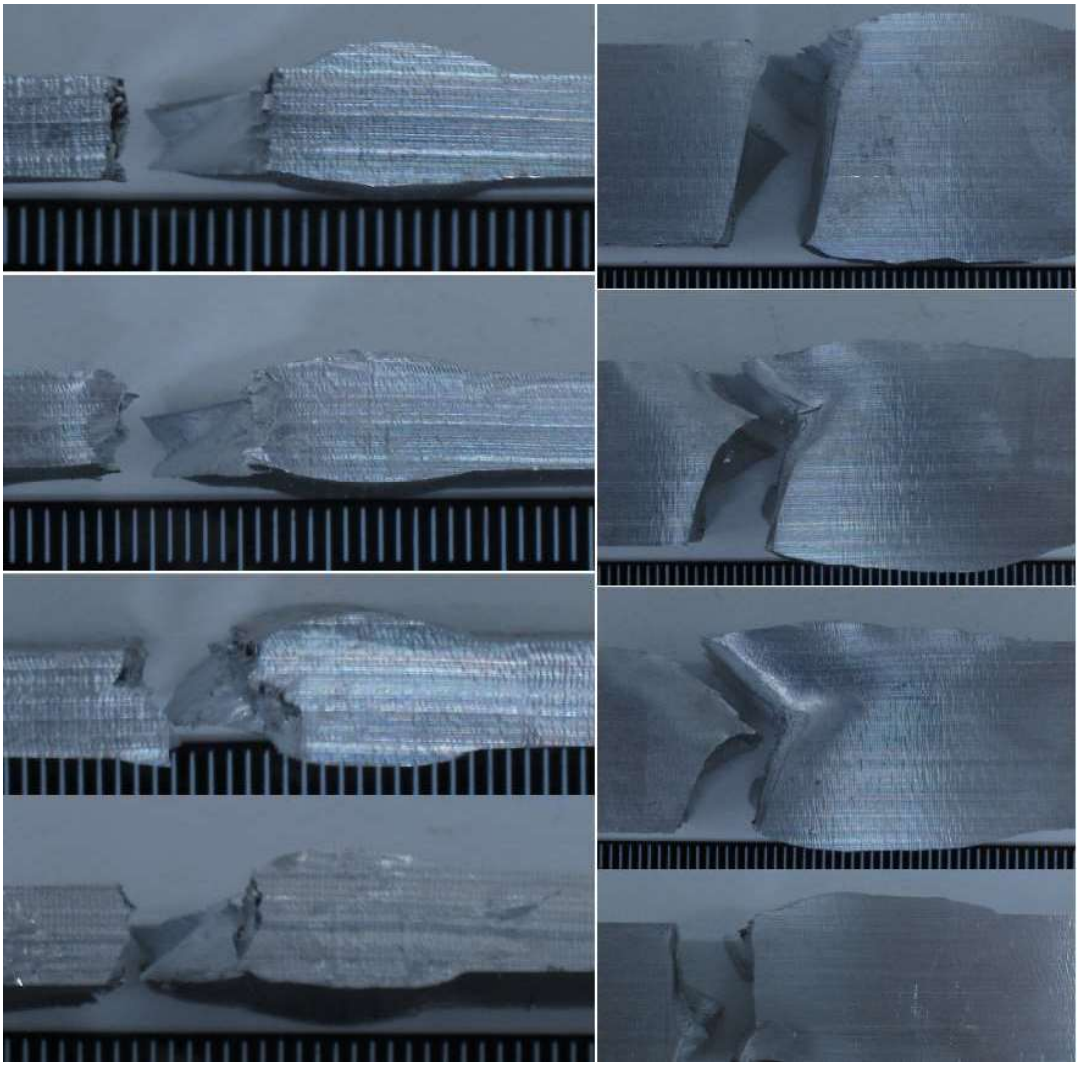

FIGURE 66: PICTURES OF FRACTURE SURFACES OF WELDED BUTT JOINTS

Finlly, a brief scheme in order to show the possible step in a welding design can be seen in figure 64, in which SED method as well compares

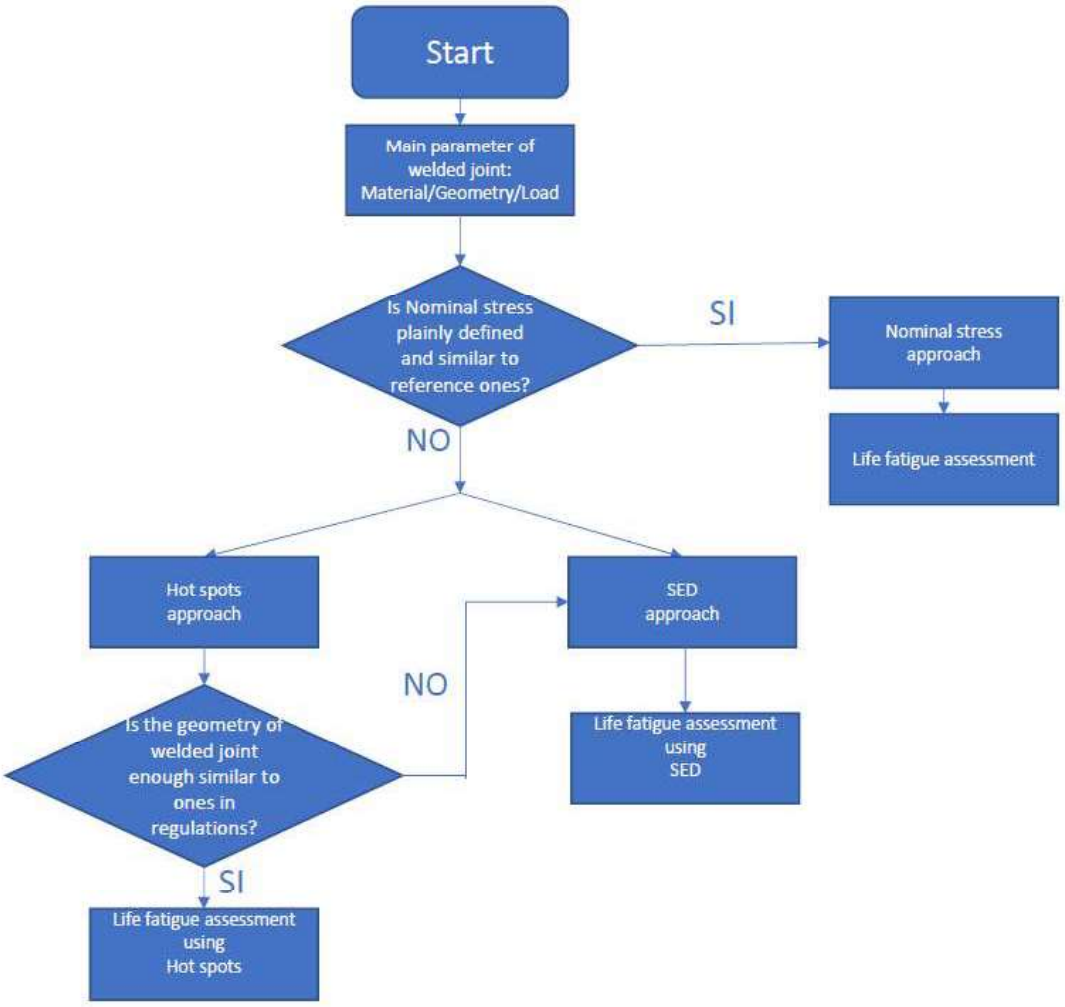

FIGURE 67: WELDING DESIGN POSSIBILITY

3.2 3D model:

In experimentals cases the model is made with plane model because of the simplicity of the samples, making some simplifying hypothesis. Consequently, the results coming from FEM model about SED values are a bit different from the 3D model. So, a 3D model has been made at first for the sample of 5 mm of thickness, studing differences between£d model and 2D one and the effects that the width of the samples generates on SED values

around the notch. As the plane model, geometry has been made without misalignement, and the values of SED have been corrected with correction factors. The first step has been making a sensitivity analysis of the SED changing and both the number os elements in the control volume and the number of division along the width. The model created in Ansys came from 2D model through extrusion, as can be seen in figure 65.

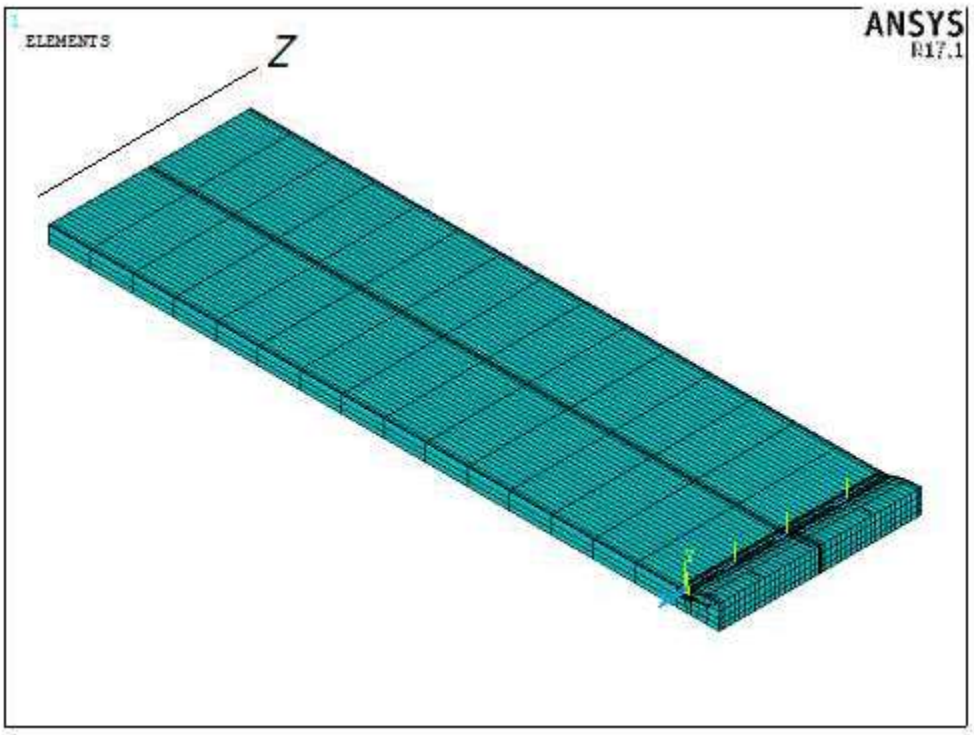

FIGURE 68: 3D MODEL OF BUTT JOINT

In the case of 3D model, the control volume becames a cilynder whose heigh is the same of critical radius (0.12 mm for aluminium) [8]. The elements used in order to optimizate the value of SED, depending from shape function, are Ansys Solid 95, that are elements with 20 nodes. The main characteristics of this elemets are listed in figure 66:

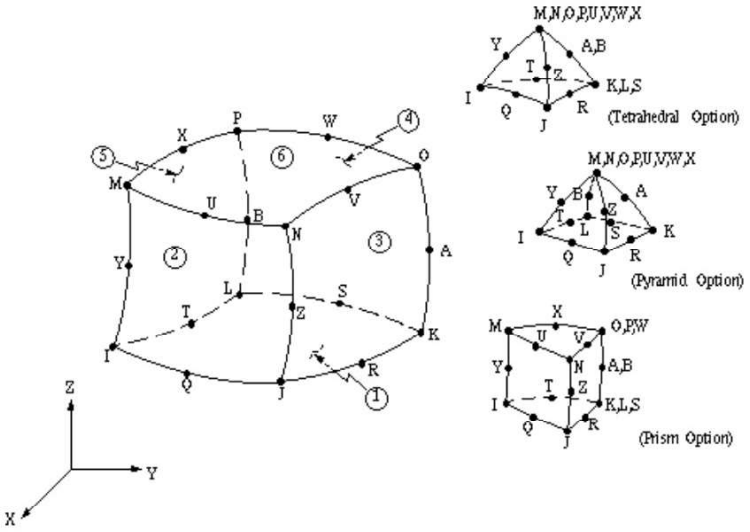

FIGURE 69: SOLID 95 ELEMENT

Dofs of the nodes are 3 (translation along X, Y and Z directions). A quarter of welded joint has been modelled and studied.

3.2.1 Sensitivity analysis

Two sensitivity analysis have been made in order to study two effects of different paramenters: the number of extrusion along the width and the number of elements in control volume. The first case can be seen in figure 67, and the error between the values of SED for different meshes are zero. The analysis has been made setting a control volume in the middle of the model and changing the number of division made along the extrusion. The lengths of the elements are 5 mm, 2.12 mm, 0.992 mm, 0.595 mm, dividing width sample in 3, 7, 15 and 25 parts respectly.

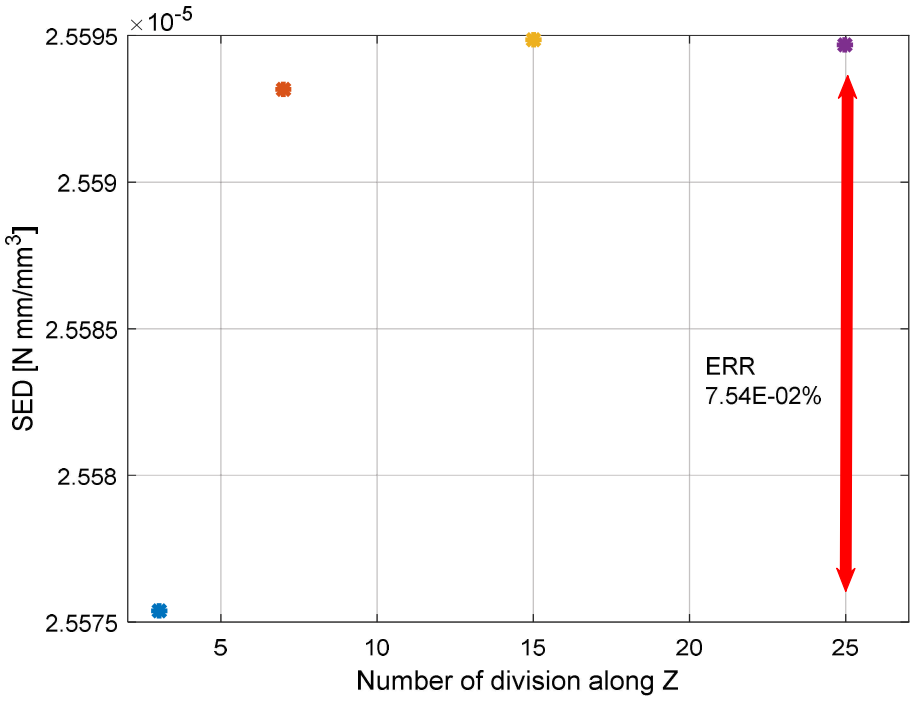

FIGURE 70: VALUES OF SED FOR DIFFERENT LENGTHS OF EXTRUSION PARTS

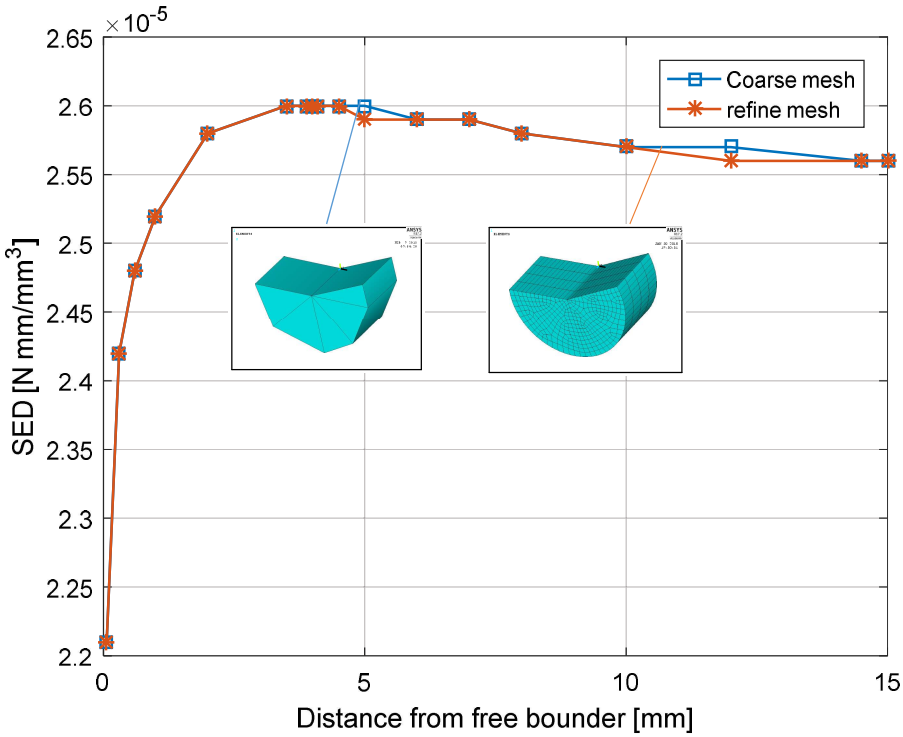

FIGURE 72: SENSITIVITY ANALYSIS CHIANGING NUMBER OF ELEMENTS IN CONTROL VOLUME

In figure 69 can be seen that the values of SED coming from in very coarse mesh and very refine mesh are the same, using twelve elements in the coarse one and more than five houndred in very refine mesh. In figure 66 can be seen too that the number of division of the width in very insensitive for SED values, underlining the fact that a vary coarse mesh can be applied in each case. The error is always under the 0.5%. So the stability of Strain Energy Density in the control volume is again valid for 3D model.

3.2.3 Analysis of quarter of joint:

In 3D model different volumes of control along the width are been made. A first step has seen to make 15 volumes in order to study a general behaviour of the parameter. In the boundary zone particular effects can be seen. Here the values of the SED increases. More simulations are made in the middle parte and near the free edge in order to have more data. The values of the SED along the notch is rapresented in figure 70 for the sample of 5 mm of thickness, with unitary input in load and without the use of correction factors. The plot describes the qualitative trend. A particular effect is in the near of free border, increasing the values of the SED.

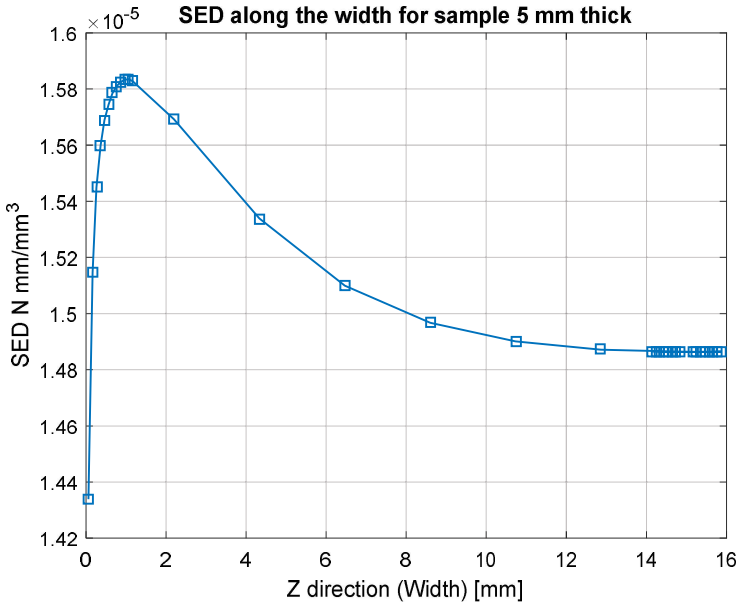

FIGURE 73: SED ALONG THE WIDTH OF THE SAMPLE 5 MM THICK

If a comparation between SED of 3D model and SED of plane model is made, in the most severe case, an error of 9% can be made near the free bounder. In the middle plane error is less then 3%. From the trend of the SED along the width, a mapping of stress field around the notch has been made in order to understand why SED increases for different values of width. Williams' model is for plane condition of strain or stress, so in 3D case this model can not be applied, and a changing along the width of the stress is expected. However Williams' model is a reference. The third dimension can not change completely the trend of the stress. The mapping of the stress has been made in two steps:

- In the first step the stress along the bisector of the corner has been to study, changing the width of the study and the distance from the V-notch
- In the second step the stress field for a costant distance from the V-notch has been to study and changing the width and the angle teta.

A fist study has been made for the sample of 5 mm of thickness. All six components of stress have been analyzed and Von mises stress has been extracted for reason of sysnthesis and because it is linked to an energetic background. All the datas are reported in figure 71. In those pictures can be noted that the main stress, in magnitude, loading the volume around the noch are the radial component, tangential component and z component. A particular trend along the width can be noted for Z-teta component, trend in according to SED one. Infact this component goes from zero values to a maximum value, keeping costant distance and changing the width. Achieved the maximum values, stress component Z-teta goes fast to zero in the free edge. The increase of the SED close to free border can be defendat to tangential stress z-teta, that increases in this part of the body. This component stress the V-notch with mode III ([17],[18]).

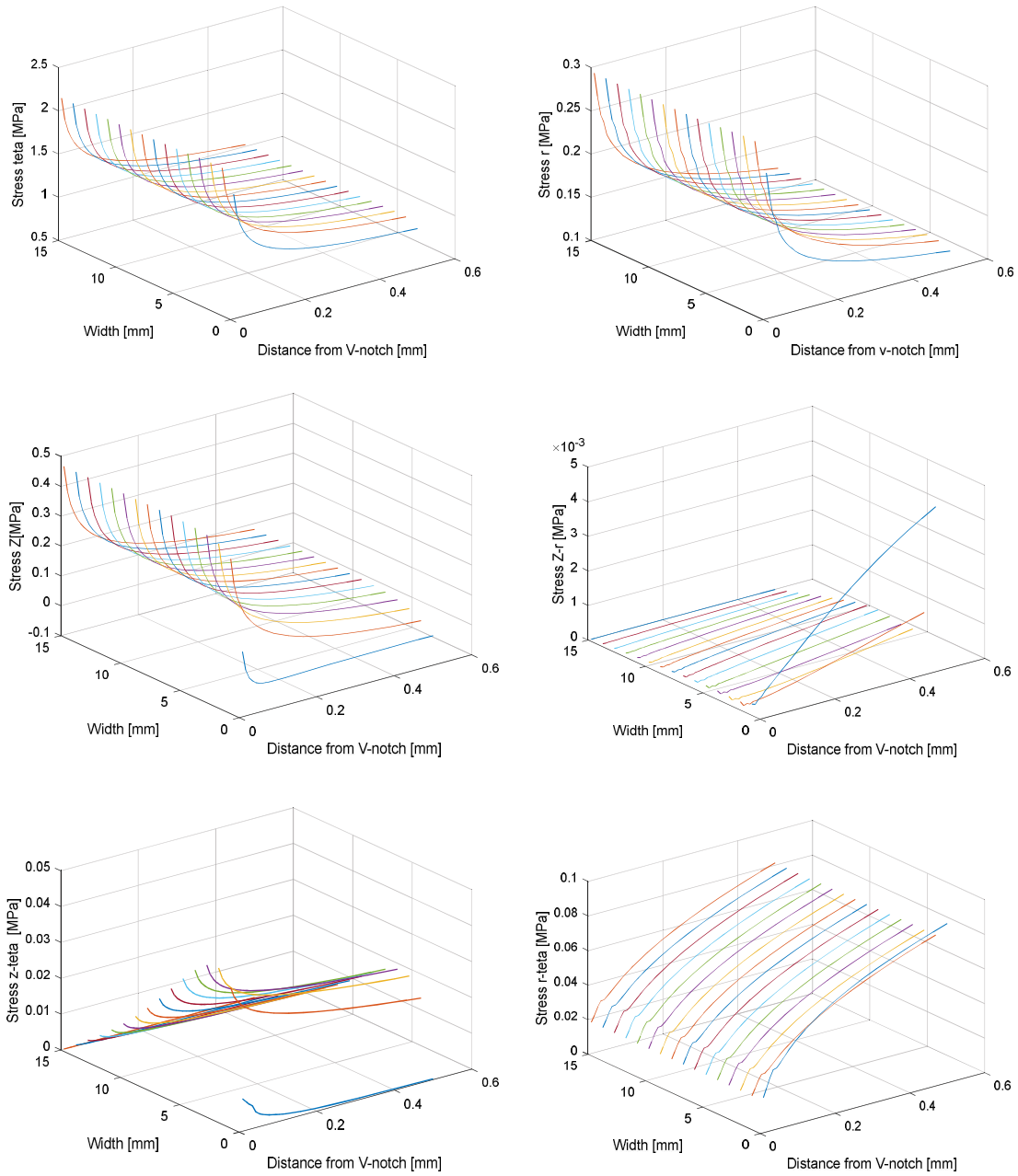

FIGURE 74: STRESS COMPONENT IN CILYNDRICAL COORDINATES ALONG BISETOR DIRECTION

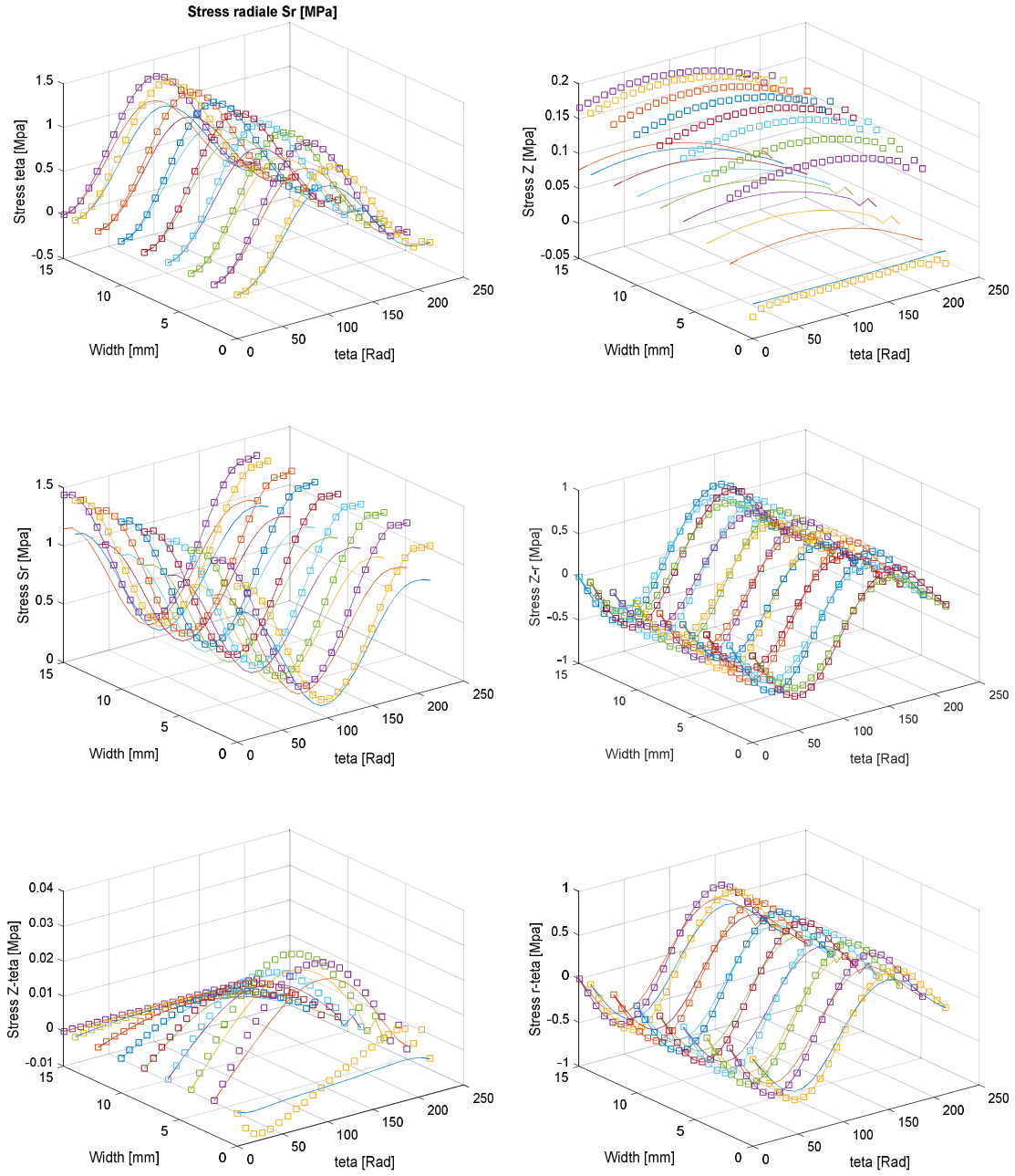

FIGURE 75: STRESS COMPONENT IN CILYNDRICAL COORDINATES ALONG CIRCONFERENTIAL DIRECTION: SQUARE USED FOR POINTS CLOSER TO V-NOTCH

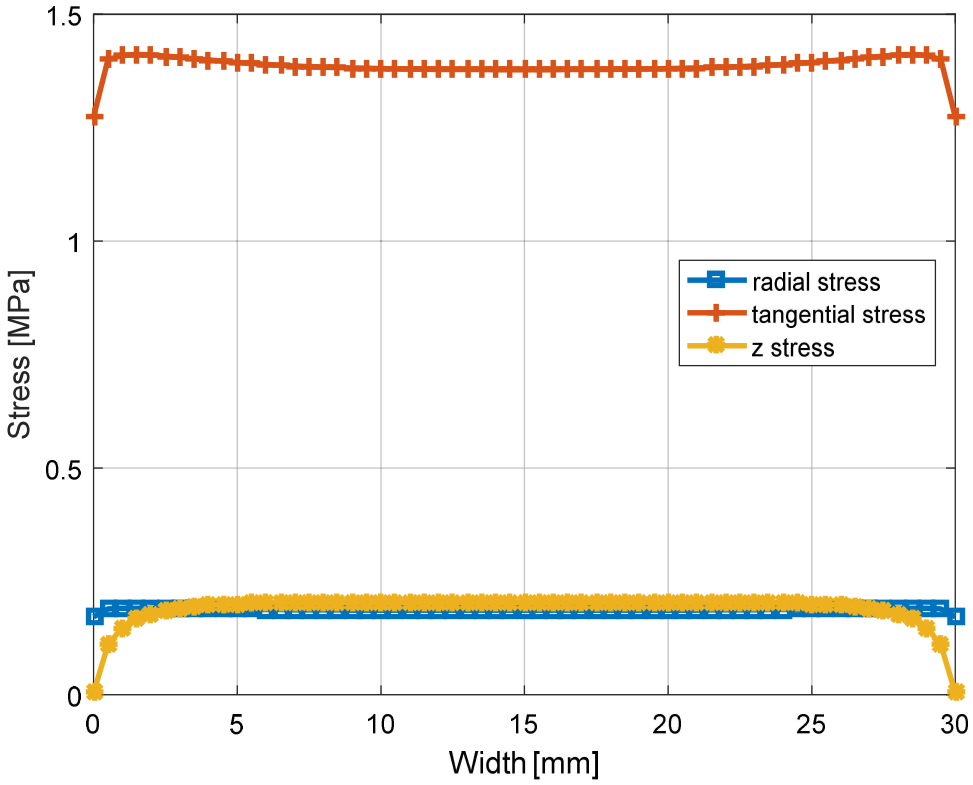

FIGURE 76: NORMAL STRESS COMPONENT ALONG THE WIDTH (DISTANCE FROM V-NOTCH 0.9MM)

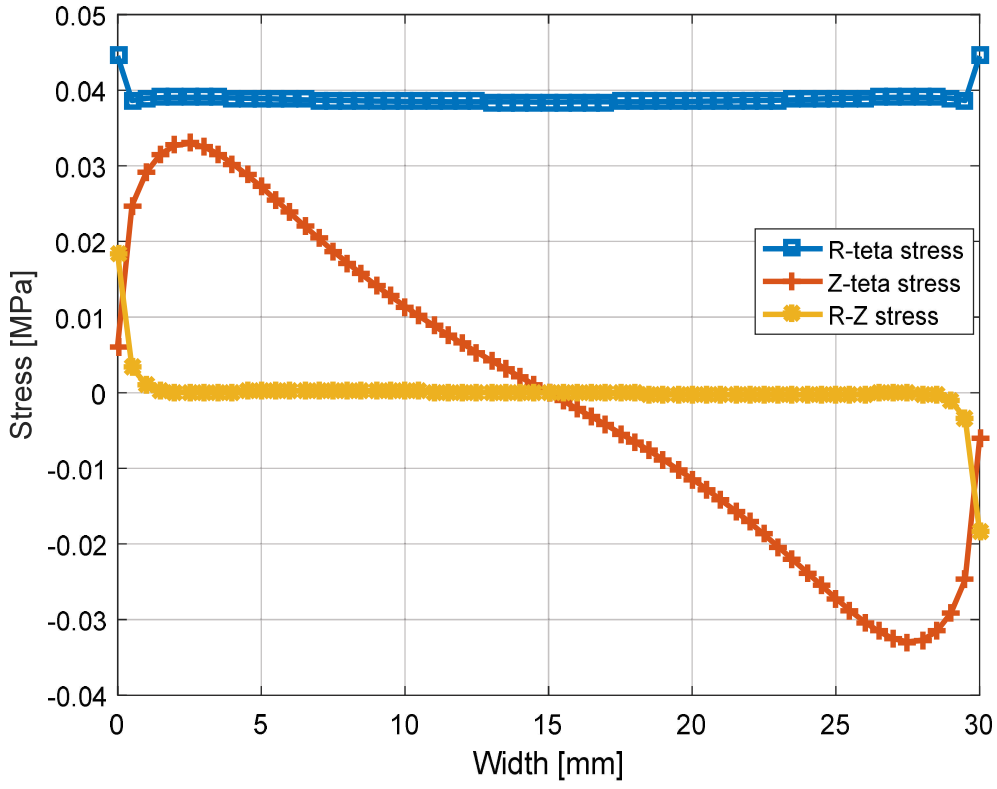

FIGURE 77: TANGENTIAL STRESS COMPONENT ALONG THE WIDTH (DISTANCE FROM V-NOTCH 0.9MM)

Infact, if we take in consideration Williams' model for mode III, can be seen that stress component loading the V-notch are the same having in 3D model in consideration. The magnitude of the stress in this area is greater than tangential stress teta-r, as can be seen in figure 74.

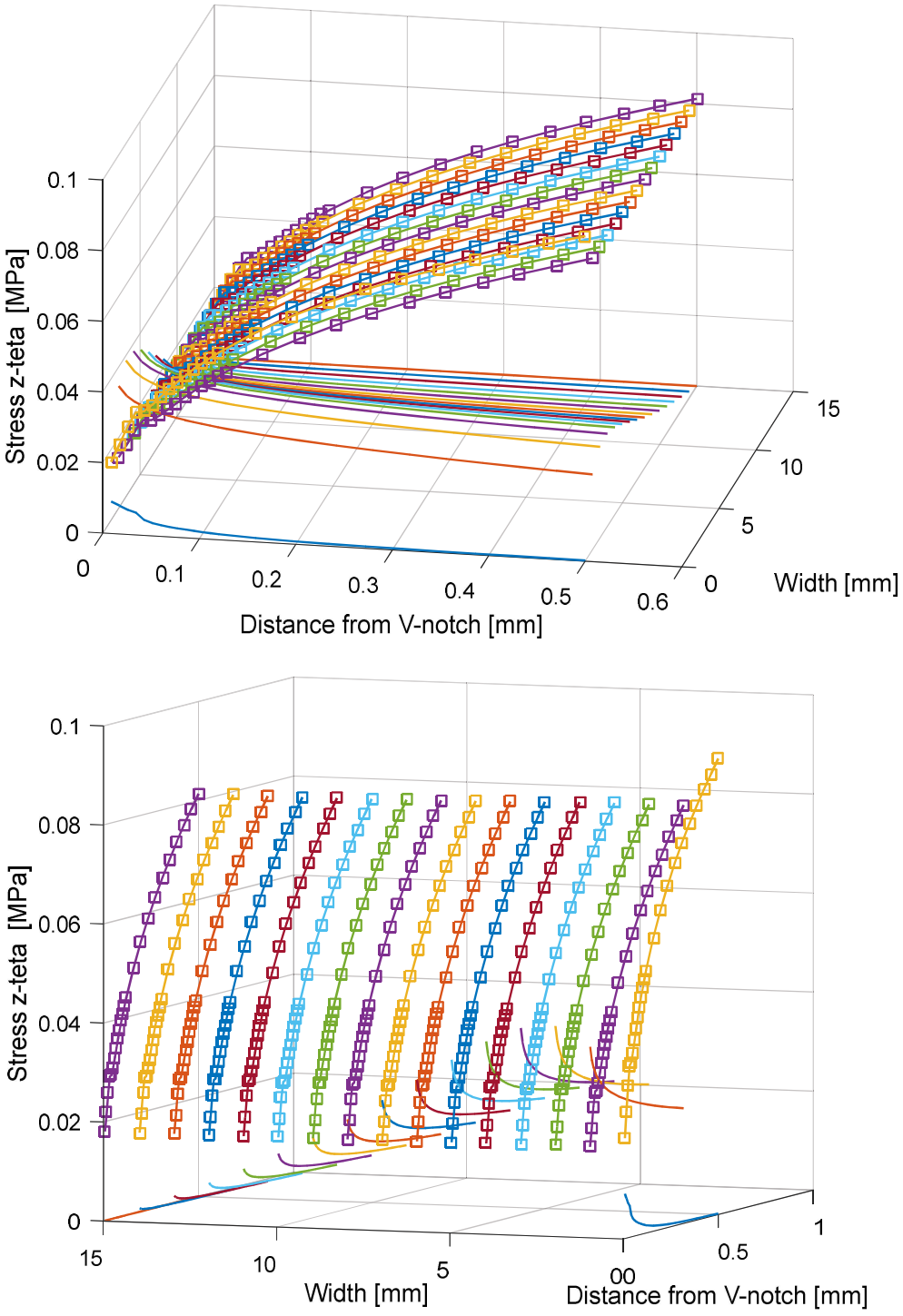

FIGURE 78:TANGENTIAL STRESS R-TETA AND Z-TETA (SQUARE BLOCKS)

The value of SED fells about to trend of stress component teta-z. If the maximun values of SED would be used in life fatigue assestmant, a little correction should be made, but this can be interesting only for notched components and not for weldments. Infact the imperfection in welding direction are so many that is not the increase of the SED near the border to fail the samples.

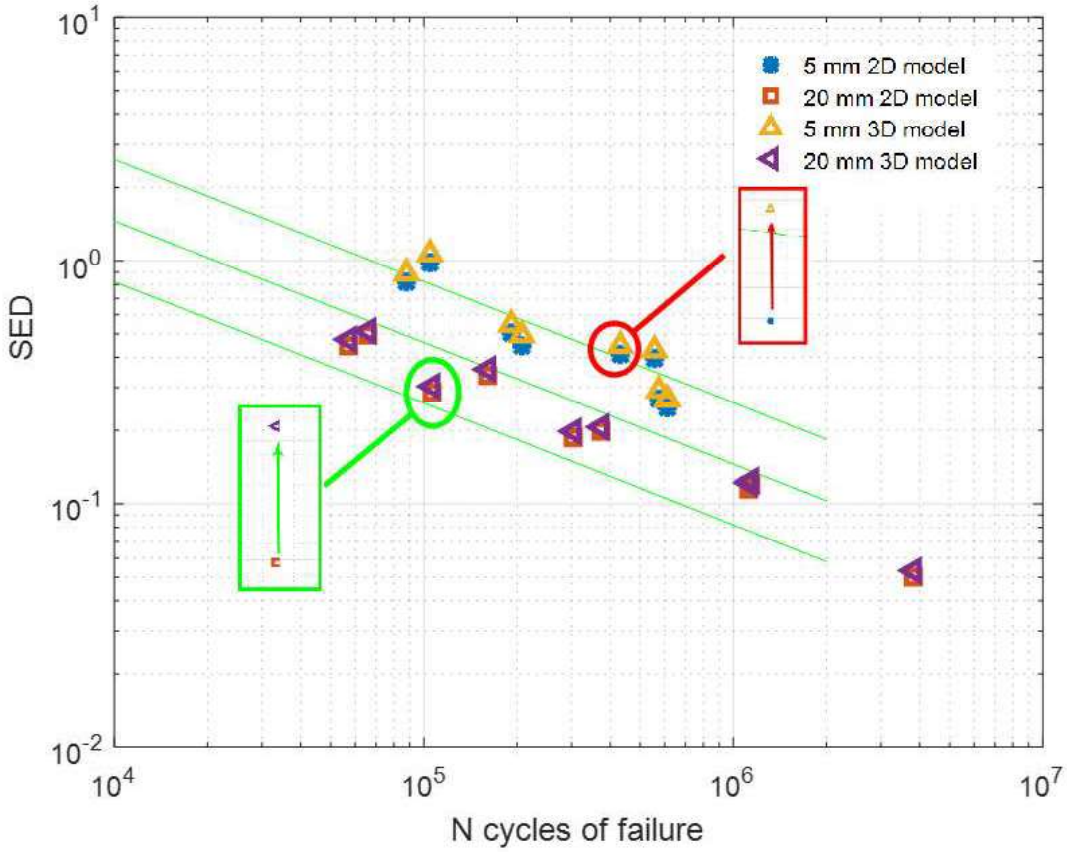

FIGURE 79: LIFE FATIGUE ASSESSMENT USING MAXIMUM VALUES OF SED [N MM/MM^3]

The error between 3D model and plane model are very little and they depend from the thickness of the speciments. For thicker samples the error is 5%, and the plane model not considering the boundary effect give an underrating of the values, like the samples 5 mm thick. In 5 mm thickness case the underrating is grater and it is about the 10%. In any case, translation of the points is the same for all the values belonging to the same thick, and the fatigue behaviour remain qualitatively the same. The linear interpolation becames higher but it doesn't change trend.

3.2.4 Comparation of plane-3D models and"Out-of-plane" effect

From 3D model "particular" effects are noted and studied. Those effects are not so important for the weldments, because of the number of imperfection along the welding are very high in number and the values of increased SED (5% and 10% respectly) is not too much to change the fatigue behavior of weldings. However, it's right to ask from where this effect came and studing like different thicknesses of the sample influence this effect. Data arising from samplel 5 an 20 mm of thickness have been taken in consideration. The values of SED along the width has been studied and the values have been related to SED coming from mono-axial state of stress in order to normalize the values of different samples because of size factor. Finally, SED values have been related to SED of 2D model in order to compare 3D model with 2D one. In figure 77 can ben seen how the SED values increase near the bounder zone for both samples, but with different "velocity" and magnitude, depending from thickness.

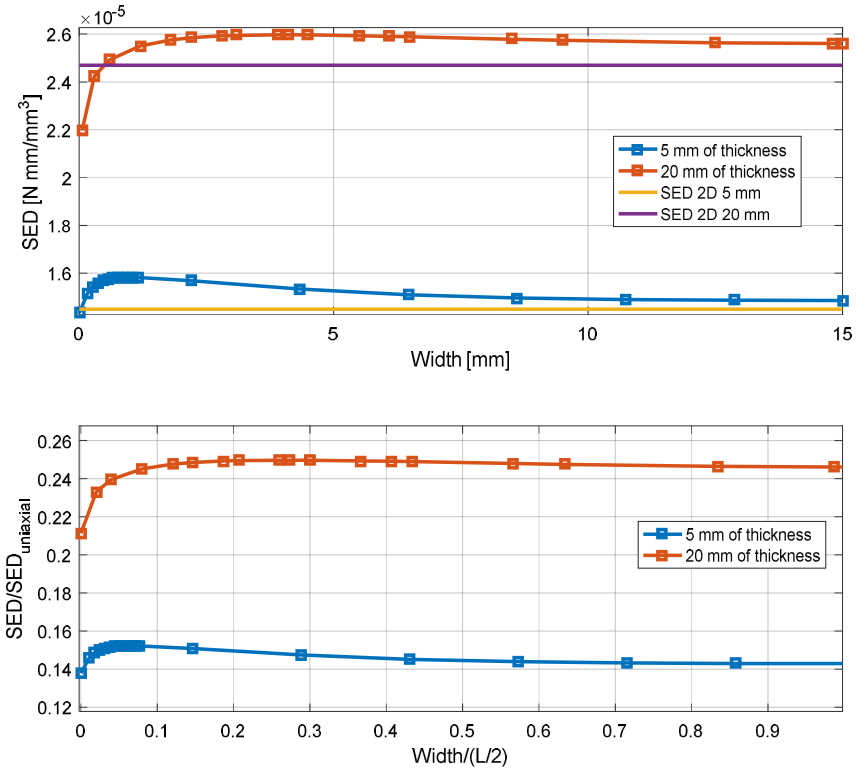

FIGURE 80: 3D SED ALONG THE WIDTH AGAINST 2D SED

Thicker is the sample, less is the maximum value of SED near the free bord, and less deep is the point where the maximum value is achieved. In all the cases the difference among 2D model and 3D one is little in the middle part.

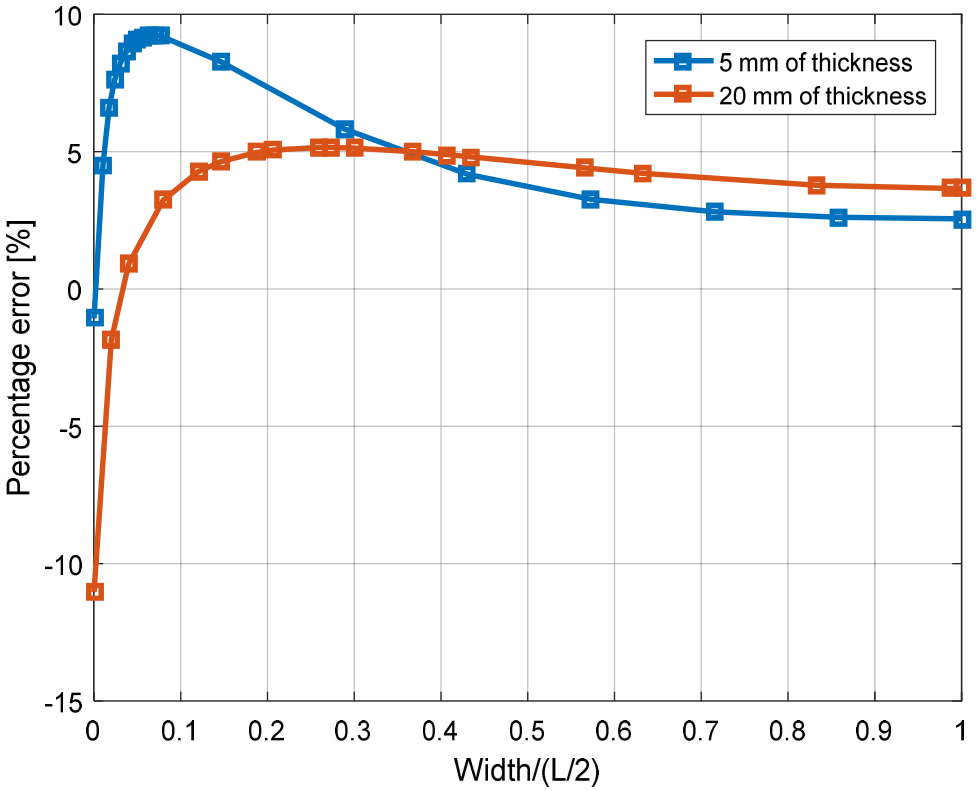

FIGURE 81: PERCENTAGE ERROR 3D VS 2D SED VALUES

In figure 78 can be seen that 2D model is good for welding pieces, and if a fatigue assessment of 3D model is faced using SED values, good results can be obtained. The boundary effects are not so important for welded pieces.

Chapter 4

Conclusions

The present work has treated design problem for aluminium weldings. In a first step, number of parameters interested in design process is very high (Material data, geometry of component, local geometry of weldments, working loads) and some complications can follow. All methods used in weldments design are based on experimental data. In some cases experiments are join with FEM models (Hot Spot and SED approaches), due to the complexity of structure. A only one best method doesn't exist. Each approarch can face problems in its application (a strict correlation of geometry-load must exist (Nominal stress) among reference curve and component, or an agreement there is respect parameter taken in count in FEM model (Hot spot stress), or the complexity of modelling in pre-processing (SED methods). Of course, when a precise reference in geometry-load doesn't exist, the most powerfull method can be SED one, that studies a only one parameter for different kind of geometries and having only one Master curve, and not a family of curves depending from particular geometries-load combinations.

The aim of this work has been approaching to SED method for welding design, to analyze advantages and disadvantages, and verify if master curve arising from lap welded joints can be apply to butt joint made in aluminium, in order to underline the powerfull of this method.

Thus, the main advantage of the Strain Energy Density approach proved in this work: its critical value and its dimensions are a constant, depending only on the material. Moreover, a very coarse mesh (figure 40), compared to the one needed by fracture mechanics based approaches or stress based approach, is able to provide an accurate value of the averaged SED in a material dependent critical volume surrounding the investigated point. A series of numerical and experimental analysies are been made. Fatigue life assessments using Nominal stress approach and SED method has been

performed and results have been compared in order to comment if SED method, that are not conventional, gives good results. Results obtained, considering a first design approach, give very good results for SED approach, in line with Nominal stress method that is, in the case of butt samples, the best one (figure 61 and 63). In the end a comparation between SED values evaluated for 3D model and 2D model has been made, in order to verify if master curves can be used for 3D models, generally more complex. The error made among two models, not considering free bounder effects, is less than 5%, very good for appling SED approach to 3D models (Figure 80).

Bibliography:

[1] P. Livieri and P. Lazzarin (2005) Fatigue strength of steel and aluminium welded joints based on generalised stress intensity factors and local strain energy values. *Internationa Journal of Fracture*, Vol. 113.

[2] L. Susmel, R. Tovo, V. Crupi (2002) La progettazione a fatica multiassiale di componenti meccanici intagliati: Lo stato dell'arte. *Atti del XVI Convegno Nazionale del Gruppo Italiano Frattura.*

[3] P. Lazzarin, P. Zambardi (2001) A finite-volume-energy based approach to predict the static and fatigue behaviour of components with sharp V-shaped notches. *International Journal of Fracture*, Vol. 112.

[4] N. E. Dowling (2013) Mechanical Behaviour of Materials. *Pearson*

[5] A. Hobbacher (1996) Fatigue design of welded joints and components, *IIW Springer.*

[6] F. Berto, P. Lazzarin (2009) The volume-based strain energy density approach applied to static and fatigue strength assessments of notched and welded structures. *Procedia Engineering, Vol. 1.*

[7] P. Lazzarin, F. Berto, F.J. Gomez, M. Zappalorto (2008) Some advantages derived from the use of the strain energy density over a control volume in fatigue strength assessments of welded joints. *International Journal of Fatigue*, Vol. 30.

[8] P. Lazzarin, F. Berto, M. Zappalorto (2010) Rapid calculations of notch stress intensity factors based on averaged strain energy density from coarse meshes: Theoretical bases and applications. *International Journal of Fatigue*, Vol. 32.

[9] P. Lazzarin, R. Tovo, L. Barosso, F. Sammaritani (1998) Fattori di intensificazione delle tensioni in giunti saldati di diverso tipo. *Atti del XIV Convegno Nazionale del Gruppo Italiano Frattura*.

[10] C. Fischer, W. Fricke, W., C. M. Rizzo (2016) Fatigue tests of notched specimens made from butt joints at steel, *Fatigue and Fracture of Engineering Materials and Structures, Vol. 39.*

[11] M. L. Williams (1961) The Bending Stress Distribution at the Base of a Stationary Crack. *Journal of Applied Mechanics,* Vol. 28.

[12] T. L. Anderson (2012) Fracture Mechanics: Fundamentals and Applications, *Taylor & Francis Group.*

[13] R.L. Taylor, O.C. Zienkiewicz (2005) The Finite Element Method, *Butterworth-Heinemann.*

[14] S. Kalpakjian, S. Steven, H. Musa (2009) Manufacturing Engineering and Technology, *Pearson*

[15] M. Groover (2013) Fundamentals of Modern Manufacturing: Materials, Processes, and Systems. *Wiley.*

[16] H.M. Westergaard (1939). Bearing pressures through a slightly waved surface or through a nearly flat part of a cylinder, and related problems of cracks, *Journal of Applied Mechanics*.

[17] C.T. Sun, Z.H. Jin (2011), Fracture Mechanics. Academic Press (Elsiever).

[18] F. Berto, P. Lazzarin, A. Kotousov, S. Harding (2011) Out-of-plane singular stress fields in V-notched plates and welded lap joints induced by in-plane shear load conditions. *Fatigue and Fracture of Engineering Materials and Structures, vol.34*

[19] G. Mathers (2012) The welding of aluminium and its alloys. CRC Press LLC.

Appendix:

Figure summary:

Table summary: